**ÇUKUROVA UNIVERSITY**
**INSTITUTE OF NATURAL AND APPLIED SCIENCES**

**PhD THESIS**

**Mehmet TONTU**

# ASSESSMENT OF AN INTEGRATED SYSTEM WITH COAL FIRED POWER PLANT FOR MULTIGENERATION

**DEPARTMENT OF MECHANICAL ENGINEERING**

**ADANA, 2018**

**ÇUKUROVA UNIVERSITY**
**INSTITUTE OF NATURAL AND APPLIED SCIENCES**

**ASSESSMENT OF AN INTEGRATED SYSTEM WITH COAL FIRED POWER PLANT FOR MULTIGENERATION**

**Mehmet TONTU**

**PhD THESIS**

**DEPARTMENT OF MECHANICAL ENGINEERING**

We certify that the thesis titled above was reviewed and approved for the award of degree of the Doctor of Philosophy by the board of jury on 15/10/2018

| | | |
|---|---|---|
| ……..... | ..……..…..…. | ……..... |
| Prof. Dr. Beşir ŞAHİN | Prof. Dr. Hüseyin AKILLI | Prof. Dr. Hüsamettin BULUT |
| SUPERVISOR | MEMBER | MEMBER |
| ……..... | ……. | |
| Prof. Dr. Mehmet BİLGİLİ | Assoc. Prof. Dr. Vedat ORUÇ | |
| MEMBER | MEMBER | |

This PhD thesis was prepared at the Mechanical Engineering division of the Institute of Nature and Science of Çukurova University.
**Registration Number**:

**Prof. Dr. Mustafa GÖK**
**Director**
**Institute of Natural and Applied Sciences**

**This thesis was supported by Scientific Researched Project Office of Çukurova University under Contract no: FDK-2016-7207.**

**ABSTRACT**
**PhD THESIS**

# ASSESSMENT OF AN INTEGRATED SYSTEM WITH COAL FIRED POWER PLANT FOR MULTIGENERATION

**Mehmet TONTU**

**UNIVERSITY OF CUKUROVA**
**INSTITUTE OF NATURAL AND APPLIED SCIENCES**
**DEPARTMENT OF MECHANICAL ENGINEERING**

Supervisor : Prof. Dr. Beşir ŞAHİN
Year: 2018, Pages: 139
Jury : Prof. Dr. Beşir ŞAHİN
: Prof. Dr. Hüseyin AKILLI
: Prof. Dr. Hüsamettin BULUT
: Prof. Dr. Mehmet BİLGİLİ
: Assoc. Prof. Dr. Vedat ORUÇ

In this thesis, a novel multigeneration energy system was introduced based on a conventional steam power plant. This system consists of four sub-systems, namely, waste heat recovery system using organic Rankine cycle, vapor compression refrigeration system, thermal vapor compression desalination system and greenhouse heating system. Energy and exergy analyzes were conducted for defining the efficiency of the sub-systems and the overall efficiency of the multigeneration energy plant. In order to better understand the system performance and to demonstrate the potential for improvement of the multigeneration system, exergoeconomic and environmental analyzes were also performed. The results revealed that the overall efficiency increased when a conventional steam power plant was converted into a multigeneration energy system. As a result, $CO_2$ emissions were reduced because of the lower consumption of coal for the same amount of electricity generation. Fossil fuel consumption and global climate change increase the advantage and importance of an efficient multigeneration power plant.

**Key Words:** Efficiency, exergoeconomic, integrated systems, multigeneration, thermodynamic analysis

# ÖZ

## DOKTORA TEZİ

**ÇOKLU ÜRETİM İÇİN ENTEGRE EDİLEN KÖMÜR YAKMALI GÜÇ SANTRALİNİN DEĞERLENDİRİLMESİ**

**Mehmet TONTU**

**ÇUKUROVA UNİVERSİTESİ**
**FEN BİLİMLERİ ENSTİTÜSÜ**
**MAKİNA MÜHENDİSLİĞİ ANABİLİM DALI**

Danışman : Prof. Dr. Beşir ŞAHİN
Yıl: 2018, Sayfa: 139
Jüri : Prof. Dr. Beşir ŞAHİN
: Prof. Dr. Hüseyin AKILLI
: Prof. Dr. Hüsamettin BULUT
: Prof. Dr. Mehmet BİLGİLİ
: Doç. Dr. Vedat ORUÇ

Bu tezde, geleneksel buhar güç santrali baz sistem alınarak yeni çoklu üretim enerji sistemi tanıtılmıştır. Bu sistem, geri kazanım sistemi için kullanılan organik Rankine çevrimi, buhar sıkıştırmalı soğutma sistemi, termal buhar sıkıştırmalı desalinasyon sistemi ve sera ısıtma sistemi olmak üzere dört alt sistemden oluşmaktadır. Alt sistemlerin verimliliğini ve çoklu üretim enerji santralinin genel verimliliğini tanımlamak için enerji ve ekserji analizleri yapılmıştır. Sistem performansını daha iyi anlamak ve çoklu üretim sisteminin iyileştirilme potansiyelini ortaya koymak için, eksergoekonomik ve çevresel etki analizleri de gerçekleştirilmiştir. Sonuçlar, geleneksel bir buhar santralinin çoklu üretim enerji sistemine dönüştürüldüğünde genel verimliliğin arttığını ortaya koymuştur. Sonuç olarak, aynı miktarda elektrik üretimi için daha az kömür tüketimi nedeniyle $CO_2$ emisyonları azaltılmıştır. Fosil yakıt tüketimi ve küresel iklim değişikliği, verimli çoklu üretim amaçlı santralin avantaj ve önemini artırmaktadır.

**Anahtar Kelimeler:** Çoklu üretim, Ekonomik analiz, entegre sistemler, termodinamik analiz, Verim

## EXTENDED ABSTRACT

The objective of this study is to conduct a thermodynamic analysis of integrated energy systems of multigeneration. The proposed system consists of base system, four different sub-systems, namely, waste heat recovery system using organic Rankine cycle (ORC), vapor compression refrigeration (VCR) system, thermal vapor compression desalination system and greenhouse heating system. Multigeneration energy system can produce electricity, distilled water and perform cooling as well as heating simultaneously. Advantages of multigeneration energy systems have a higher plant efficiency comparing to the conventional power plant, less thermal losses and wastes, lower running costs, lower gas emissions, efficient use of resources, multiple generation options, high standard of reliability.

In this study, first of all, three different steam power plants were compared operating under ultra-supercritical, supercritical and subcritical conditions. Energy and exergy analyses were conducted in order to determine the performance of each system and the efficiencies of the fundamental equipment, as well as the overall efficiency of power plants were compared. According to the results obtained, the overall exergy efficiency of the ultra-supercritical cycle was found to be higher due to lower coal consumption. The energy efficiency of the subcritical, supercritical and ultra-supercritical thermal power plants was determined to be 41.5%, 43.8% and 46.0%, respectively. Also, comparable exergy efficiency values of thermal power plants were determined to be 39.1%, 40.8% and 41.9%, respectively. The chemical reaction is the most significant exergy destruction source which occurs in the combustion chamber of the boiler system. Exergy destruction can be decreased with a preliminary heating procedure for air delivered into the combustion chamber and hence decreasing the air/coal ratio. Among all elements of plants, the highest level of exergy destruction occurs in the boiler unit.

In the first attempt, the integrated system which was an organic Rankine cycle (ORC) system for power generation driven by the waste heat of a coal-fired

thermal power plant was designed. To conduct energy, exergoeconomic and environmental analyses, industrial data obtained from the coal-fired power plant operating at a maximum capacity of 660 MW was used. As a working fluid, R245fa, R236fa, R600 and R236ea refrigerants were considered in the present system. These working fluids were chosen because the critical temperatures of these working fluids are close to the flue gas temperature of the thermal power plant. Chen et al. (2010) suggested using a dry fluid in the case of organic Rankine cycle to prevent working fluid droplet which impinges to the ORC turbine blades during the expansion of a dry fluid. The effects of the flue gas temperature, the flue gas mass flow rate, the steam power plant unit load and the evaporator pinch point temperature on the performance level of the system were determined. According to the results obtained, the ORC system integrated with the steam power plant could generate a net output power of 4.7 MW at a design point. Calculations indicate that the exergy efficiency increases with an increase in the flue gas mass flow rate and steam power plant unit load. On the other hand, this exergy efficiency decreases with an increase in flue gas temperature and evaporator pinch point temperature. In addition, the net power output generated by the ORC system is increased with increasing flue gas temperature, flue gas mass flow rate and steam power plant unit load. But, this net power output is reduced with rising evaporator pinch point temperature. The originality of this work is the feasibility study of the ORC system that is integrated with a currently operating steam power plant.

In the second integrated system, exergoeconomic analysis was conducted theoretically for a steam turbine driving vapor-compression refrigeration system using R134a, R410a, R407c and R717 in this study. Dual purpose system was designed by eliminating the expansion valve to fulfill the demand of cooling load of the steam power plant. Primarily steam turbine was investigated by changing turbine inlet parameters. Afterward, the effect of steam turbine inlet parameters on the cooling load, the coefficient of performance (COP), exergy efficiency of vapor compression cycle (VCC) and equipment both exergy efficiency and exergy

destruction rate were investigated. Among all examined working fluids, R134a was suggested as the best candidate from thermodynamic and thermoeconomic viewpoints. The COP values are determined to be 2.73, 2.29, 1.8 and 1.15 for R134a, R410a, R407c and R717 respectively. Also, exergy efficiencies of VCR are found to be 18.61 %, 13.93 %, 14.97 % and 18.38 % for R134a, R410a, R407c and R717 respectively. On the other hand, the general exergy efficiency of the whole steam power plant was 39.1%. As a consequence of integrating VCC, general exergy efficiencies of the whole system were found to be 39.36%, 39.32%, 39.27% and 39.21% for four different working fluids respectively.

In the third integrated system, a multi-effect distillation system that is presently in use in a thermal power plant was analyzed. In this system, a thermal steam compressor uses the energy of the superheated steam filtered from the steam turbine more efficiently, and this compressor can provide additional steam circulation. In addition to the analysis of the exergy efficiency of the multi-effect distillation system under higher operating loads, the desalination capacity of the system has also been examined. Taking the increasing operating plant load and seawater temperatures into consideration, the overall exergy efficiency were analyzed in order to define the optimum seawater temperature. The unit cost of distilled water is less when the operating load is increased. In summary, a thermo-economic analysis of the Multi-Effect Distillation System (MED-TVC) integrated with a steam power plant was conducted by taking the actual industrial data into account for different plant loads, seawater temperatures and upper brine temperatures. As seen in the subsystem exergy analysis conducted in this study, the vast majority of the exergy destruction in the (MED-TVC) system occurred in the vapor ejector.

In the fourth integrated system, greenhouse heating system was analyzed and the amount of heat recovery was calculated considering different sea water and ambient air temperatures.

Examining the overall efficiency, the calculated exergy efficiency of a single generation is 39.1 %. In the case of the cogeneration system, the systems' efficiency becomes 39.25 %, furthermore, using trigeneration systems the efficiency increase to a value of 39.49 %. Besides the multigeneration system exergy efficiency increase to a value of 39.84% when desalination plant and organic Rankine cycle are integrated to the conventional steam power plant. As in the case of exergy efficiency, energy efficiency is 41.5 % for only power generation. On the other hand, the overall energy production efficiency with cogeneration becomes 41.66 %. In the case of trigeneration application, this efficiency increases up to 41.92 %. Finally, after integration of the desalination plant and the organic Rankine cycle, multigeneration overall energy efficiency becomes 42.29%. On the other hand, the $CO_2$ emissions are lowered from 230 kg/MWh to 225 kg/MWh by integrating four subsystems with the conventional steam power plant.

## GENİŞLETİLMİŞ ÖZET

Bu çalışmada ulaşılmak istenen amaç, entegre çoklu üretim enerji sistemlerinin termodinamik analizini uygulamaktır. Bahsi geçen sistem bir baz sistem ve 4 farklı alt sistemden oluşmaktadır, isimleri ile sırasıyla atık ısının sisteme geri kazanımını sağlayan organik Rankine çevrimi (ORC), buhar sıkıştırmalı soğutma sistemi (VCR), desalinasyon sistemi ve sera ısıtma sistemidir. Çoklu üretim sistemleri aynı anda elektrik üretimi, su arıtma, ısıtma ve soğutma sağlayabilir. Çoklu üretim sistemleri, konvansiyonel güç santrallerine kıyasla daha yüksek verim, daha düşük ısıl kayıplar, düşük işletme maliyetleri, düşük emisyon salınımları, kaynakların daha verimli kullanımı, çoklu üretim opsiyonları, daha yüksek güvenilirlik standartları yönünden avantajları vardır.

Öncelikli olarak bu çalışmada, birbirinden farklı 3 farklı buhar santrali ultra-kritiküstü, kritiküstü ve kritikaltı şartlarda incelenmiştir. Bu santrallerin genel verimlilikleri kıyaslanırken, santrallerin temel ekipmanlarının her birinin performans verimleri enerji ve ekserji yönünden analiz edilmiştir. Sonuçlardan elde edilenler doğrultusunda, ultra-kritiküstü çevrimlerde kömür tüketiminin düşük olmasından dolayı genel ekserji verimi daha yüksektir. Enerji verimlilikleri kritikaltı, kritiküstü ve ultra-kritiküstü termik santrallerde sırasıyla % 41.5, % 43.8 ve % 46.0 olduğu belirlenmiştir. Ayrıca bu santrallerin ekserji verimlilik değerleri sırasıyla % 39.1, % 40.8 ve % 41.9 olduğu belirlenmiştir. Kimyasal reaksiyonlar ekserji yıkımının en çok gerçekleştiği durumlardır, bu durumda en yüksek ekserji yıkımı kazanda yanmanın gerçekleştiği kısımda meydana gelir. Ekserji yıkımı, yanma odasına gönderilen hava için ön ısıtma prosedürü ile azaltılabilir ve böylece hava / kömür oranının düşmesi sağlanır. Santraldeki tüm elemanların içinde en yüksek ekserji tersinmezliği kazanda görülmektedir.

İlk denemede, kömür yakıtlı bir termik santralin atık ısısından yararlanan elektrik üretimi için organik Rankine çevrimi (ORC) sistemi olan bir entegre

sistem tasarlandı. Enerji, eksergokonomik ve çevresel analizler yapmak için, 660 MW'lık maksimum kapasitede çalışan kömür santralinden elde edilen endüstriyel veriler kullanılmıştır. Mevcut sistemde iş akışkanı olarak R245fa, R236fa, R600 ve R236ea düşünülmüştür. Bu akışkanların seçilme sebebi ise akışkanların kritik sıcaklıklarının santralin baca gazı sıcaklıklarına yakın olmasıdır. Chen ve ark. (2010) organik Rankine çevrimi esnasında, iş akışkanının genleşmesi sonucu türbin kanatları üzerinde damlacık oluşumunu engellemek için ORC'de kuru iş akışkanı kullanılması önerilmiştir. Baca gazı sıcaklığının , baca gazı debisinin, santralin ünite yükünün ve buharlaştırıcı akışkan sıcaklıkları yaklaşım sıcaklığının sistemin performansına etkileri belirlenmiştir. Elde edilen sonuçlara göre, tasarım aşamasında santrale entegre edilen ORC sistemiyle birlikte 4.7 MW'lık net çıkış gücü üretilebilir. Hesaplamalar, baca gazı debisi ve buhar santrali ünite yükü arttıkça ekserji verimliliğinin arttığını göstermektedir. Diğer taraftan, baca gazı sıcaklığı ve buharlaştırıcı akışkan yaklaşım sıcaklığı arttıkça ekserji verimliliği azalmaktadır. Ayrıca, baca gazı sıcaklığı, baca gazı debisi ve santralin ünite yükünün artışı ile ORC sistemi tarafından üretilen net çıkış gücü artırılır. Ancak, net güç çıkışı yükselen buharlaştırıcı akışkan yaklaşım sıcaklığı ile azalır. Bu çalışmanın özgünlüğü, hali hazırda çalışan buhar çevrimli bir santral ile entegre edilmiş olan ORC sisteminin fizibilite çalışmasıdır.

İkinci entegre sistemde, çalışmada R134a, R410a, R407c ve R717 kullanarak buhar türbin tahrikli buhar sıkıştırmalı soğutma sistemi için teorik olarak eksergokonomik analizi yapılmıştır. Çift amaçlı tasarlanan sistem, buhar santralinin soğutma talebini karşılamak için genleşme vanasını ortadan kaldırarak tasarlanmıştır. Öncelikli olarak buhar türbini, türbin giriş parametrelerini değiştirilerek incelenmiştir. Sonrasında, buhar türbini giriş parametrelerinin soğutma yükü üzerindeki etkisi, performans katsayısı (COP), buhar sıkıştırmalı soğutma çevriminin (VCC) ekserji verimliliği ve ekipmanların ekserji verimlilikleri ile ekserji yıkım oranları incelenmiştir. Test edilen tüm akışkanlar arasında R134a'nın termodinamik ve termoekonomik açıdan en iyisi olduğu tespit

edilmiştir. COP değerleri R134a, R410a, R407c ve R717 için sırasıyla 2.73, 2.29, 1.8 ve 1.15 olarak belirlenmiştir. Ayrıca VCR ekserji verimlilikleri R134a, R410a, R407c ve R717 için sırasıyla %18.61, %13.93, %14.97 ve %18.38 olarak belirlenmiştir. Diğer taraftan, buhar çevrimli santralin genel ekserji verimi %39.1 olarak görülmüştür. VCC'nin entegrasyonu sonucunda, tüm sistemin genel ekserji verimliliği 4 farklı akışkan için sırasıyla %39.36, %39.32, %39.27 ve %39.21 olarak bulunmuştur.

Üçüncü entegre sistemde, hali hazırda bir termik santralde kullanımda olan çok etkili bir desalinasyon sistemi analiz edilmiştir. Bu sistemde, bir termal buhar kompresörü, buhar türbinden daha verimli bir şekilde geçirilen aşırı ısıtılmış buharın enerjisini kullanır ve bu kompresör, ilave buhar dolaşımını sağlayabilir. Daha yüksek çalışma yükü altında arıtma sisteminin ekserji verimliliğinin analizine ek olarak, sistemin tuz giderme kapasitesi de incelenmiştir. Artan sistem yükü ve deniz suyu sıcaklıkları dikkate alınarak, optimum deniz suyu sıcaklığını tanımlamak için genel ekserji verim analizleri yapılmıştır. Sistemin çalışma yükü arttıkça distile suyun birim maliyeti azalmaktadır. Özet olarak, buhar santraline entegre edilen çok etkili desalinasyon sistemi (MED-TVC)'nin bir termoekonomik analizi endüstriyel veriler doğrultusunda farklı çalışma yükleri deniz suyu sıcaklıkları ve en yüksek tuzlu su sıcaklıkları dikkate alınarak gerçekleştirilmiştir. Bu çalışmada yapılan alt sistem ekserji analizinde görüldüğü gibi (MED-TVC) sistemindeki ekserji yıkımının büyük çoğunluğu buhar ejektöründe meydana gelmiştir.

Dördüncü entegre sistemde, sera ısıtma sistemi analiz edilmiş ve farklı deniz suyu ve ortam sıcaklıkları dikkate alınarak ısı geri kazanım miktarı hesaplanmıştır.

Genel verimlilik incelendiğinde, sadece elektrik üretimi yapan santralin ekserji verimliliği %39.1 olduğu hesaplanmıştır. Kojenerasyon durumunda sistem verimliliği %39.25 olmaktadır, ayrıca trijenerasyon sistemi kullanılarak verim %39.49'a yükseltilebilir. Yanı sıra, konvansiyonel buhar çevrimli santrale

desalinasyon ve organik Rankine çevrimi entegre edildiğinde çoklu üretim sistemi ekserji verimliliği %39.84 değerine yükselmektedir. Ekserji verimliliğindede olduğu gibi, sadece elektrik üretimi için enerji verimliliği %41.5 olarak belirlenmiştir. Diğer taraftan, kojenerasyonla birlikte enerji üretim verimliliği %41.66 olmaktadır. Trijenerasyon uygulaması ile birlikte bu oran %41.92'e kadar çıkmaktadır. Son olarak, desalinasyon tesisinin ve organik Rankine çevriminin entegrasyonuyla birlikte çoklu üretim santrali genel verimliliği %42.29 olur. Öte yandan konvansiyonel buhar santraline 4 alt sistemin entegrasyonuyla birlikte $CO_2$ emisyonları 230 kg/MWh' ten 225 kg/MWh'e düşürülmüştür.

**ACKNOWLEDGMENTS**

This list endless if I have to thank all the people that made possible this work. My first thanks go to my advisor Prof. Dr. Beşir ŞAHİN for his support, guidance and encouragement. He has been a great source of motivation, both personal and technical. His generous advice, encouragements and constant faith have made my time with him is a very challenging and rewarding experience.

I am so grateful to Prof. Dr. Mehmet BİLGİLİ for his motivation, support and encouragement starting from my graduate study. I learned so many things from him. I always received his support both mentally and scientifically during this study to construct and reinforce my research way properly.

I would like to present my endless thanks to the head of Mechanical Engineering Department Prof. Dr. Hüseyin AKILLI for his contributions starting from the undergraduate to the end of PhD studies.

I would like to thank my committee members, Prof. Dr. Hüsamettin BULUT and Assoc. Prof. Dr. Vedat ORUÇ for their valuable discussions and helpful suggestions about my thesis, despite their busy schedules.

In addition, I would like to thank my colleagues Ozan AKGÖZ, Osman AKTAŞ and Muhammed Ali GÜMÜŞ for providing me with a good environment and facilities to complete this thesis.

Last but not least, I would like to thank my mother Sevgi TONTU, my father Ergün TONTU, my sister Pınar KARAKURT and my younger sister Gamze HAZIR, for their patience and trust.

Finally, my special thanks go to my wife Ahsen Sultan TONTU for her patience and endless support.

**CONTENTS** **PAGE**

**LIST OF TABLES** **PAGE**

**LIST OF FIGURES** **PAGE**

**NOMENCLATURE**

| | |
|---|---|
| CV | : Control volume |
| $\dot{C}$ | : Cost rate ($/h) |
| c | : Unit cost rate ($/kJ) |
| D | : Distilled water |
| dc | : Steam ejector discharge condition |
| e | : Evaporator |
| ej | : Ejector |
| ev | : Entrained vapor |
| E | : Energy (kJ) |
| ex | : Specific exergy (kJ/kg) |
| $ex^{ch}$ | : Chemical exergy per unit mass (kJ/kg) |
| $ex_{in}$ | : Exergy at inlet (kJ/kg) |
| $ex_{out}$ | : Exergy at outlet (kJ/kg) |
| $ex^{ph}$ | : Physical exergy per unit mass (kJ/kg) |
| fg | : Flue gas |
| h | : Enthalpy (kJ/kg) |
| $h_0$ | : Enthalpy at dead state (kJ/kg) |
| $h_{in}$ | : Enthalpy at inlet (kJ/kg) |
| $h_{out}$ | : Enthalpy at outlet (kJ/kg) |
| HP | : High pressure |
| I | : Irreversibility (kW) |
| ICE | : Internal combustion engine |
| IP | : Intermediate pressure |
| L | : Specific latent heat (kJ/kg) |
| LP | : Low pressure |
| m | : Mass flow rate (kg/s) |
| M | : Molar mass |

$m_f$ : Fuel mass flow rate (kg/s)

$m_{in}$ : Inlet mass flow rate (kg/s)

$m_{out}$ : Outlet mass flow rate (kg/s)

$m_{fg}$ : Flue gas flow rate (kg/s)

MED-TVC : Multi effect distillation-thermal vapor compression

MRA : Minimum required amount of air (kg/s)

n : Molar ratio

P : Pressure (bar)

$P_0$ : Ambient pressure (bar)

Q : Heat (kW)

$Q_f$ : Heat due to fuel (kW)

$Q_{in}$ : Input heat (kW)

$Q_l$ : Heat loss (kW)

$q_{out}$ : Output heat per unit mass (kJ/kg)

$Q_{out}$ : Output heat (kW)

RAA : Required amount of air (kg/s)

s : Entropy (kJ/kgK)

spp : Steam Power Plant

$s_0$ : Entropy at dead state (kJ/kgK)

$S_{gen}$ : Entropy generation (kW/K)

SOFC : Solide oxide fuel cell

T : Temperature (°C)

$T_0$ : Ambient temperature (°C)

$T_{fg}$ : Flue gas temperature (°C)

$T_k$ : Surrounding temperature (°C)

$V_{in}$ : Inlet velocity ($m^2/s$)

$V_{out}$ : Outlet velocity ($m^2/s$)

$W_{net}$ : Work (kW)

w : Work per unit mass (kJ/kg)

$W_p$ : Input work to pump (kW)

$W_t$ : Output work from turbine (kW)

$W_{rev}$ : Reversible work (kW)

X : Exergy (kW)

$X_D$ : Exergy destruction (kW)

$X_f$ : Fuel exergy (kW)

$X_{in}$ : Inlet exergy (kW)

$X_l$ : Exergy loss (kW)

$X_{out}$ : Outlet exergy (kW)

$\eta_I$ : Energy efficiency (%)

$\eta_{II}$ : Exergy efficiency (%)

$\lambda$ : Excess air coefficient

*y* : Exergy destruction ratio (%)

Z : Component procurement cost ($/h)

# 1. INTRODUCTION

For the economic growth and social development, energy is indispensable input. Urbanization, industrial developments, economic progress and increasing the world's population growth raise energy demand and consumptions worldwide. Global energy demand has grown rapidly almost every year and the total energy consumption is predicted to go up by 40% approximately between 2015 and 2030 (Al-Sulaıman et al., 2012). On the other hand, global concerns are the reduction of coal and natural gas consumptions and the depletion of greenhouse exhaust emissions. Therefore, during any process releasing heat to the environment must be recovered back for using preconditioning the same process or using for other purposes in order to raise the ratio of energy generation per unit of fuel. Using waste heat at low temperature provide improving more efficient and effective systems. Global warming and reduction of fossil fuel consumptions are major concerns in re-using waste heat and trying to increase the utility of renewable energy sources worldwide. In this regards, significant efforts must be put on developing more efficient energy systems. Presently, conventional thermal power plants based on single energy generation have efficiency, in general, less than 40%. This means that 60 % of a plant's energy is not converted into useful power. That is to say, most of the various processes input energy is usually wasted in different forms (Ahmadi et al., 2012a). Issues of climate change and fossil fuel depletion force researches to invent significantly efficient multigeneration energy systems (Khanmohammadi et al., 2015). Nowadays, multigeneration systems have designed as a permanent solution to these problems. Recently, multigeneration is considered as one of the achieving a more efficient method to use fuel, to fulfill part of energy demand. The integration of multigeneration systems with traditional plant could increase the entire plant efficiency by up to 80%. In general, multigeneration system consists of a conventional system, electrolyzer, desalination plant, absorption chiller and water heater. These are integrated systems that combine key

power cycles to improve processes with high efficiency, such that, ultimately the power production platform can convert waste energy sources and generate additional power to improve net outputs. Multigeneration systems enhance profitability due to an increase in the number of re-generated outputs (Dincer and Zamfirescu, 2014). An abstract representation of multigeneration is shown in Figure 1.1. Electricity, heating, cooling, hydrogen production and desalination and many more processes can simultaneously be produced in the case of multigenerations systems (Suleman et al., 2014).


Figure 1.1. Abstract representation of multigeneration system

### 1.1. Steam Power Plants

The abundance of coal is very high compared to other fossil fuel sources utilized for producing electrical power worldwide (Hasti et al., 2013), and it is the second main energy source which corresponds to 30% of worldwide energy consumption. It plays a vitally important role in electricity production around the world. For instance, steam power plants now account for 41% of global electricity,

and coal fuels in some countries account for a higher percentage of electricity generation. Despite the significance of coal in recent years, there are two crucial global issues: Environmental pollution and the depletion of fossil fuels. The main global energy source is fossil fuels, and the decrease in their reserves creates problems in terms of energy shortages in the future. Another issue is that using fossil fuels contributes to global warming and environmental pollution. In order to solve these two problems, researchers are focused on two following solution proposals: (a) Inventing new energy sources (particularly renewable energy sources) and (b) Increasing energy efficiency (Hepbasli et al., 2009).

According to their temperature and pressure differences, the thermal power plant technology is classified as subcritical, supercritical, ultra-supercritical and advanced ultra-supercritical (WER, 2016). Around 75% of the steam power plants in the world use a subcritical boiler. The thermal efficiency of subcritical technologies is approximately 30%, and these technologies are the most widespread power plant types in the world because they can be installed in a shorter time at a lower cost than the others. Supercritical plants constitute 22% of thermal power plants globally, and their thermal efficiency is about 40%. Because the plant operates at high steam pressures and temperatures, the materials used in these applications require large amounts of alloying and other necessary welding techniques. For this reason, supercritical technologies have the highest capital costs. Furthermore, the $CO_2$ emission of a supercritical plant is approximately 20% lower in comparison to a subcritical plant. Similar to supercritical thermal power technology, ultra-supercritical technology also operates at elevated temperatures and higher pressures to increase the efficiency to a value of 45%. Today, approximately 3% of global steam power plants use this technology. This power technology also reduces $CO_2$ emissions at a rate of one third compared to subcritical power plants with the same amount of energy output. In addition, ultra-supercritical power plants utilize fairly high quality, low ash coal. The capital expenses for ultra-supercritical power plants are approximately 40 to 50% higher

than subcritical plants. Currently, ultra-supercritical plants can work at 620°C, with mainline steam pressures between 25 MPa and 29 MPa. Apart from these technologies, there is advanced ultra-supercritical technology, which is a further modification of ultra-supercritical technology. In advanced ultra-supercritical technology, using steel that contains high levels of nickel is required to give it a higher melting temperature because these thermal power plants operate at even higher temperatures and pressures. This makes them more expensive to install than ultra-supercritical plants. Emissions for the advanced ultra-supercritical plant are expected to be 20% lower than supercritical plants, and the efficiency of these advanced ultra-supercritical plants can be almost 50% (WER, 2016). Figure 1.2 presents the historical process of developing steam conditions and the material transition point. In this figure, the numbers on the stages of historical development of the thermal power plants indicate the nominal pressure the minimum temperature and the maximum temperature respectively.

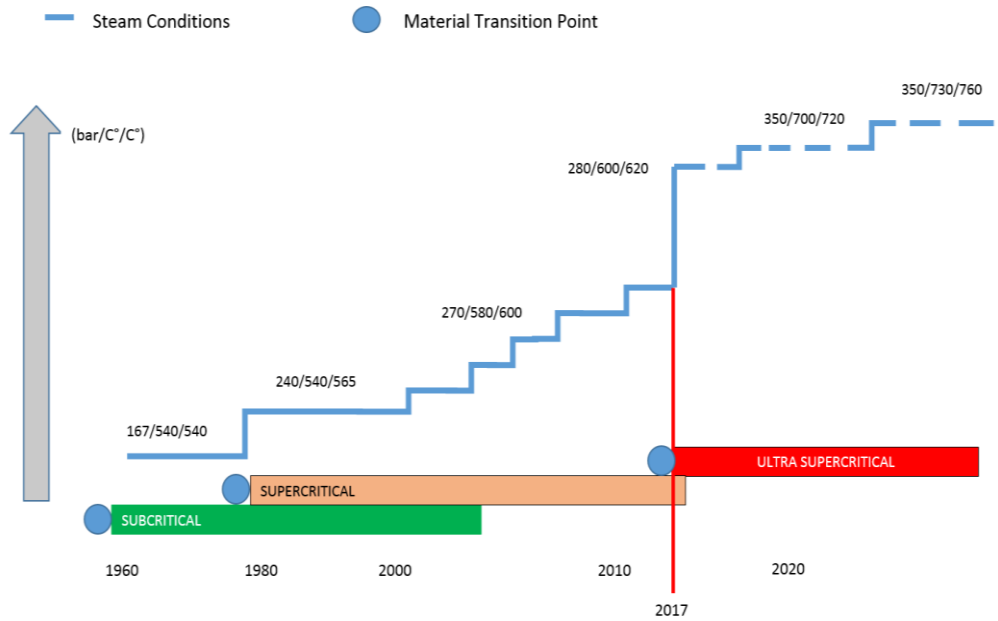


Figure 1.2. The historical process of developing steam conditions and material transition point (Sahin and Aydın, 2012)

### 1.2. Organic Rankine Cycle

In parallel with industrial developments, a tremendous amount of waste heat is released into the environment. These wastes include exhaust gases from the fossil fuel powering thermal power plants, furnaces used in vast variety of domestic and industrial applications and internal combustion engines that deliver huge amount of heat to the atmosphere as a waste heat and environmental pollutions to upgrade the worsening of global warming (Dai et al., 2009; Li et al., 2018a). Furthermore, waste heat emerges as a result of unused heat in combustion processes, chemical reactions and thermal processes. Discharged exhaust gases contain not only high exergy values but also high amounts of contaminants such as carbon dioxide ($CO_2$), nitrogen oxides ($NO_x$) and sulfur oxides ($SO_x$), which are responsible for greenhouse gases and a high rate of global warming. Because of these catastrophic problems, those countries with advanced industries have evaluated the potential of waste heat recovery to reduce harmful gas emissions, as well as reducing the use of fossil fuels (Tchanche et al., 2011).

Low-grade waste energy usage has become substantially important due to the inadequacy and future exhaustion of fossil fuels, as well as increasing global warming. When combined with low-temperature renewable energy and dissimilar thermodynamic cycles, problems of the energy storage system can be efficiently reduced. In recent years, the waste heat recovery techniques have attracted attention of engineers significantly for improving the efficiency of energy systems to minimize the waste heat. Different approaches have been adopted for waste heat recovery systems, including thermoelectric, absorption cooling and the Rankine Cycle. Regarding thermodynamic cycles, numerous approaches have been suggested including the ORC, the Kalina cycle, the supercritical $CO_2$ cycle, the triangle cycle and heat-pump system to obtain electrical power from low-grade waste heat sources. The ORC is a more practical methodology, and it has been used in many areas of industry. The ORC is considered to be a highly efficient technique

compared to other methods in recovering waste heat (Seyedkavoosi et al., 2017; Long et al., 2014).

The working principle of the ORC system resembles with that of conventional steam cycles and energy conversion systems. However, it uses an organic fluid such as refrigerants and hydrocarbons-whereas conventional systems use water (Tchanche et al., 2011; Wang et al., 2011b). The usage of an ORC is a good solution for recovering waste energy between low temperature and medium temperature (Carcasci and Winchler, 2016). At the same time, the ORC system is highly flexible, very safe and requires low-maintenance procedures. The ORC system can be integrated with energy systems such as steam power plants to reduce the steam power plant losses and increase its efficiency so that high-grade energy from the steam power plant can be obtained in terms recovering waste heat which is defined as low-grade energy. The use of ORC systems decreases the emission of pollutants including $CO_2$ and $SO_2$. In addition, the heat that is recovered by the ORC system can be used in driving chillers or any other purposes (Wei et al., 2007).

It has been presented that the ORC system is regarded as an efficacious approach in the case of recovering waste heat with temperatures ranging from low to medium temperatures to generate power (Safarian and Aramoun, 2015). The ORC processes yield relatively high efficiencies for applications on a smaller scale and/or low-temperature heat sources. In addition to other positive aspects, the ORC systems can be successfully utilized at low temperatures in numerous industrial applications including biomass burning, solar, desalination systems and geothermal systems. Also, it has been reported that the ORC systems are reliable, secure and flexible. When a comparison is made between the steam power plant and the ORC systems, the past works report that the ORC has advantages of physical properties of working fluids which have a lower boiling point, a higher vapor pressure, a higher molecular mass and a higher mass flow. All these properties have better advantages in terms of turbine efficiency compared to water vapor properties (Dai

et al., 2009; Eyidogan et al., 2016). In the ORC systems, regeneration by integration of the regenerator or feed fluid heaters, or by the process occurring at the critical point in transcritical or supercritical cycles, yield higher efficiencies. Many studies on this subject have revealed that this technology has shown much promise over the last few years (Tchanche et al., 2014).

Studies on the exploitation of low-quality energy sources for power production have recently increased (Galloni et al., 2015). The majority of industrial processes and power plants work at exhaust temperatures below 300ºC. It is not economically feasible to use traditional methods to recover waste energy from such exhausts (Chen et al., 2010). Therefore, the ORC is a good alternative at low to medium temperatures to regain waste heat energy and use for electricity generation (Vélez et al., 2012). The ORC has garnered interest in studies on waste heat recoveries at low temperatures (Sun et al., 2017). But, the Rankine cycle is not a preferable option except for recovering waste heat (Kaşka, 2014). Regarding energy sources having a low-temperature characteristic, the ORC has a better efficiency compared to that of conventional power generators. But, when it comes to high-temperature heat sources, conventional power generators are more efficient than the ORC systems. Therefore, it is vitally important to conduct further studies on the advantages of the ORC (Sun et al., 2017).

### 1.3. Vapor Compression Refrigeration

The cooling process is an interesting area where various disciplines come together, with a multidisciplinary character where science and engineering meet to solve the refrigeration and cooling needs of humanity in a wide range of applications from the cooling of electronic devices to cooling of many other industrial systems.

Over the past two decades, the refrigeration industry has expanded considerably to play an important role in societies and economies. Therefore, the economic effect of cooling technology on the world has become more influential

and will continue to be even more effective in the future, due to the growing demand for cooling systems and applications. Of course, this technology helps to develop living standards in countless ways (Dincer and Kanoglu, 2010).

One of the world's heaviest needs is energy demand for air-conditioning and refrigeration appliances (Aphornratana and Sriveerakul, 2010). In order to improve the performance energy systems and hence decrease waste heat, researchers and engineers should discover new technological methods for recovering industrial waste heat. Currently, high-temperature heat pumps and power cycles are two common methods of recycling industrial waste heat (Deng et al., 2017; Lu et al., 2015Even though cooling technologies which are thermally activated often used as absorption coolers for large-scale industrial applications. It is worth mentioning that the COP is commonly low for a single stage absorption cycle (Wang et al., 2011a). An absorption cooling system and an ejector cooling process can start functioning by a heat source having a temperature interval between 100 °C and 200 °C. They have various advantages such as simple structure, reliability, lower initial capital cost, low level of maintenance, long lifetime, and lower operating cost (Saleh, 2016). On the other hand, both absorption and jet cooling systems are not convenient for available thermal energy lower than 60 $^{o}$C and also are not convenient for operation in high temperature environments (Aphornratana and Sriveerakul, 2010).

The Rankine cycle can be associated with an immersion cooling cycle, or it can be changed to have the ability of cooling. In this combined power and cooling process, low-grade heat sources varying from 60 $^{o}$C to 150 $^{o}$C can be used to generate cooling and power. Also, the cycle can be used for mid-grade heat source temperatures ranging from 200 $^{o}$C to 350 $^{o}$C to generate power only. Power is produced by the expansion of a high-pressure vapor through an expander and cooling comes from the sensible heating of the expander exhaust. In general, about two-thirds of the energy input in thermal power plants is transferred as a waste heat to the environment during mechanical energy conversions. For residential and

industrial purposes, waste heat from the main thermal power plant can be recovered using refrigerating or heat pump cycles as the bottoming cycles. If this waste energy is used to generate power or cooling, it increases the entire conversion efficiency of the waste heat source and provides additional economic benefits. This application improves the entire efficiency of the power plant (Demirkaya et al., 2013).

### 1.4. Desalination System

Most of the thermal power plants have been built by the seaside in order to meet the demand with more economic seawater required by the steam power plants. It should be noted that in these plants, energy efficiency is significantly dependent on seawater temperature, and the amount of water used in the condenser unit is enormous. Since clean water productions have become increasingly important in many countries, the Multi-Effect Desalination (MED) method has become an alternative solution parallel to other methods for clean water production as well as generating electricity by integrating Multi-Effect Desalination (MED) units into steam-powered plants. Efficiency, the rate of water production or the capacity of double-purpose (electricity and water) plants depends on the seawater temperature. With an increase of seawater temperature in clean water production, the MED desalination unit for a certain rate of clean water production requires a greater rate of heat transfer and more surface area, in other words, a larger heat exchanger (Askari et al., 2018).

Depending on the world population growth, an increase in clean water demand combined with occasional droughts around the planet, necessitate the discovery of new and alternative clean water resources (Khalid et al., 2018). Desalination has become one of the world's most important, traditional water processes in recent years and is especially important in areas where water is less available (Zarzo and Prats, 2018). Desalination is one of the distillation methods where a large number of components of various sizes are used consumes a large

amount of energy. Energy losses in these units are a major issue in terms of a design and the operation of plants. Separating salts from salty water is a costly process because it consumes much more energy compared to other freshwater supply and treatment options (Li et al., 2018b). In order to be economically viable in comparison to the other clean water procurement methods, this method needs to bring down the energy demand for water treatment processes such as removing salts from the seawater.

There are two main groups of operations within different desalination technologies: evaporation and membranes. Evaporation processes can be managed by a heat source, such as Multi-Stage Flash (MSF) and Multi-Effect Distillation (MED), or by an electrical power supply with mechanical compression (Vapor Compression or VC). With the exception of a few emerging technologies (for example, membrane evaporation or evaporation), the related membrane technologies are managed in a variety of ways by supplying electric energy. For example, direct current is passed between the electrodes to decompose ions by membrane pressurization – Reverse Osmosis (RO) and Nanofiltration (NF) – or by ionic membranes – Electrodialysis Reversal (EDR). Other processes that can be used to remove salts from seawater, such as ion exchange, decanting or freezing, are not used for large scale desalination. Desalination types are shown in Figure 1.3 (Zarzo and Prats, 2018). One of the earliest desalination processes was the multi-effect evaporation (MEE) process, which technologically had fundamental problems in the past such as fouling problems as well as low production capacity. The technological developments taking place in the past years related to the MEE system have improved the MEE process. For example, in the new technology, the seawater falls onto the heat exchanger surface in thin film layer form producing steam more efficiently with a higher capacity. Today, the MEE process has various different systems and methods (Al-Mutaz and Wazeer, 2014). It is worth stating that energy requirements vary from application to application and from process to process. There is no doubt that the seawater reverse osmosis process technology

consumes significantly less specific energy than MSF and MED technologies. For this reason, the efficiency and energy requirement of MED and MSF processes for thermal desalination is mainly related to the temperature values of the heat source and heat sink, and to the thermodynamic paths (Fitzsimons et al., 2015; Brogioli et al., 2018).

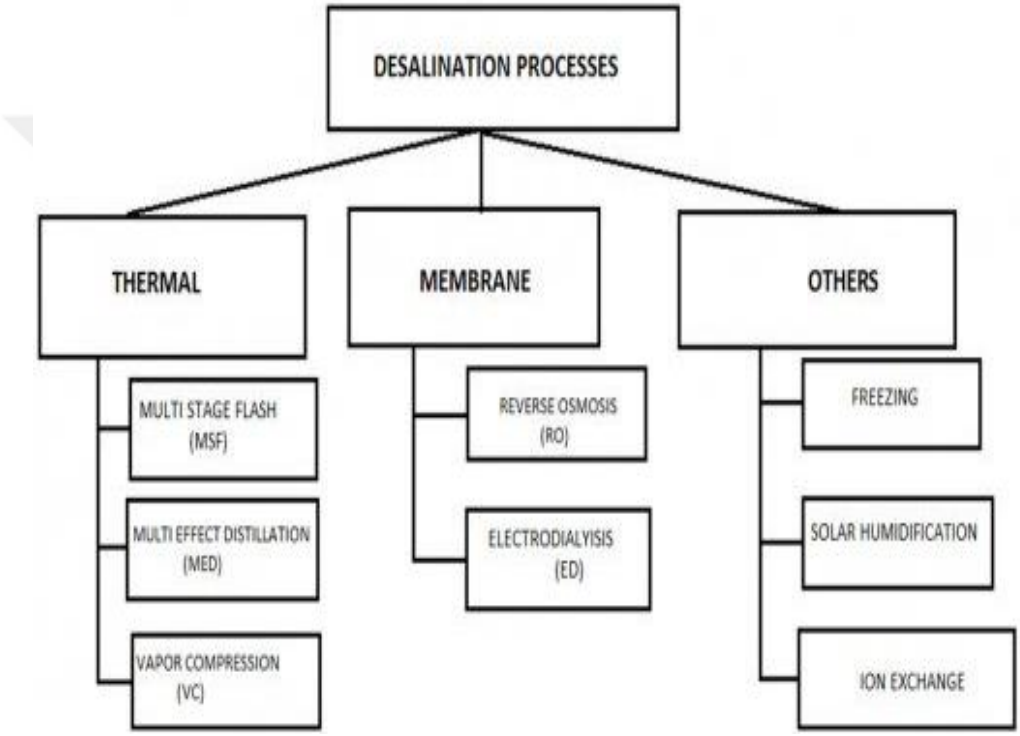


Figure 1.3. Desalination types (Zarzo and Prats, 2018)

### 1.5. Greenhouse Heating

Greenhouse farming industry has been expanding all over the world because the need for agricultural products increases as the population of the world increases. Therefore, greenhouse cultivation is one of the most convenient ways to meet increasing food demand year around. All plant growing parameters can be regularly checked and maintained at an optimum level in greenhouses. The

greenhouse is a very high-priced way to produce crops and there are many variables that should be taken into consideration before the farmer decides to take this route.

The consumption of energy in agriculture has risen significantly with the meet of highly-productive varieties and mechanized-crop production practices. The use of fossil fuel to warm up a greenhouse causes higher costs, so greenhouse growers are turning to alternative energy sources. Generally, the heating cost in the greenhouse constitutes 60% to 80% of the total production cost in Turkey which is very high. The necessary condition in the greenhouse for plant planning and cultivation is essential. Therefore, while keeping the operating cost to a minimum level, greenhouse production is applied by using suitable climatic conditions. For this reason, most greenhouses are kept warm conditions to avoid frost, except for internal plant production. Therefore, greenhouse production is made by using appropriate climatic conditions while minimizing operating costs. However, most greenhouses have warm conditions to prevent frost formation and have the necessary air-conditioning for optimum growth of plants.

Greenhouse farming is the fastest growing agricultural sector due to the presence of suitable climatic conditions in Turkey. However, a healthy greenhouse production needs auxiliary heating, particularly for cold winter nights. Greenhouse heating is one of the most energy-consuming events throughout winter months in Turkey. Because of the high relative energy cost, the minority of greenhouse growers can only use auxiliary heating. Therefore, the use of a low-cost waste heating system is essential for a greenhouse to ensure optimum internal conditions during the winter period. Various alternatives to the traditional greenhouse heating methods are heat pumps, waste heat and cogeneration systems. Attempts to reduce energy demand have directed plants producers and engineers to utilize different energy sources for greenhouse heating.

The greenhouse is needed to be adapted according to the variety of agricultural products to be raised in it. Because the greenhouse indoor conditions should be kept at the plant growth temperature (Esen and Yuksel, 2013).

### 1.6. Multigeneration

More than three different output systems called a multigeneration energy system were obtained from the same energy source input. These outputs can contain electricity, refrigeration, heating, warm water, hydrogen and distilled water. Multigeneration system should be considered for large apartments, hotels, power plants and other locations where a large number of beneficial outputs are needed. In the design phase of the multigeneration system, the location and requirements of the process should be considered as the main factor. As a clear example, any multigeneration system used to address the required in a place where distilled water needs are vital should give priority to this objective.

In the previous studies, there is not enough research based on investigating and evaluating multi-generation energy systems. Multigeneration systems are one of the greatest challenges and opportunities in this century for the efficient use of energy and are seen as a partial solution to global warming problems. It should be noted that multigeneration energy systems have different methods to achieve every goal. Therefore, the implementation of each subsystem is very crucial in fulfilling the requirements of the system. Figure 1.4 shows a real-word multigeneration plant to generate electricity, refrigeration, power and warm water that operates based on the Brayton cycle.

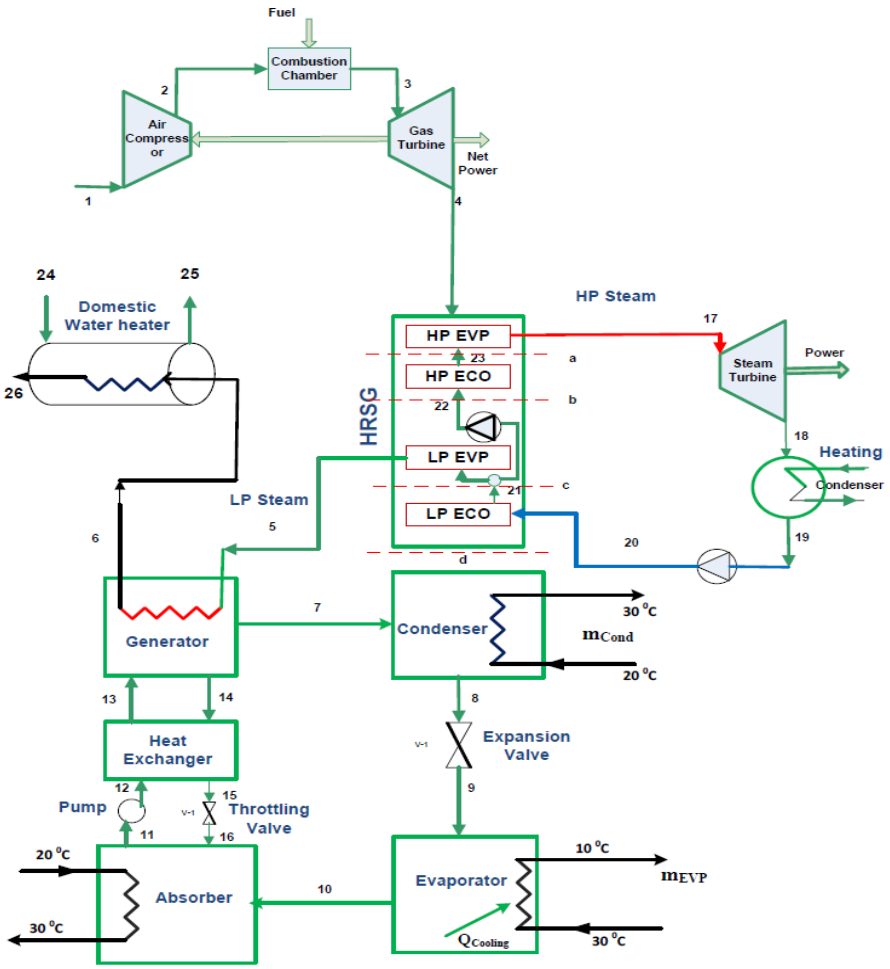


Figure 1.4. Example of the multigeneration system (Ahmadi et al., 2012a).

### 1.7. Benefits of Multigeneration

Multigeneration energy systems have many different benefits. These systems provide advantages such as higher flexibility, higher plant efficiency, better source utilization, lower energy losses, lower atmospheric gas emissions, shorter transmission lines, greater reliability and multiple products outputs (Dincer and Zamfirescu 2012). Multigeneration application develops the entire efficiency of the power plant further and decreases running costs. The entire efficiency of traditional energy systems that use fossil fuel with a single energy output is

generally less than 40%. That is, higher than 60% of the energy of the fuel input to the traditional power plant is rejected to outside. Conversely, the entire efficiency of a traditional power plant that generates electrical power and thermal waste separately is around 60% (Ahmadi et al., 2012a).

However, with the use of the waste heat from the input energy, the efficiency of multigeneration systems could increase up to 80% (Khaliq et al., 2009). In a multi-generation plant, waste heat from the power production unit is used to run cooling and heating systems without supplying additional energy. But, the conventional power plant needs additional energy supply for those auxiliary units. Thus, a multigeneration energy system consumes less energy to generate the same output as a traditional plant and has correspondingly lower running costs.

Multigeneration also reduces greenhouse gas emissions (GHG). A multigeneration power system emits fewer GHGs than a conventional power plant because it produces more output as a useful work and thus consumes less amount of fuel. Less energy losses and costs due to the need for less power transmission lines and fewer distribution units are indirect benefits of multigeneration energy systems. The production of conventional electricity is usually obtained from a centralized plant that is commonly placed away from the end user. Electric energy losses from the power plant to the end-user are around 9% due to the transmission and distribution of electricity losses (Ahmadi et al., 2012b).

These advantages and superiority have inspired engineers and scientist to improve multigeneration energy systems. A progress in inefficiency is often the most important parameter in executing a multigeneration plant. Detail evaluations before choosing a multigeneration systems, such as the assessment of investment and running costs, are required to be known to confirm efficient and economic multigeneration system structure and performance.

An integrated system in power plants is separated into two categories, such as renewable based and non-renewable based multigeneration plant. In a multigeneration plant, it is important to choose a suitable input energy to fulfill the

required demand. Hence, the selection of this component is one of the main concerns for engineering practices. Input energy is classified according to stated categories and shown in Figure 1.5.

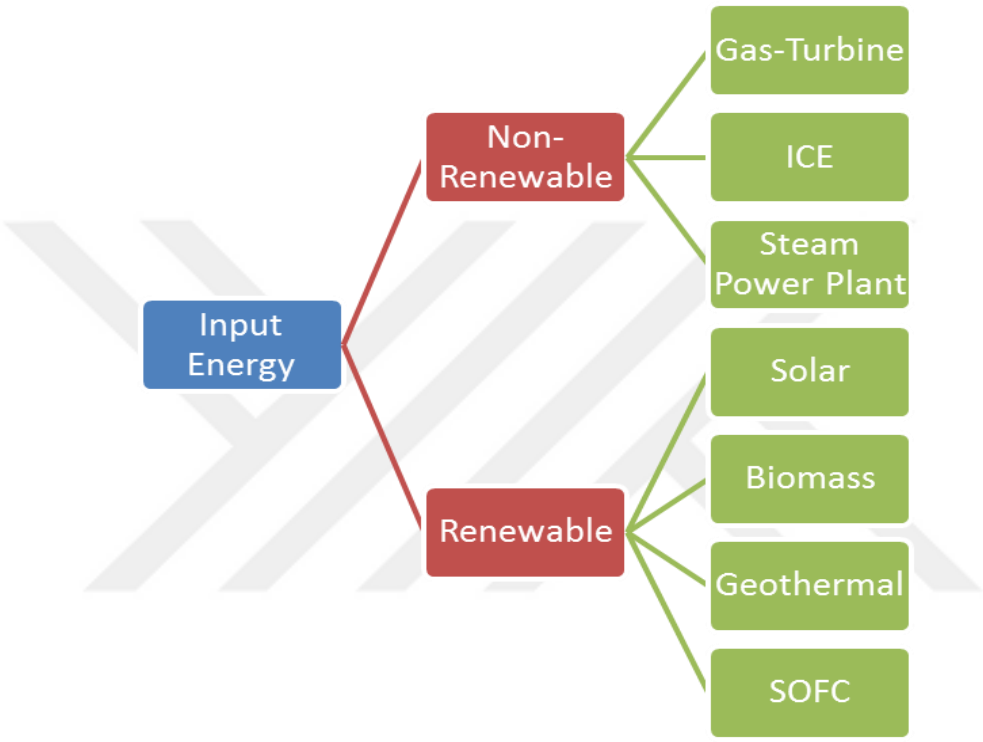


Figure 1.5. Classification of input energy that used in the multigeneration system

**1.8. Objectives of Study**

A multigeneration energy system has the capability to generate more than three different outputs, such as electrical power, distilled water, heating and cooling, warm water, and plant heat requirement with the same source of the prime mover. Such systems have many improvements, such as flexible plant operation, minimized thermal and energetic losses, decreased material waste, reduced running and maintenance costs, reduced GHG influences, improved resource allocation, enhancement reliability and also fewer electrical grid failure per energy output as

well as providing multiple generation procedures. Multigeneration systems for combined production of useful commodities are rapidly distributed around the world since they offer several advantages, such as lower working cost, higher plant efficiency, decreased the environmental effect.

In this study, both thermo-economic modeling and environmental studies will be undertaken for a novel integrated multigeneration system, including an ORC to produce additional electricity, vapor compression cycle for cooling, a heat exchanger for greenhouse heating and a thermal vapor compression desalination unit to produce distilled water. The method of analysis of the multigeneration system is shown in Figure 1.6.

In the present work, our main objective is to examine the effect of supplementary integrated systems on the performance of a conventional steam power plant and define performance and destruction of each component of subsystems.

The exergoeconomic analysis is conducted to indicate the thermodynamic losses in each system. Also to understand system performance more comprehensively, a parametric study is carried out to investigate the influence of various significant design factors on the energy and exergy efficiencies of the system.

Environmental impact analysis is decided to be performed for calculation of $CO_2$ emissions of the system and to obtain the effect of emissions on the multigeneration system.

This study aims to increase overall plant efficiency and reduce harmful gas emissions by integrating additional systems to existing steam power plants operating under subcritical conditions.

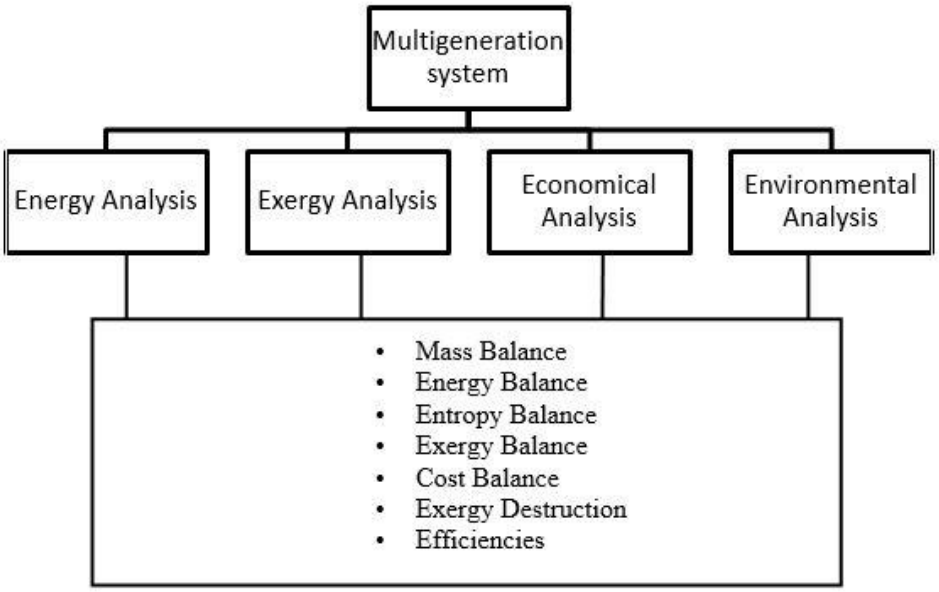


Figure 1.6. Method of analysis of the multigeneration system

## 2. LITERATURE SURVEY

In the literature, there have been various studies associated with CHP and trigeneration energy systems, through a comprehensive study of a multigeneration energy system has not yet appeared in the literature. However, the related papers, their aims, a method of analysis and brief conclusions are presented in this section.

Al-Sulaiman et al. (2012) applied energy and exergy analyses of trigeneration system based on the biomass energy system which consist of biomass burner, ORC and the absorption refrigeration system. The best performance of the trigeneration system is found at the minimum organic Rankine cycle evaporator pinch temperature considered, Tpp = 20 K. Furthermore, the highest exergy efficiency of the ORC is computed as a 13% and, when trigeneration is applied, this efficiency reaches to value of 28%. Moreover, this study shows that the electricity consumption to the cooling load can be controlled by variations of the ORC evaporator pinch point temperature and/or the pump upstream temperatures. Ahmadi et al. (2012a) conducted exergo-environmental analysis of an integrated ORC for trigeneration applications. This trigeneration system composed of a Brayton cycle, ORC, single-effect absorption refrigeration and an internal water heater. Energy and exergy analyses, environmental effect evaluations and parametric works are conducted, and parameters that measure environmental effect and sustainability are investigated. The results also reveal that carbon dioxide,

$Co_2$ emissions for the trigeneration system are lower than for a single energy generation system. The exergy analysis demonstrates that the combustion chamber has the largest irreversibility of the plant equipment, due to chemical reactions and the finite temperature differences between the working fluid and flame temperatures. The parametric assessments illustrate that the compressor pressure proportion, the gas turbine entry temperature and the gas turbine

isentropic efficiency considerably impact the exergetic efficiency and environmental effect of the trigeneration system.

Ozturk and Dincer (2013) carried out performance evaluations of a multigeneration system based on a solar-aided coal gasification system. The coal gasification system is combined with a solar power to utilize the concentrating solar power generation. This multi-generation system consists of the six integrated systems, energetic and exergetic efficiencies of the integrated systems vary between 19.43% and 46.05% and 14.41% and 46.14%, respectively, and the multigeneration system has the highest energy and exergy efficiencies which are found to be 54.04% and 57.72%, respectively. Besides, parametric works presenting the thermal performance of the multigeneration system components are performed by changing some main variables used for design parameters, namely environment temperature, compressor pressure ratio, and nitrogen supply ratio for the combustion chamber and gas turbine entry temperature. Al-Ali and Dincer (2014) reported new integrated energy systems for multigeneration based on combine geothermal-solar system to generate electricity, refrigeration, indoor heating, warm water and heat generation for industrial usage. System is assessed in terms of energy and exergy point of view in order to report the efficiency of the overall cycle and compare the outcomes of a single generation with cogeneration, trigeneration and multigeneration systems. Parametric works are performed to examine the influences of working conditions and environmental variables on the plant performance. The energy efficiencies for power generation and multigeneration plant are determined to be 16.4% and 78%, respectively, which corresponds to the exergy efficiencies of 26.2% and 36.6%. The results reveal that 75% of the irreversibilities occur in the solar collector system. Suleman et al. (2014) designed a novel integrated system based on solar and geothermal energy system for multigeneration implementations, which consist of two ORC for electricity production, an absorption system cycle for refrigeration and a drying system. In order to define the exergy destructions, almost all the plant elements are

investigated from energy and exergy point of view. The general energy and exergy efficiencies of the plant are calculated to be 54.7% and 76.4%, respectively. Furthermore, to assess the system clearly, parametric studies are also carried out to observe the influence of dissimilar variables such as both ORC turbine inlet pressure and temperature and reference environmental temperature to examine the changing in the system performance in terms of the energetic and exergetic efficiencies. Ahmadi et al. (2014) conducted exergoeconomic studies and multiobjective optimization for biomass-based multigeneration energy systems. In this study, biomass is used as the prime mover and system consisting of an organic Rankine cycle, absorption refrigeration for cooling, a heat exchanger, PEM electrolyzer to generate hydrogen, an internal water heater to obtain warm water and a reverse osmosis (RO) desalination plant to supply distilled water demanded by the system. This study involves performance analysis in terms of energy and exergy as well as environment impact assessment. Also, multi-objective optimization performed to define the optimum operating parameters for the integrated energy system. Khanmohammadi et al. (2015) investigated the exergoeconomic performance of a combined gas turbine and ORC united with a biomass gasifier. The temperature of gasification of biomass, combustion temperature, gas turbine upstream temperature, both gas turbine and compressor isentropic efficiencies, compressor pressure proportion and highest ORC working pressure are elected as a major decision parameter of multigeneration systems. The total cost rate and exergy efficiency of the system is selected as the key objectives. A process of data obtaining called artificial neural network and multi-objective optimization is used for modeling the influences of the seven decision parameter on both specified expressions. The outcome of multi-objective optimization illustrates that the exergy efficiency of the multigeneration plant is 15.6%, which can be increased to a value of 17.9% in the optimal state.

Khalid et al. (2015) conducted energetic and exergetic analyses of biomass and solar combined system for multigeneration of useful outputs, in which two

renewable energy sources are integrated to produce multiple commodities. Energetic and exergetic studies are used to evaluate the efficiencies of the cycle and the influences of different system variables on energy and exergy efficiencies of the general system and integrated systems were investigated. The general energy and exergy efficiencies of the system are calculated as 66.5% and 39.7% respectively. Moreover, the influence of reference-environmental temperature on energy and exergy efficiencies is also examined for the plant.

Malik et al. (2015) examined a renewable energy-based multigeneration plant. In their study biomass and geothermal energy are used as an input energy for electric power generation, heating and cooling, domestic purposes producing hot water and hot air to dry products using ORC cycle, absorption chiller, heat exchanger and drying unit respectively. Also, energy and exergy analyses conducted to determine the performance of the plant. Energy efficiency of the overall plant is calculated to be 56.5% and exergy efficiency is found to be 20.3%. The highest irreversibility takes place in both units combustion chamber and boiler. Ozlu and Dincer (2015) analyzed a solar-wind hybrid multigeneration system. The systems produce heating and chilling, electrical power, hydrogen simultaneously. In this application, energetic, exergetic, exergoeconomic and exergo-environmental studies are performed. The impact of different input parameter on the plant performance are examined throughout both energy and exergy efficiencies, and an optimization work is undertaken of system efficiency and power generation are obtained. Energy and exergy efficiencies are bigger than an equivalent single generation. The system has 43% highest energetic efficiency and 65% highest exergetic efficiency. Yuksel et al. (2016) analyzed thermodynamically a new solar energy based multigeneration system for generating electrical power, hydrogen, warm water, heating and chilling. Energy and exergy analyses are carried out for the overall system and its integrated systems, which are a parabolic trough collector system, a double-stage ORC, a proton exchange membrane electrolyzer, a PEM fuel cycle and a quadruple effect absorption cooling system. The parametric

jobs are conducted in order to observe the effect of some main parameters on the integrated system performance. According to the analysis, a rise in environmental temperature enhances the exergy performance of the Quadruple Effect Absorption Cooling System. In addition, an increase in solar intensity, temperature of absorber pipes inner surface and concentration of ammonia in working fluid mixture has a positive effect on the production of electricity from expanders and turbines, and hydrogen from the PEM electrolyzer.

Bicer and Dincer (2016) examined novel renewable energy based multigeneration system, which integrates a solar PV/ T system and a geothermal plant to generate electrical power and heat for power, heating, refrigeration, warm water and drying air. They conducted investigations on the design parameters, analyses and evaluation of this integrated system. The psychometric processes are made use for obtaining required dry agent from the environmental air, and an air circulation system is used to benefit from heat transferred from the PV modules to the air, which ultimately raises the PV/T efficiency- and hence the general efficiency. Through energy and exergy analyses, for a chosen common case general energy and exergy efficiencies are determined to be 11% and 28%, respectively. Literature survey studies are summarized in Table 2.1.

Table 2.1. Literature survey studies

| Author | Input Energy | Integrated Systems |
|---|---|---|
| **Al-Sulaiman et al. (2012)** | Biomass | ORC |
| | | Absorption Chiller |
| **Ahmadi et al. (2012a)** | Gas Turbine Cycle | ORC |
| | | Absorption Chiller |
| | | Hot Water |
| **Ozturk and Dıncer (2013)** | Solar | PEM |
| | | Coal Gasifier |
| | | Rankine Cycle |
| | | Gas turbine Cycle |
| | | Absorption Chiller |
| **Al-Ali and Dıncer (2013)** | Solar & Geothermal | ORC |
| | | Absorption Chiller |
| | | Hot water |
| | | Rankine Cycle |
| **Suleman et al. (2014)** | Solar & Geothermal | ORC |
| | | Absorption Chiller |
| | | Drying |
| **Ahmadi et al. (2014)** | Biomass | ORC |
| | | Absorption Chiller |
| | | PEM |
| | | RO |
| | | Hot water |
| **Khanmohammadi et al.(2015)** | Biomass | ORC |
| | | Gas turbine Cycle |
| | | Hot water |
| **Khalid et al. (2015)** | Biomass & Solar | Gas turbine Cycle |
| | | Rankine Cycle |
| | | Absorption Chiller |
| | | Hot Air |
| **Malik et al. (2015)** | Biomass & Geothermal | ORC |
| | | Absorption Chiller |
| | | Rankine Cycle |
| | | Drying |
| | | Liquefaction |

| | | |
|---|---|---|
| **Ozlu and Dıncer (2015)** | Solar & Wind | Rankine Cycle |
| | | Absorption Chiller |
| | | Hot water |
| | | PEM |
| **Yüksel et al. (2016)** | Solar | Absorption Chiller |
| | | PEM |
| | | PEM Fuel Cell |
| | | Rankine Cycle |
| | | TES |
| **Bicer and Dıncer (2016)** | Solar & Geothermal | TES |
| | | ORC |
| | | Drying |
| | | Absorption Chiller |
| | | Vapor Compression Refrigeration |

## 3. MATERIAL AND METHOD

Supplementary systems are integrated with the conventional steam power plant. These are organic Rankine cycle, vapor compression refrigeration, greenhouse heating and desalination plant. They are combined with the conventional Rankine cycle to produce different products and achieve better efficiency. As it is known that steam power plant has waste energy which should be decreased or regained to enhance the plant overall efficiency. For this purpose, one of the present objectives was to use the organic Rankine cycle to recover waste heat energy from the combustion chamber of the boiler. The second objective was to install the desalination system which was adequate to produce demineralized water to decrease the cost of distilled water and make this distilled water available continuously. In general, a continuous supply of the distilled water is essential for the water-steam cycle and it is necessary as make-up water to top-up the working fluid. Presently considered power plant is located in Adana where air-conditioning of indoors is vitally important for about 6 months in summertime due to very high humidity and the temperature of the atmosphere. Therefore, as a third objective of the present work was to integrate the vapor compression refrigeration system by removing the expansion valve where the motive steam pipeline of desalination systems is placed. Also, the heat exchanger is designed to recover waste heat energy from the steam condenser of seawater line. Lastly, as a fourth objective of the present work the heating system of a greenhouse was also integrated to the process of the conventional power plant for the purpose of supplying heat to keep the interior temperature of the greenhouse at the desired level for growing plants in the winter season.

### 3.1. Steam Power Plant

#### 3.1.1. System Description

Apart from those objectives reported above, three steam power plants operating under different conditions were investigated in terms of both energy and exergy. A steam power plant basically consists of a boiler, a pump, a condenser and a boiler feed pump. The efficiency of the basic equipment strongly affects the overall efficiency. The operating conditions of the steam power plants are given in Table 3.1. The subcritical steam power plant is installed in the southern part of Turkey. The subcritical steam power plant is actively operating for 15 years and there is no drop in efficiency due to a regular maintenance. Coal is used as the main fuel, and it is imported from Colombia or South Africa to obtain the utmost energy input. The subcritical boiler is called a one-pass tower type plant. The supercritical steam power plant is situated in the eastern Mediterranean region of Turkey. The supercritical steam power plant has been operating for 5 years and it was built by a Chinese company. And the power plant has been working with the same efficiency since it was founded. It uses imported coal like a subcritical power plant. The supercritical boiler is a double-pass system to absorb heat efficiently; in addition, no evaporation occurs at the evaporator tube to cover the latent heat of steam. An ultra-supercritical steam power plant is new technology, and it is operated at higher temperatures and pressures associated with a supercritical steam power plant. This ultra-supercritical power plant is located in the north-west of Turkey. The ultra-supercritical power plant steam power plant is newly established and has just emerged from the commissioning period. Currently, the power plant is operating under normal operating conditions. Cooling water is provided by the Sea of Marmara.

A subcritical power plant is operated at below critical point pressure such that water boils first and then is converted to superheated steam. At supercritical power plant, feed water is heated to produce superheated steam without boiling

above critical point. The steam power plant is called as an ultra-supercritical in case of the main steam parameters exceed 280 bar and 600 °C.

It is worth mentioning that measured data for three steam power plants operating under ultra-supercritical, supercritical and subcritical conditions were obtained from the plant managers. The data obtained are monitored using the measuring instruments calibrated by the internationally accredited company regularly. Also, each parameter was measured by 3 independent devices and the parameter value was taken by means of averaging.

Table 3.1. The operating conditions of the steam power plants

| Parameter | Unit | Subcritical | Supercritical | Ultra-Supercritical |
|---|---|---|---|---|
| Power Plant Capacity | MW | 660 | 615 | 660 |
| Main Steam Pressure | bar | 177 | 242 | 280 |
| Main Steam Temperature | $^0$C | 541 | 566 | 600 |
| Main Steam Flow Rate | t/h | 1886 | 1683.9 | 1792.4 |
| Reheat Steam Pressure | bar | 49 | 38.8 | 56.68 |
| Reheat Steam Temperature | $^0$C | 539 | 566 | 610 |
| HP Turbine Output Pressure | bar | 52 | 43.11 | 61.61 |
| Condenser Pressure | bar | 0.03 | 0.049 | 0.035 |
| Sea Water Temperature | $^0$C | 18 | 20 | 20 |
| Feed water Temperature | $^0$C | 268 | 276.3 | 304.4 |
| Coal Consumption | t/h | 220 | 195 | 200 |
| Coal Lower Heating Value | kJ/kg | 25,800 | 25,800 | 25,800 |

The coal-fired steam power plant considered in the present study is located in Adana, Turkey as shown in Figure 3.1 (ISKEN, 2018). It operates with the Rankine cycle supplying competitive power to the national grid under acceptable environmental protection. The power plant generally consists of pumps, turbines, boiler, condensers and heaters also includes flue gas desulfurization unit and

electrostatic filters. The present thermal power plant has one high-pressure turbine (HP), one intermediate Pressure (IP) turbine and two low pressure (LP) turbines. HP turbine is a single flow type and has 13 stages. IP is a double flow type and has three uncontrolled steam extraction points and 14 stages. LP turbines are double flow type and each LP turbine has three uncontrolled steam extraction points and 14 stages. All turbines directly coupled with the generator which rotates at a speed of 3000 rpm (50 Hz). Gross outlet power is 660 MW and net power is 605 MW at a full load for each unit. The boiler of coal-fired sub-critical plant includes heating packages such as evaporators, super-heaters, economizer and reheaters. The economizer is the parallel flow type and placed on the top of the boiler. A heat exchanger device heats up fluids or recovers residual heat from the flue gases in the thermal power plant before being released through the air preheater. Feed water enters the evaporator after the economizer. The feed water in the evaporator tubes receives heat from the combustion gases and boils further. In the exit of evaporator tubes, the evaporation process is completed.

There are three super-heater packages the one which examined. Super-heaters have a large heat transfer surfaces in which heat is transferred to the saturated steam in order to increase its temperature and available energy. Super-heaters are placed above banks of water tubes to protect them from the combustion flames and high temperatures. After the unit of super-heater, steam becomes superheated steam and moves into the HP turbine. There are two reheater packages in one unit. Exhaust steam of HP turbine returns to the reheaters for an additional superheating process before it enters the IP turbine. When the exit steam temperature becomes excessive, the attemperator sprays feed water into superheated steam in order to eliminate fluctuation of superheated steam temperatures. An imported coal with a calorific value of 25,800 kJ/kg is used as the main fuel source. These coals are pulverized by the mill and conveyed pneumatically to the pulverized coal burners. But oil is used as a fuel for start-up,

shut-down conditions and stabilizing the flame temperature during the combustion. Also, there is a soot blowing system to reduce fouling around the pipe.

Figure 3.1. A view of the steam power plant (ISKEN 2018)

An air preheater is a regenerative heat exchanger installed at an exit of the boiler. The air preheater transfers thermal energy from the flue gas to the cold combustion air. Preheated air accelerates combustion by producing more rapid ignition, increasing plant efficiency and reducing fuel consumption. The feed water tank is a mixing chamber installed between condenser and boiler. It is used to remove the air from the condensed water. This operation is necessary because an air in water produces corrosion in pipes. Besides condensed water is heated by the steam which is drawn from the IP turbine. The present thermal power plant has four LP heaters and two HP heaters. HP heaters are located after the feed water pump before the economizer in the process line of the power plant. LP heaters are located in the process line between the feed water tank and condenser. Closed-type

feedwater heaters are used to maintain fluids separately. Feed water is conveyed inside the tubes and steam outside the tubes in the case of a shell-and-tube type heat exchanger named as the HP feedwater heater. The wet steam leaving the LP turbine is condensed in terms of cooling water. The fundamental objective of using cold water-based steam condenser in a steam power plant is to keep up a low back pressure at the outlet of LP steam turbine. In the present power plant, steam is generated at a pressure and temperature of 177 bar and 541 °C in the boiler. This superheated steam is fed to the HP turbine. Then steam is returned to reheaters to regain 541 °C steam temperature with high energy availability. Afterward, the steam goes back into the IP turbine and lastly expansion of steam continues through LP turbines. The exhaust steam leaves LP turbines at wet conditions nearly 90%. Finally, the steam is condensed by condensers under the vacuum pressure at about 0.03 bar. Water-steam cycle and T-s diagram of this power plant are shown in Figures 3.2 and 3.3, respectively.

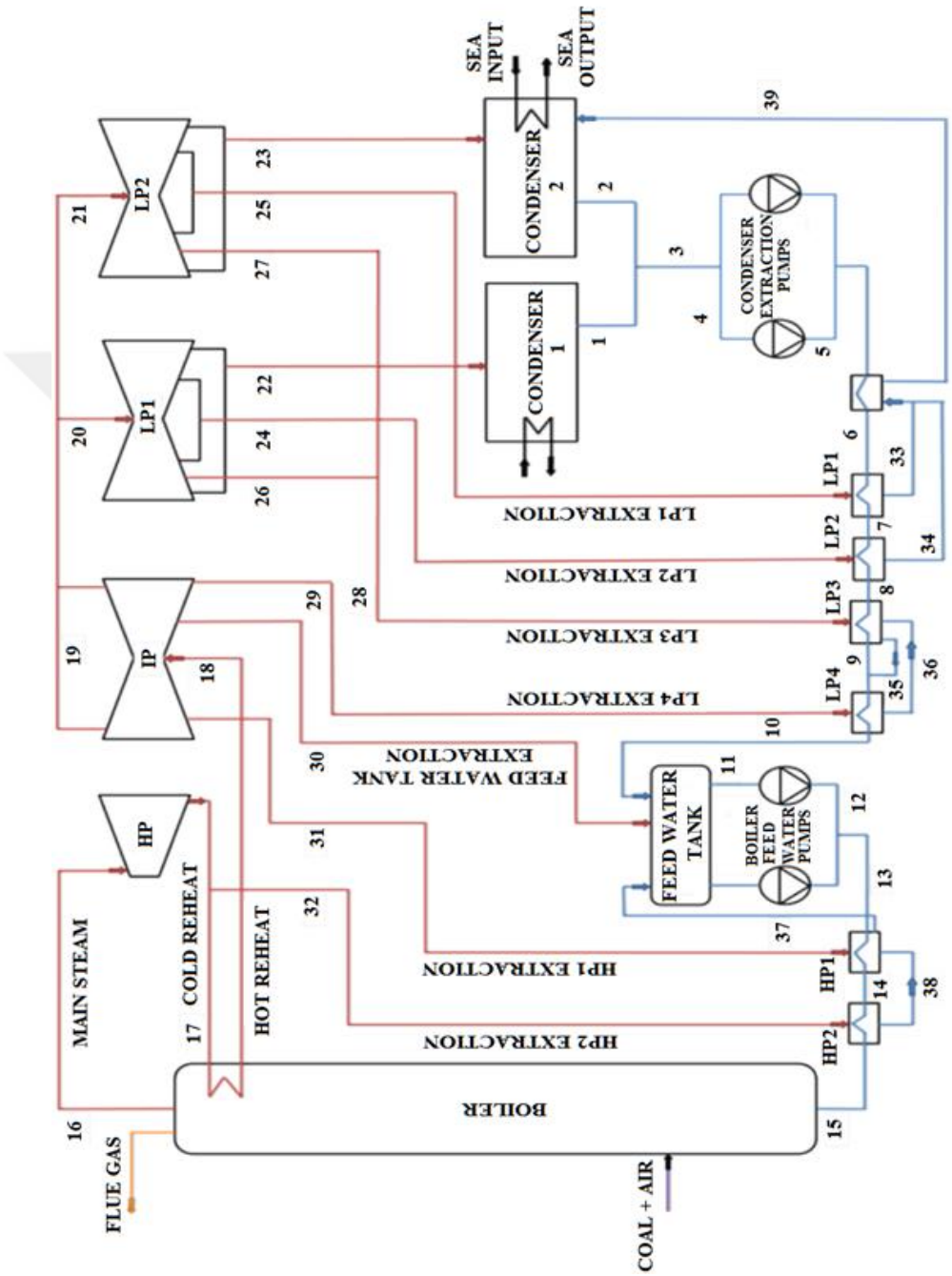


Figure 3.2. Water steam cycle of present the subcritical steam power plant

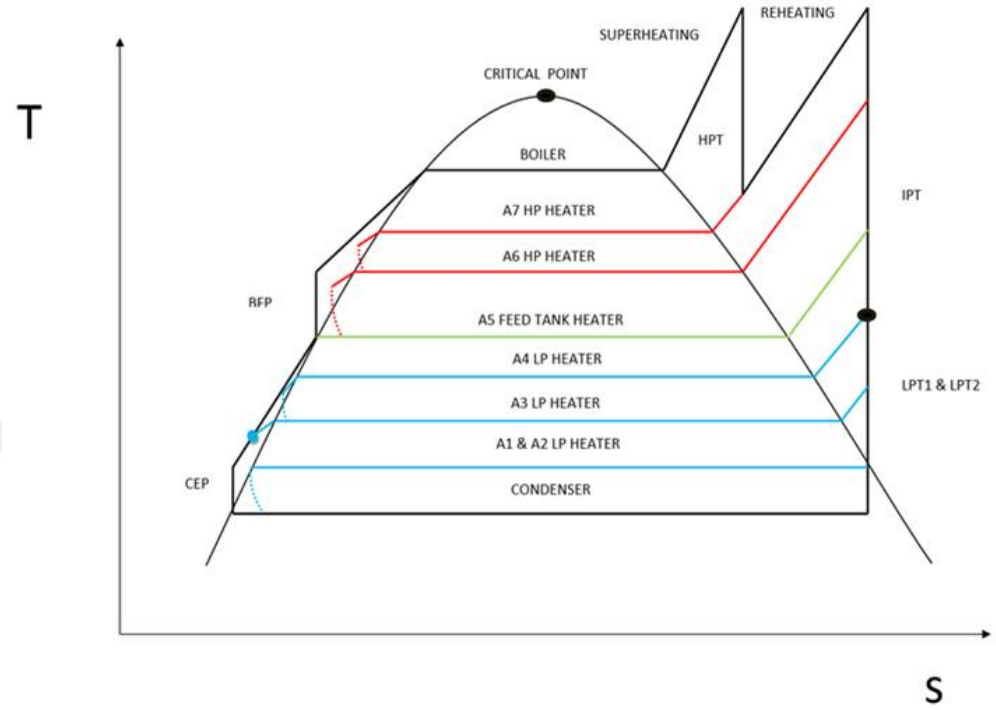


Figure 3.3. T-s diagram of present the subcritical steam power plant

### 3.1.1. Analysis

#### 3.1.1.1. Energy and Exergy Analyses

The total energy content remains constant in the case of the mass balance during the steady-state operation, for example, $E_{in}=E_{out.}$ The energy efficiency $(\eta_I)$ is defined as the first-law efficiency, which can be expressed as the ratio of the work rate to the fuel energy input rate:

$$\eta_I = \frac{W_{net}}{Q_{in}} \tag{3.1}$$

In the exergy analysis of this study, at the dead state, the properties are symbolized by subscript zero. For instance, $P_0$ and $T_0$ refer to the dead-state pressure and temperature, respectively. Here, $T_0$ is assumed to be 25$^{o}$C (298 K) and

$P_0$ is assumed to be 1 bar. The use of exergy analysis eliminates the restrictions of the first law. The locations and amount of waste energy in a process can clearly be identified by using exergy analysis based on both the first-law and the second law. This evaluation leads the researchers to advance operational procedures and improve the technological status of the thermal power plants. Exergy analysis is also capable of defining the quantity and quality of waste heat in a stream. Exergy assessment offers the necessary tools for indicating poor spots in the process (Dinçer and Rosen, 2011; Dinçer and Rosen, 2007; Afanasyeva and Mingaleeva, 2015).

The exergy assessment for the present subcritical power plant was carried out for each device of the subsystem in order to evaluate the exergy destruction and then the exergy assessment which was conducted for the overall subsystems considering devices individually to obtain exergy destruction of each subsystem. Lastly, overall exergy evaluation for the coal-fired steam power plant was carried out and the second-law efficiency was computed. A quantitative measure of a disorder called entropy of the system was also examined at a microscopic level.

Entropy generation, $S_{gen}$ of the system is presented as follows:

$$S_{gen} = \sum_{out} ms - \sum_{in} ms - \frac{Q_l}{T_0} \tag{3.2}$$

Exergy balance can be obtained by using the following equation:

$$\sum \left(1 - \frac{T_o}{T_k}\right) Q_l - W + \sum_{in} m(ex) - \sum_{out} m(ex) - X_D = 0 \tag{3.3}$$

Where $T_k$ is the surrounding temperature. Irreversibility can be calculated as:

$$I = T_0 S_{gen} \tag{3.4}$$

=

Considering no kinetic and potential energy, the expression for exergy becomes;

$$ex = (h - h_o) - T_o(s - s_o) \tag{3.5}$$

For a steady state operation, and choosing each power plant equipment in Fig. 3.2 as a control volume, the irreversibility and the exergy efficiency, are defined as shown in Table 3.2.

Table 3.2. The irreversibility and exergy efficiency equations for plant equipment (Aljundi, 2009)

| **Plant equipment** | **Irreversibility** | **Exergy efficiency** |
|---|---|---|
| Boiler | $I_{boiler} = X_f + X_{in} - X_{out}$ | $\eta_{\Pi,boiler} = \frac{X_{out} - X_{in}}{X_f}$ |
| Pumps | $I_{pump} = X_{in} - X_{out} + W_{pump}$ | $\eta_{\Pi,pump} = 1 - \frac{I_{pump}}{W_{pump}}$ |
| Heaters | $I_{heaters} = X_{in} - X_{out}$ | $\eta_{\Pi,heaters} = 1 - \frac{I_{heaters}}{X_{in}}$ |
| Turbine | $I_{turbine} = X_{in} - X_{out} - W_{turbine}$ | $\eta_{\Pi,turbine} = 1 - \frac{I_{turbine}}{X_{in} - X_{out}}$ |
| Condenser | $I_{condenser} = X_{in} - X_{out}$ | $\eta_{\Pi,condenser} = \frac{X_{out}}{X_{in}}$ |
| Cycle | $I_{cycle} = \sum all\ components$ | $\eta_{\Pi,cycle} = \frac{W_{out}}{X_f}$ |

### 3.1.1.2. Fuel and Combustion Analyses

Boilers need a heat source with a certain temperature level in order to generate steam under a high pressure using fossil fuel in the combustion chamber. It is known that the main element of coal is carbon. Coal also comprises oxygen,

hydrogen, nitrogen, sulfur, moisture, and ash with varying amounts as given in Table 3.3. In the present thermal power plant, imported coal with a high calorific value is used. Lower calorific value of coal is defined as 25,800 kJ/kg (Unal, 2009).

Table 3.3. Chemical compositions of presently used coal

| **Coal Components (% ratio)** | | | | | | |
|---|---|---|---|---|---|---|
| C | H | N | S | O | Ash | Water |
| 66 | 3.66 | 1.5 | 0.9 | 4.16 | 13.78 | 10 |

During the combustion process, both the carbon and the oxygen are oxidized releasing a large quantity of energy. A fuel is said to be combusted completely if all carbon existed in the fuel is burned to form carbon dioxide, $CO_2$, water, $H_2O$ and sulfur dioxide, $SO_2$. Nitrogen, $N_2$ acts like an inert gas and does not react with other chemical elements during the combustion, but it forms a very small amount of nitric oxides, NO. In general, pure oxygen, $O_2$ is used only in the special application of combustion but in this study, air is used for combustion (Moran and Shapiro, 2000).

The combustion process of coal in this study is presented as:

$$(cC+hH+nN+sS+oO+wH_2O)+1.5a\,(O_2+3.76N_2) \rightarrow (xCO_2+yN_2+zH_2O+tSO_2)$$

Excess air coefficient is assumed to be $\lambda = 1.2$

$$RAA = (MAA)\,(\lambda) \tag{3.6}$$

Flue gas flow rate can be calculated after obtaining the required amount of combustion air. As a result of the combustion of 1 kg of coal, the flue gas flow rate is 1+ RAA kg. Coal energy supplied to the boiler is (Kotas, 1995):

$$Q_f = m_f h_f \tag{3.7}$$

Flue gas enthalpy and molar ratio components of flue gases are:

$$x = \frac{n_i}{n_{total}} \tag{3.8}$$

Enthalpy of flue gas can be calculated at the desired temperature using the following equations:

$$\bar{h}_{fg} = x_{CO_2}\bar{h}_{CO_2} + x_{N_2}\bar{h}_{N_2} + x_{SO_2}\bar{h}_{SO_2} + x_{H_2O}\bar{h}_{H_2O} \tag{3.9}$$

$$h_{fg} = \frac{\bar{h}_{fg}}{M_{fg}} \tag{3.10}$$

The entropy of components forming the flue gas is calculated as:

$$\bar{s}_{CO_2} = \bar{s}_{K,CO_2} - R\ln x_{CO_2} \tag{3.11}$$

$$\bar{s}_{N_2} = \bar{s}_{K,N_2} - R\ln x_{N_2} \tag{3.12}$$

$$\bar{s}_{SO_2} = \bar{s}_{K,SO_2} - R\ln x_{SO_2} \tag{3.13}$$

$$\bar{s}_{H_2O} = \bar{s}_{K,H_2O} - R\ln x_{H_2O} \tag{3.14}$$

$$\bar{s}_{fg} = x_{CO_2}\bar{s}_{CO_2} + x_{N_2}\bar{s}_{N_2} + x_{SO_2}\bar{s}_{SO_2} + x_{H_2O}\bar{s}_{H_2O} \tag{3.15}$$

$$s_{fg} = \frac{\bar{s}_{fg}}{M_{fg}} \tag{3.16}$$

Chemical exergy of flue gas by summing up exergies of chemical elements forming flue gas is presented with the following equations:

$$\overline{ex}_{fg}^{ch} = x_{CO_2}\overline{ex}_{CO_2} + x_{N_2}\overline{ex}_{N_2} + x_{SO_2}\overline{ex}_{SO_2} + x_{H_2O}\overline{ex}_{H_2O} + RT_O(x_{CO_2}lnx_{CO_2} + x_{N_2}lnx_{N_2} + x_{SO_2}lnx_{SO_2} + x_{H_2O}lnx_{H_2O} \quad (3.17)$$

$$ex_{fg}^{ch} = \frac{\overline{ex}_{fg}^{ch}}{M_{fg}} \quad (3.18)$$

$$X_{fg}^{ch} = m_{fg}ex_{fg}^{ch} \quad (3.19)$$

Similarly, chemical exergy of combustion air is determined by considering exergies of chemical elements forming flue gas with the following equations:

$$\overline{ex}_{air}^{ch} = x_{O_2}\overline{ex}_{O_2} + x_{N_2}\overline{ex}_{N_2} + RT_O(x_{O_2}lnx_{O_2} + x_{N_2}lnx_{N_2} \quad (3.20)$$

$$ex_{air}^{ch} = \frac{\overline{ex}_{air}^{ch}}{M_{air}} \quad (3.21)$$

$$X_{air}^{ch} = m_{air}ex_{air}^{ch} \quad (3.22)$$

Finally, the chemical exergy of coal is presented as:

$$\Phi = 1.0437 + 0.1882\,\frac{h}{c} + 0.0610\,\frac{o}{c} + 0.0404\,\frac{n}{c} \quad (3.23)$$

$$ex_f = \phi\left(h_f + w\frac{2467.3}{4.18}\right) \quad (3.24)$$

$$X_f = \dot{m}_f(ex_f) \tag{3.25}$$

### 3.2. Organic Rankine Cycle

#### 3.2.1. System Description

It is known that in a steam power plant, heat energy with the exhaust gas is released with a certain level of temperature into the atmosphere to avoid acid deformations in the flue gas channel. This acid deformation depends on the level of sulfur and water content of the coal and most importantly this acid deformation generally occurs below 120°C of the exhaust gas temperature. That is to say, if the thermal power plant does not have a desulfurization unit, it is a requirement to keep the temperature of the flue gas channel and chimney more than 120 °C. In doing this, too much waste heat is transferred out of the existing system. Figure 3.4 shows the temperature profile of a boiler through the flue gas. The temperature downstream of the induced-draft fan is higher than the acid deformation temperature, so the Organic Rankine Cycle is integrated with the steam power plant flue gas line to recover waste heat. The properties of the organic fluids used in the system are given in Table 3.4. The ORC operation principle is similar to the conventional Rankine Cycle, but in the ORC system, the working fluid used is an organic compound with a low boiling temperature instead of water vapor. Thus, the temperature required for evaporation is relatively low. The schematic diagram of the ORC system used in this study is shown in Figure 3.5. The nominal power of this proposed ORC system in the present work is 4.7 MW. The ORC system consists of a circulation pump, an evaporator powered by exhaust heat, a turbine and a water-cooled condenser. The pump feeds the working fluid to the evaporator, where the working fluid is heated up and vaporized by the exhaust heat. The high-pressure steam produced is delivered into the turbine where power is generated and then directed to the low-pressure steam condenser and condensed with water. The fluid moves back to the evaporator, and this phenomenon take place at the end of

each cycle. A recuperator can also be utilized to improve the use of the energy from the expanded vapor, by applying a pre-treatment procedure to the fluid. Figure 3.6 exhibits the T-s diagram of the present ORC.

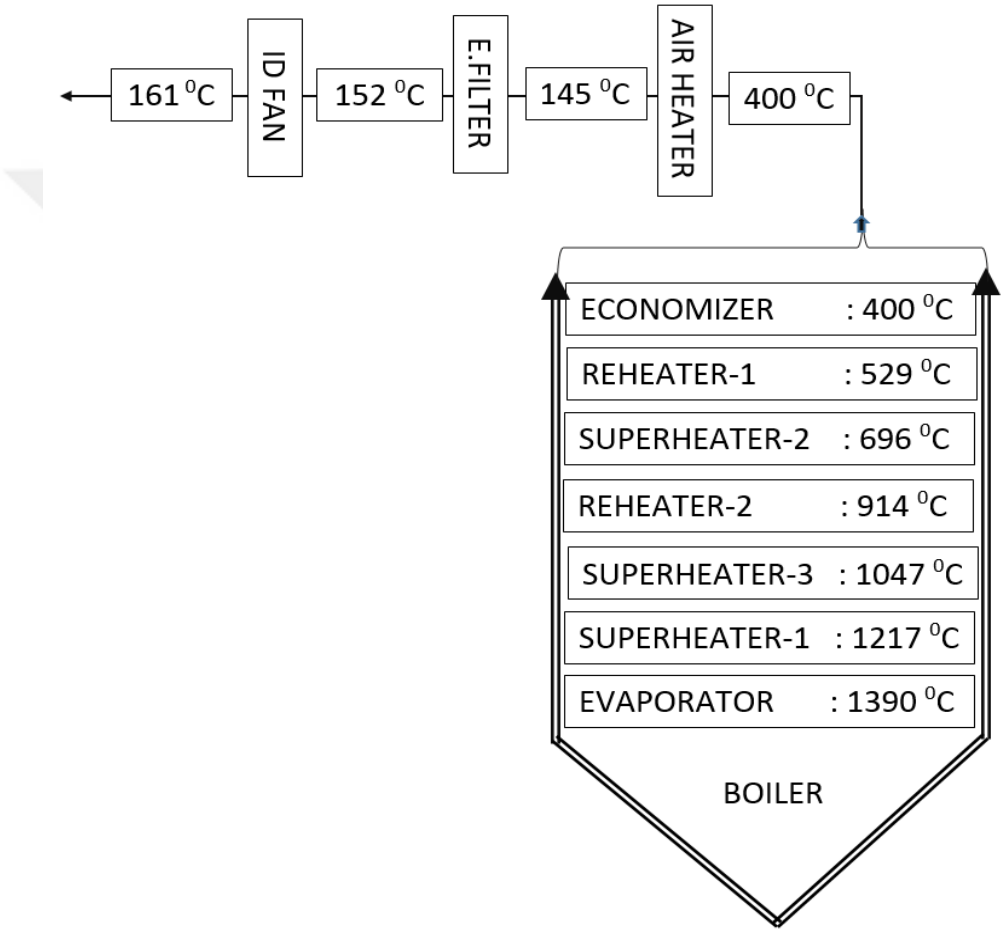


Figure 3.4. Profile of temperatures through the steam boiler

Table 3.4. Thermodynamic properties of organic fluids used in this study

| Name | Molecular weight (g/mol) | $T_c$ (K) | $P_c$ (bar) | $c_p$ (J/kgK) | Latent heat (kJ/kg) |
|---|---|---|---|---|---|
| R-245fa | 134.05 | 427.20 | 36.4 | 980.90 | 177.08 |
| R-236ea | 152.04 | 412.44 | 35.0 | 973.69 | 142.98 |
| R-600 | 58.12 | 425.13 | 38.0 | 1965.59 | 336.82 |
| R-236fa | 152.03 | 397.92 | 32.0 | 377.21 | 161.69 |

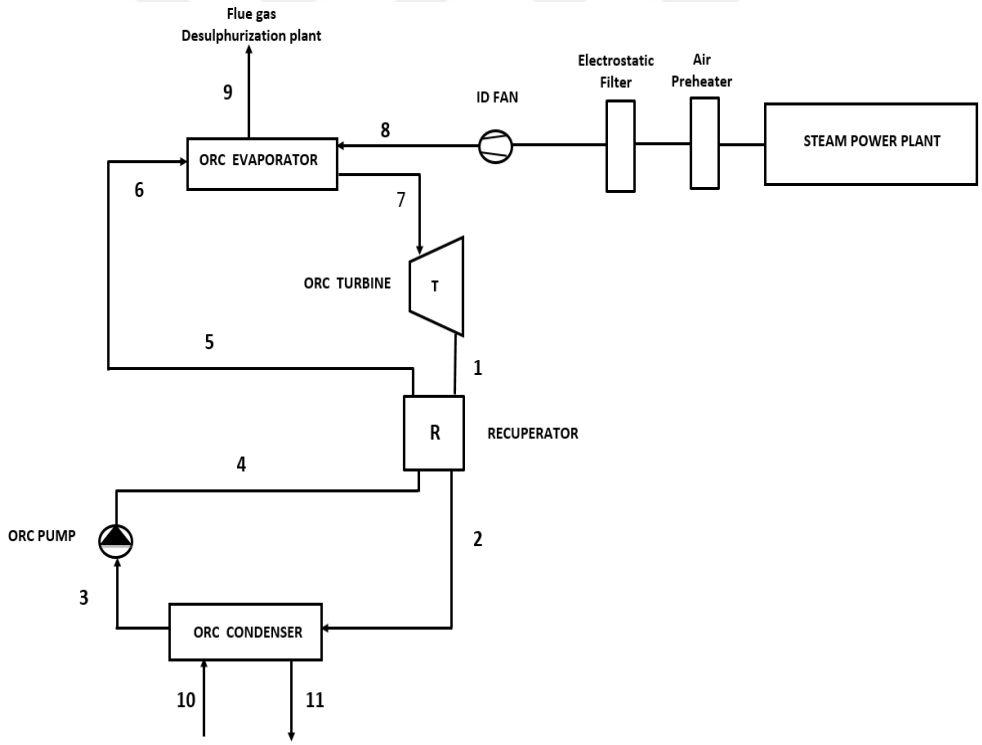


Figure 3.5. Schematic diagram of the ORC system used in this study

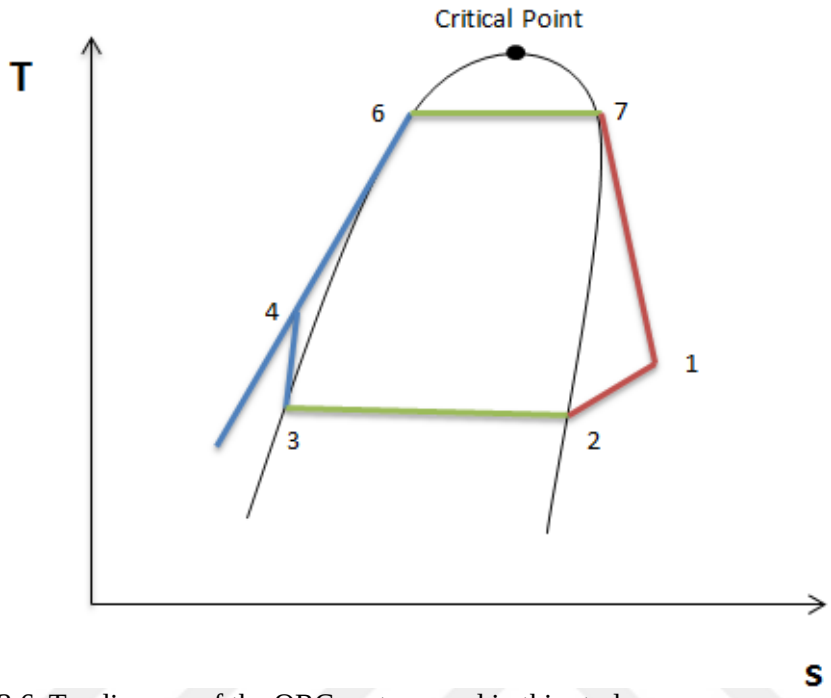


Figure 3.6. T-s diagram of the ORC system used in this study

### 3.2.2. Energy and Exergy Analyses

Work, heat, exergy of flow, thermodynamic properties, and energy and exergy efficiencies can be determined by applying balances of mass, energy, exergy, and cost values for every component of the system. The following exhibits the numerous rate balance values based on energy and exergy analyses for system components. The equations for a steady-state system are given below:

$$\sum m_{in} = \sum m_{out} \tag{3.26}$$

$$Q - W = \sum E_{out} - \sum E_{in} \tag{3.27}$$

$$X_Q - W = \sum X_{out} - \sum X_{in} + X_D \tag{3.28}$$

Where the net exergy transfer by heat $X_Q$ at temperature T is determined by the following expression:

$$X_Q = \sum \left(1 - \frac{T_0}{T}\right) Q \tag{3.29}$$

And the specific exergy is determined by the following equation:

$$ex = h - h_0 - T_0(s - s_0) \tag{3.30}$$

Table 3.5 exhibits the exergy destruction rate and the exergy efficiency values for a steady state, and the selection of each component of the ORC system as a control volume. There are numerous methods to define the exergy efficiency of the power cycle. Also, the definition will let us know the exergy efficiency of the power cycle in addition to providing information on the exergy destruction associated with fuel combustion and the exergy lost through exhaust gases from the boiler.

The fuel exergy is determined as follows:

$$\Phi = 1.0437 + 0.1882\ \frac{h}{c} + 0.0610\ \frac{o}{c} + 0.0404\ \frac{n}{c} \tag{3.31}$$

$$ex_f = \Phi \left(h_f + \frac{w\ 2467.3}{4.18}\right) \tag{3.32}$$

$$X_f = m_f ex_f \tag{3.33}$$

The ORC exergy efficiency can be calculated as follows:

$$n_{ORC} = \frac{W_{ORC}}{X_8 - X_9} \tag{3.34}$$

Overall plant exergy efficiency is:

$$n_{overall} = \frac{W_{ORC}+W_{spp}}{X_f} \quad (3.35)$$

Table 3.5. Energy and exergy analysis equations

| **Components** | **Energy balance** | **Exergy destruction rate** | **Exergy efficiency** |
|---|---|---|---|
| Condenser | $E_2 + E_{10} = E_3 + E_{11}$ | $X_D = X_2 + X_{10} - X_3 - X_{11}$ | $n_c = \frac{X_{10} - X_{11}}{X_2 - X_3}$ |
| Recuperator | $E_1 + E_4 = E_2 + E_5$ | $X_D = X_1 + X_4 - X_2 - X_5$ | $n_r = \frac{X_4 - X_5}{X_1 - X_2}$ |
| Pump | $E_3 + W_P = E_4$ | $X_D = X_3 + W_P - X_4$ | $n_p = \frac{X_4 - X_3}{W_p}$ |
| Evaporator | $E_6 + E_8 = E_7 + E_9$ | $X_D = X_6 + X_8 - X_7 - X_9$ | $n_e = \frac{X_6 - X_7}{X_8 - X_9}$ |
| Turbine | $E_7 = E_1 + W_t$ | $X_D = X_7 - W_t - X_1$ | $n_t = \frac{W_t}{X_7 - X_1}$ |

### 3.2.3. Exergoeconomic Evaluation

Exergoeconomics can be defined as the combination of exergy analysis and economic evaluation that helps to comprehend the costs and the optimization of the system. To determine the cost of inefficient factors and to enhance the cost efficiency, a formulation of a cost balance for the ORC can be made as follows (Bejan et al., 1996):

$$\dot{C}_{q,k} + \sum_i \dot{C}_{i,k} + \dot{Z}_k = \sum_i \dot{C}_{e,k} + \dot{C}_{w,k} \quad (3.36)$$

For each flow in a system, a parameter called the flow cost rate $\dot{C}$ (\$/h) is defined, and a cost balance is written for each component:

$$\sum_i (c_e X_e)_k + c_{w,k}\dot{W}_k = c_{q,k}X_{q,k} + \sum_i (c_i X_i)_k + \dot{Z}_k \quad (3.37)$$

$$\dot{C}_j = c_j X_j \quad (3.38)$$

In this study, fuel and product exergy should be determined. While the product exergy is determined for every element of the ORC system, the fuel represents the consumed source for the process of the products. Both products and fuels are expressed in terms of exergy. The cost ratios of inputs and outputs related to fuels ($\dot{C}_F$) and products ($\dot{C}_P$) are provided by modifying the exergy ratios (X). In the cost-equivalenced formulation, there is no cost term immediately related to exergy destruction of each process. Accordingly, the cost due to the destruction of the exergy of a process is a hidden cost. If one integrates both exergy destruction and cost equivalences, one can get:

$$X_{F,k} = X_{P,k} + X_{D,k} \quad (3.39)$$

$$X_{F,k} = X_{P,k} + X_{L,k} + X_{D,k}c_{P,k} = c_{F,k}X_{F,k} - \dot{C}_{L,k} + Z_k \quad (3.40)$$

In this way, the cost of exergy destruction is given as:

$$\dot{C}_{D,k} = c_{F,k}X_{D,k} \quad (3.41)$$

The calculation of the investment cost rate is as follows:

$$\dot{Z}_k = \frac{Z_k.CRF.\varphi}{Nx3600} \quad (3.42)$$

*Z* corresponds to the procurement cost of the element, and *CRF* is the capital recovery factor. *CRF* is associated with equipment lifetime and the interest rate and can be found by the following equation:

$$CRF = \frac{i.(1+i)^n}{(1+i)^n-1} \tag{3.43}$$

Here, *i* correspond to the interest rate and *n* is the total operating period of the system in years. In addition, *N* refers to the annual number of operating hours for the unit, and φ is the maintenance factor (usually 1.06).

The variable shows the relative increase in the average cost per exergy unit between the fuel and the unit of product. The relative cost difference helps to assess and optimize the system components. The relative cost difference is defined by:

$$r = \frac{c_{P,k}-c_{F,k}}{c_{F,k}} \tag{3.44}$$

The exergoeconomic factor is an important variable for the evaluation of the performance. It is determined as follows:

$$f = \frac{\dot{Z}_k}{\dot{Z}_k+c_{F,k}(X_{D,k}+X_{L,k})} \tag{3.45}$$

One of the methods of the exergy-aided cost analysis is exergoeconomics. Accordingly, the cost rate equivalence is implemented in that the sum of cost rates related to whole departing exergy streams equals the sum of the cost rates of whole incoming exergy streams plus the capital investment, and the maintenance and operating costs. Table 3.6 exhibits the auxiliary equations and cost rate equivalences for every element of the ORC system (Anvari et al., 2015).

Table 3.6. Cost rate balances and auxiliary equations for components

| **Components** | **Cost rate balance** | **Auxiliary equations** |
|---|---|---|
| Condenser | $C_2 + C_{10} + Z_C = C_3 + C_{11}$ | $c_2 = c_3$ |
| Recuperator | $C_1 + C_4 + Z_R = C_2 + C_5$ | $c_1 = c_2$ |
| Pump | $C_3 + C_{w,p} + Z_p = C_4$ | **-------** |
| Evaporator | $C_6 + C_8 + Z_e = C_7 + C_9$ | $c_8 = c_9$ |
| Turbine | $C_7 + Z_t = C_1 + C_{w,t}$ | $c_1 = c_7$ |

Table 3.7 summarizes the definitions of the cost rate associated with the fuel and product of the components. The cost rate related to the fuel of components contains the cost rates of the same streams used in the same order and with the same sign as in the definition of the exergy of the fuel.

Table 3.7. Cost rate associated with fuel and product

| **Components** | **Cost rate of fuel ($C_F$)** | **Cost rate of product ($C_p$)** | **Variable** |
|---|---|---|---|
| Condenser | $C_2 - C_3$ | $C_{11} - C_{10}$ | $c_{11}$ |
| Recuperator | $C_1 - C_2$ | $C_5 - C_2$ | $c_5$ |
| Pump | $C_{w,p}$ | $C_4 - C_3$ | $c_4$ |
| Evaporator | $C_8 - C_9$ | $C_7 - C_6$ | $c_7$ |
| Turbine | $C_7 - C_1$ | $C_{w,t}$ | $c_{w,t}$ |

The capital cost of ORC components, the *Z* value, can be described as a function of related parameters. Capital cost equations for the system components are given in Table 3.8 (Dincer et al., 2017).

Table 3.8. Capital cost equations for system components

| **Components** | **Capital cost** |
|---|---|
| Condenser | $Z_c = 516.62(A_c)^{0.6}$ |
| Recuperator | $Z_r = 1000(A_r)^{0.65}$ |
| Pump | $Z_p = 200\left(W_p\right)^{0.65}$ |
| Evaporator | $Z_e = 309.14(A_e)^{0.85}$ |
| Turbine | $Z_t = 4750(W_t)^{0.65}$ |

### 3.2.4. Environmental Impact Analysis

Two cases are evaluated to determine the $CO_2$ emissions. Firstly, the power cycle is utilized for producing electricity, while in the second one the whole system for multiple products is taken into account. The $CO_2$ emission values produced in each case can be written as follows (Dincer et al., 2017):

$$\varepsilon_{single} = \frac{m_{CO_2}}{W_{net}} \tag{3.46}$$

$$\varepsilon_{multi} = \frac{m_{CO_2}}{W_{total} + X_{other}} \tag{3.47}$$

The adiabatic flame temperature in the main combustion zone of the boiler can be written as shown below:

$$T_{flame} = A\sigma^{a}\exp(\beta(\sigma+\lambda)^2)\pi^{x^*}\theta^{y^*}\psi^{z^*} \tag{3.48}$$

The CO and $NO_x$ produced in a boiler and the combustion reaction depends on the adiabatic flame temperature. The CO and $NO_x$ emissions can be found by the following equations:

$$m_{NO_x} = \frac{0.15E16\ \tau^{0.5} \exp\left(-\frac{71100}{T_{Flame}}\right)}{P^{0.05}\left(\frac{\Delta P}{P}\right)^{0.5}} \tag{3.49}$$

$$m_{CO} = \frac{0.179E9\ \tau^{0.5} \exp\left(-\frac{7800}{T_{Flame}}\right)}{P^{2}\tau\left(\frac{\Delta P}{P}\right)^{0.5}} \tag{3.50}$$

## 3.3. Vapor Compression Refrigeration

### 3.3.1. System Description

In this study, industrial data provided from the coal-fired power plant operating at a maximum capacity of 660 MW was used. This steam power plant is situated in the southern region of Turkey as stated before. It operates with the Rankine cycle supplying competitive power to the national grid under acceptable environmental protection. The subcritical coal-fired power plant is actively operating for 15 years and there is no decline in the efficiency due to a comprehensive regular maintenance. Coal is used as the main fuel, and it is imported from Colombia or South Africa to provide the utmost energy input rate. The subcritical boiler is called a one-pass tower type plant. The power plant commonly consists of pumps, turbines, boiler, condensers and heaters also includes flue gas desulfurization unit and electrostatic precipitators. The operating conditions of the steam power plants are presented in Table 3.9.

Table 3.9. Operating conditions of power plants

| Parameter | Unıt | Value |
|---|---|---|
| Power plant capacity | MW | 660 |
| Main steam pressure | bar | 177 |
| Main steam temperature | $^{o}$C | 541 |
| The main steam flow rate | t/h | 1886 |
| Intermediate reheat steam pressure | bar | 49 |
| Intermediate reheat steam temperature | $^{o}$C | 539 |
| High pressure turbine output pressure | bar | 52 |
| Condenser pressure | bar | 0.03 |
| Circulating seawater cooling temperature | $^{o}$C | 18 |
| Boiler feed water temperature | $^{o}$C | 268 |
| Coal consumption | t/h | 220 |
| Design coal lower heating value | kJ/kg | 25,800 |

Figure 3.8 displays a schematic diagram of a steam turbine which drives the vapor compression refrigeration (STD-VCR) system. As seen in Figure 3.7, the expansion valve is used for pressure drop in order to feed a desalination system with steam under a desired pressure value in the current system. Super-heated steam delivered to the expansion valve, for example, has the thermodynamic properties of 55 bar pressure, 355 $^{o}$C temperature and 6 kg/s mass flow rate for maximum distilled water production. These steam properties may change according to the steam power plant production load. The steam pressure of the distillation unit for the water distillation and salt separation from seawater is adjusted by the expansion valve to keep the pressure at 16 bar. Since saturated steam is required in the desalination process, it is not possible to extract steam from HP and IP turbines. The desalination system is operated at 16 bar steam pressure in order to provide a required vacuum inside the effects. As can be seen from Figure 3.9, pressure differences of about 40 bar generated for the desalination unit can be used for power generation by using a steam turbine instead of the expansion valve.

For this aim, in the study, a novel system, steam turbine-driven vapor compression refrigeration (STD-VCR) system is proposed. In order to activate vapor compression refrigeration (VCR) system, a steam turbine, which is integrated into the steam power plant with multiple effect distillation-thermal vapor compression (MED-TVC) technology, is used. So that, both the desalination unit is fed and the extra cooling load is achieved.

Normally vapor compression cycle input energy is supplied by electricity, but in this study, the steam turbine is placed to drive the compressor. Before integrating the steam turbine, an expansion valve used to drop the pressure to the desired level to feed the desalination system as a motive steam. But, in the present work, it is decided to recover energy losses caused by the expansion valve a steam turbine is used instead of expansion valve to deliver the necessary steam under desired pressure to the desalination unit. The basic VCR system consists of a compressor, an expansion valve an evaporator and a condenser. The refrigerating is provided in the cold zone by removing the heat during evaporation of the refrigerant in the evaporator. The refrigerant vapor from the evaporator is compressed with a high pressure that the saturation temperature in the compressor is higher than the ambient temperature or any other heat sink. For this reason, the refrigerant with high temperature passes through the condenser. At the high pressure, condensation of the vapor into the liquid phase is substituted by heat rejection. To fulfill the cycle, the high pressure fluid is made to flow through an expansion valve. The refrigerant temperature drop and pressure drop take place in the expansion valve. At this low pressure and low temperature, the refrigerant vapor evaporates by taking the heat from the cold region in the evaporator. The system needs to receive an input energy in the form of mechanical energy. The characteristics of the refrigerants used in this study are displayed in Table 3.10. Refrigerants with different characterizes were selected to consider the effect on the power plant in terms of performance point of view.

Table 3.10. Features of refrigerants

| Refrigerants | Molecular Weight (g/mol) | Boiling Point (°C) | Freezing Point (°C) | Critical Temperature (°C) | Critical Pressure (bar) |
|---|---|---|---|---|---|
| R134a | 102.03 | -26.11 | -96.67 | 101 | 40.15 |
| R410a | 72.6 | -48.56 | -155 | 72.2 | 46.96 |
| R407c | 86.2 | -43.56 | -160 | 86.74 | 45.6 |
| R717 | 17.02 | -33.33 | -77.72 | 133 | 112.7 |

Vapor compression refrigeration, which is subjected to phase changes of the refrigerant, is one of the refrigeration cycles and is the most commonly used method for the air conditioning purposes.

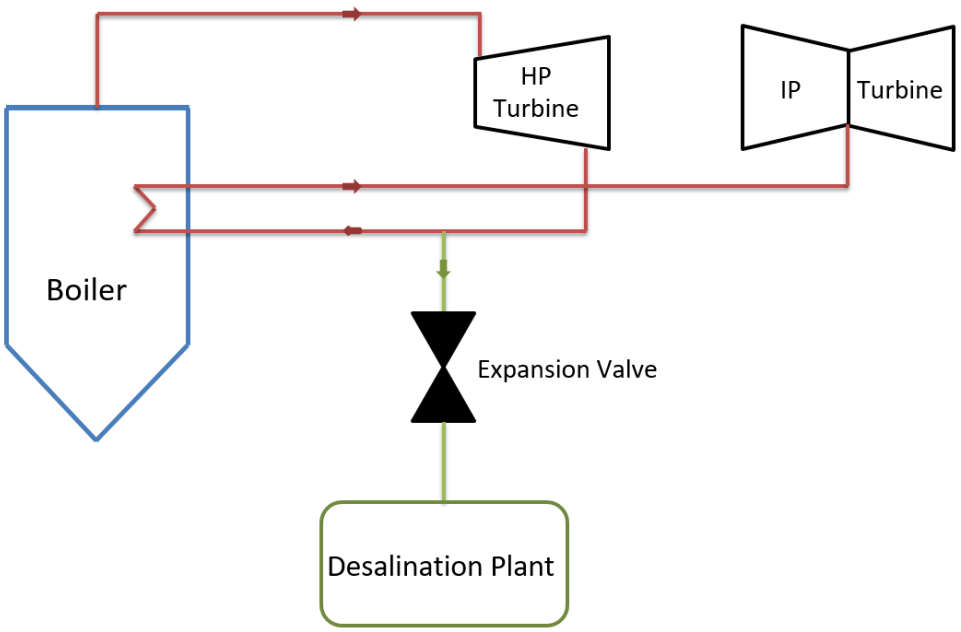


Figure 3.7. Current system: Expansion valve used in the steam power plant with multiple effect distillation-thermal vapor compression (MED-TVC)

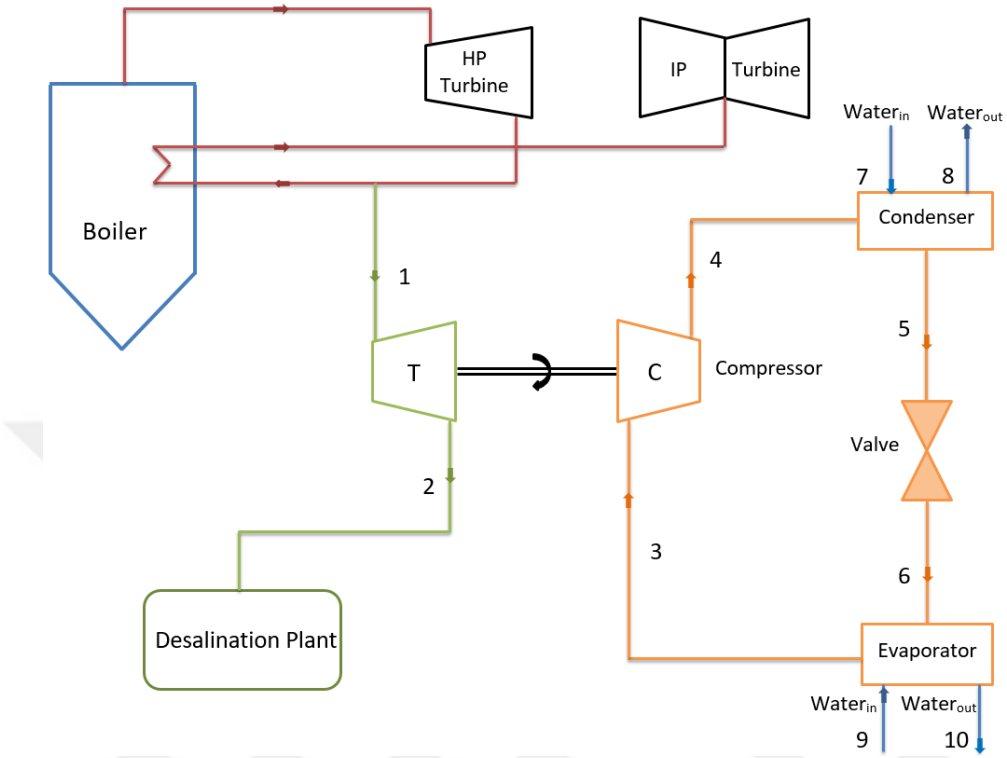


Figure 3.8. Turbine-driven vapor compression refrigeration (STD-VCR) system

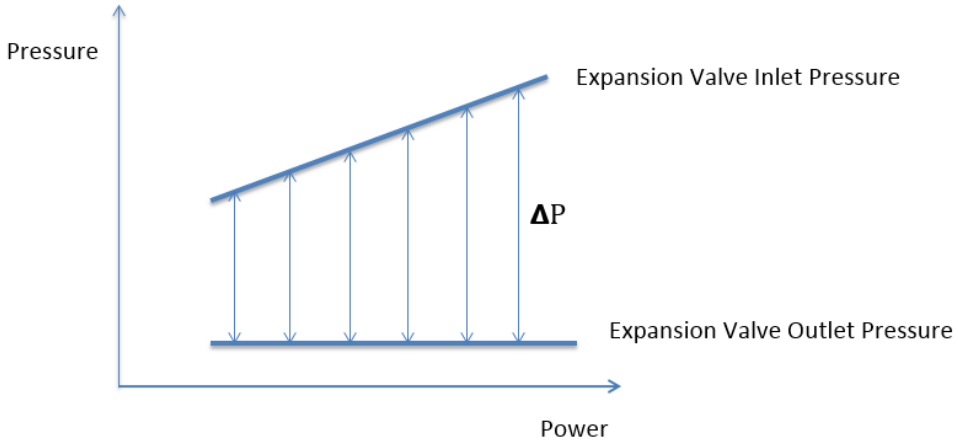


Figure 3.9. Pressure differences inlet and outlet of expansion valve

### 3.3.2. Energy and Exergy Analyses

In this part of the work, energy and exergy analyses were performed for a simple vapor compression refrigeration cycle. As it is known the steam compression system has four main elements: condenser, compressor, expansion valve and evaporator. To analyze a VCR system, we can think of a steady stream of states and apply the first law of thermodynamics to each of the major elements of equipment. Energy and mass are conserved in every element and also in the entire system. Table 3.11 displays the energy and energy equivalence and changes in the equation of exergy efficiency for each component (Dincer and Kanoğlu, 2010).

The coefficient of performance (COP) of the refrigeration system would be expressed as,

$$COP = \frac{Q_e}{W_{in}} \tag{3.51}$$

The COP value of a cooling cycle running between the $T_L$ and $T_H$ temperature limits based on the Carnot cooling cycle,

$$COP_{carnot} = \frac{T_L}{T_H - T_L} \tag{3.52}$$

The exergy efficiency of the VCR cycle is defined as,

$$n_{vcr} = \frac{COP}{COP_{carnot}} \tag{3.53}$$

The exergy efficiency of entire plant efficiency,

$$n_{overall} = \frac{Wspp+X_e}{X_{in}} \quad (3.54)$$

Table 3.11. Expressions used for energy and exergy analyses

| **Components** | **Energy Balance** | **Exergy Destruction Rate** | **Exergy Efficiency** |
|---|---|---|---|
| Turbine | $E_1 = W_t + E_2$ | $X_D = X_1 - W_t - X_2$ | $n_t = \frac{W_t}{X_1 - X_2}$ |
| Compressor | $E_3 + W_{Comp} = E_4$ | $X_D = X_3 + W_{comp} - X_4$ | $n_{comp} = \frac{X_4 - X_3}{W_{comp}}$ |
| Condenser | $E_4 + E_7 = E_5 + E_8$ | $X_D = X_4 + X_7 - X_5 - X_8$ | $n_c = \frac{X_8 - X_7}{X_4 - X_5}$ |
| Expansion Valve | $E_5 = E_6$ | $X_D = X_5 - X_6$ | $n_v = \frac{X_6}{X_5}$ |
| Evaporator | $E_6 + E_9 = E_3 + E_{10}$ | $X_D = X_6 + X_9 - X_3 - X_{10}$ | $n_e = \frac{X_3 - X_6}{X_9 - X_{10}}$ |

### 3.3.3. Exergoeconomic Analysis

An economic analysis of the cycle based on the provided product of exergy is made to calculate the cost per unit of excellence of the total return product. In this context, every element, the cost equilibrium equation and the auxiliary equations for each element of equipment are applied. In order to determine the inefficiency costs and thus increase the cost-effectiveness of the system, cost equivalence has been prepared for the VCR using equation (3.36).

For every flow of the system, parameter named the flow cost ratio Ċ ($/ h) is determined and the cost equivalence is performed for each element considering equations (3.37) and (3.38).

In this study, fuel exergy and product exergy should be determined. While the product exergy is determined for every element, the fuel represents the consumed source in the production process of the product. In conclusion, exergy analysis of product and fuel are conducted. The cost ratios of an element related to fuel ($\dot{C}_F$) and product ($\dot{C}_P$) are provided by modifying the exergy ratios (X). In the cost-equivalenced formulation, there is no cost term immediately related to exergy destruction of each element. Accordingly, the cost due to the destruction of the exergy of an element or process is a hidden cost. Both exergy destruction and cost equivalences is determined using equations (3.39) and (3.40).

In accordance with, the statement for the exergy destruction cost is determined in terms of equation (3.41). The investment cost rate for the elements is calculated using equation (3.42).

The variable emits the relative increase in the average cost per exergy unit between the product and fuel. The relative cost difference is a relevant tool for evaluating and optimizing system elements. The relative cost difference is determined by equation (3.44). In evaluating the performance of elements equation of (3.45) is used providing that exergoeconomic factor should be known. Exergoeconomics is the cost analysis method and it is performed by means of exergy analysis. In this method, a cost ratio equivalence is applied in which the sum of the cost ratios in relation with all exergy flows is even out the sum of the costs of whole incoming exergy flows plus the sum of operating and capital investment as well as maintenance costs. Cost ratio equivalences and auxiliary equations are placed in Table 3.12 for every element of the system.

Table 3.12. Cost rate equivalences as well as auxiliary equations for plant elements

| **Components** | **Cost rate balance** | **Auxiliary equations** |
|---|---|---|
| Turbine | $C_1 + Z_t = C_2 + C_t$ | $c_1 = c_2$ |
| Compressor | $C_3 + C_{comp} + Z_{comp} = C_4$ | **-------** |
| Condenser | $C_4 + C_7 + Z_c = C_5 + C_8$ | $c_4 = c_5$ |
| Expansion Valve | $C_5 + Z_v = C_6$ | **-------** |
| Evaporator | $C_6 + C_9 + Z_e = C_3 + C_{10}$ | $c_9 = c_{10}$ |

Table 3.13 summarizes the definitions of cost rate related to the fuel and product of the plant elements. The cost rate related to the fuel of elements contains the cost rates of the identical streams used in identical order and with the identical sign when the fuel exergy is defined.

Table 3.13. Cost rate associated with fuel and products of plant elements

| **Components** | **Cost rate of Fuel ($C_F$)** | **Cost rate of Product ($C_p$)** | **Variable** |
|---|---|---|---|
| Turbine | $C_1 - C_2$ | $C_t$ | $c_t$ |
| Compressor | $C_{comp}$ | $C_4 - C_3$ | $c_4$ |
| Condenser | $C_4 - C_5$ | $C_8 - C_7$ | $c_8$ |
| Expansion Valve | $C_5$ | $C_6$ | $c_6$ |
| Evaporator | $C_9 - C_{10}$ | $C_6 - C_3$ | $c_3$ |

The capital cost of vapor compression refrigeration cycle elements *Z* value can be described as a combination of related parameters. Capital cost equations of system elements are displayed in Table 3.14 (Dincer et al., 2017).

Table 3.14. Capital cost equations for system elements

| Components | Capital cost |
|---|---|
| Turbine | $Z_t = C\ (W_t)^{0.7}\ \left[1+\left(\frac{0.05}{1-n_t}\right)^3\right]\left\{1+exp\left(\frac{T_1-866K}{10.42K}\right)\right\}$ |
| Compressor | $Z_{comp} = \frac{573\ \dot{m}_{ref}}{0.8996-n_{comp}}\left(\frac{P_{cond}}{P_{eva}}\right)\log\left(\frac{P_{cond}}{P_{eva}}\right)$ |
| Condenser | $Z_c = 516.62A_c + 268.45$ |
| Expansion Valve | $Z_v = 37\left(\frac{P_5}{P_6}\right)^{0.68}$ |
| Evaporator | $Z_e = 309.14A_e + 231.95$ |

### 3.4. Desalination System

#### 3.4.1. System Description

The existing desalination plant has been commissioned to fulfill the water requirements of the steam power plant. It is based on the MED with thermal vapor compression technology and contains four effects (Plate type heat exchangers) at full load with a total capacity of 2.000 $m^3$/day. A schematic diagram of the MED-TVC system is presented in Figure 3.10. The system comprises four horizontally falling film evaporators. The incoming seawater is preheated in a distiller cooler and in an end condenser. A fraction of the feed water is returned to the sea when necessary and the remainder is divided into 4 equal flows to form the water supply. A small proportion of the live steam is removed by turbine flows into the vacuum ejector, and the remaining steam is transferred to the steam ejector as motive steam. The flow of steam from the nozzle forms a vacuum that draws the steam

formed into the final effect. The combined vapor streams are then compressed in the ejector to meet the first thermal requirement. The condensate leaving the first effect is divided into two streams. The heated steam causes the feed from the top to evaporate the brine. The steam generated by the first effect is then fed to the tube side of the next effect, which features the same condensation and a repetition of the evaporation process. The brine produced in the first effect is stepped down to the next effect for flashing. In the last effect, seawater is discharged as brine. Distilled water collected from the four effects feed the water– the steam cycle of the steam power plant (Hamed et al., 1996). Operating parameters about desalination plants at full load are given in Table 3.15.

Table 3.15. Operating conditions

| **Parameters** | **Value** |
|---|---|
| Capacity ($m^3$/day) | 2000 |
| Salinity (ppm) | 44000 |
| Top brine temperature, $T_1$ (°C) | 66 |
| Discharged temperature, $T_d$ (°C) | 42 |
| Last brine temperature, $T_4$ (°C) | 54 |
| Temperature drop / effect, $\Delta T$ (°C) | 4 |
| Number of effects | 4 |
| Motive steam pressure, $P_s$ (bar) | 15 |
| Motive steam flow rate, S (kg/s) | 3 |
| Feed seawater temperature, $T_f$ (°C) | 23 |
| Feed seawater flow rate, F (kg/s) | 350 |
| Boiling point elevations (BPE) (°C) | 0.8 |

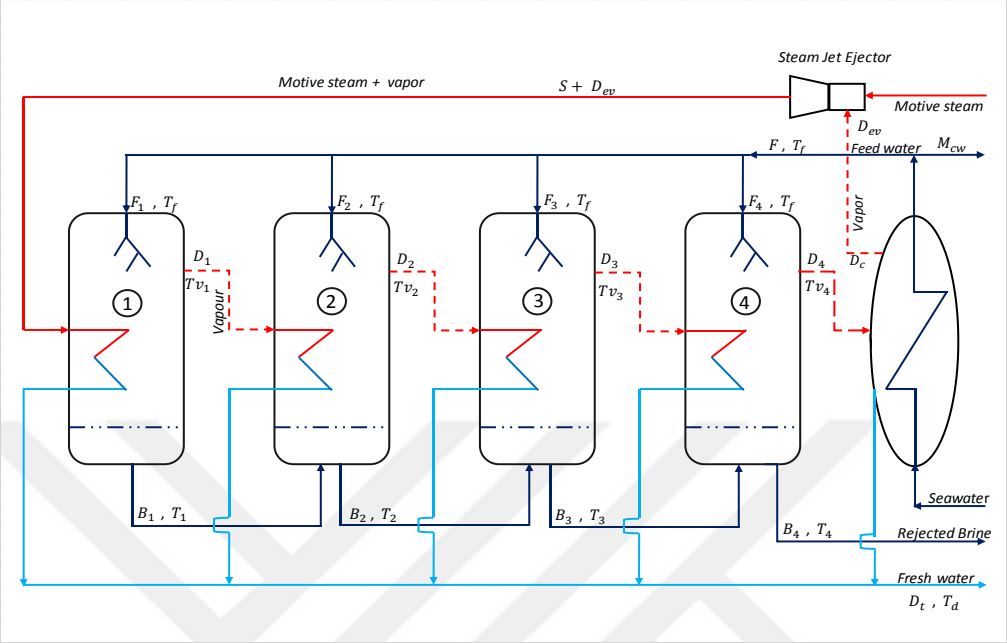


Figure 3.10. Schematic diagram of the MED-TVC system

### 3.4.2. Analysis

The energy and exergy analyses on the MED-TVC were carried out by applying mass and energy conservation laws to subsystems such as end condensers, evaporators and vapor ejectors. Some assumptions were made in applying the analysis: steady-state operation, equal temperature difference throughout the feed heaters, distillation (without distillation contributions from each effect), and specific temperature changes, as well as temperature, salinity and boiling point elevation were ignored (Bin Amer, 2009).

Most of the thermodynamic analyzes of steam plants and TVC systems are based on the first law of thermodynamics. Since both thermal, kinetic and potential energy are used in steam power plants, the first law of thermodynamics has a special significance for evaluating systems. Although the first law of thermodynamics is a significant tool in evaluating the overall performance of the thermal vapor compression desalination plant, this analysis does not add to the

quality of the transferred and converted energy. A thermodynamic analysis using the first law cannot illustrate where the maximum loss of available energy happens and concludes that energy loss to the environment and blowdown (brain rejects) are the only important losses. In this sense, exergy analysis is necessary to place all energy interactions on the same basis and to provide appropriate guidance for process improvement (Mabrouk et al., 2007). The TVC system performance parameters are given in Table 3.16.

Table 3.16. Thermal vapor compression desalination system performance parameters (Fellah et al., 2014)

| **Parameter** | **Unit** | **Equation** |
|---|---|---|
| Gain output ratio (GOR) | - | $GOR = \frac{D}{S}$ |
| Specific energy consumption | kWh/m$^3$ | $\frac{Q}{D} = S(h_s - h_c)$ |
| Specific exergy consumption | kWh/m$^3$ | $\Delta ex = \frac{\Delta X}{D}$ |
| Exergy efficiency | % | $n_{ıı} = \frac{X_D}{X_{in}}$ |

The total loss of exergy consists of the individual exergy losses of the plant subsystems. The exergy efficiency deficit of each subsystem is defined one by one (Alasfour and Alajmi, 2010).

- **Steam Ejector**

Equations used for calculations of the energy balance and exergy destruction are as follows:

$$Sh_s + D_{ev}h_{ev} = (S + D_{ev})h_{dc} \quad (3.55)$$

$$I_{ej} = \Delta\Psi_{ej} = S[(h_s - h_{dc}) - T_0 (s_s - s_{dc})] + D_{ev} [(h_{dc} - h_{gn}) - T_0 (s_{dc} - s_{gn})] \quad (3.56)$$

- **First effect (or stage)**

Equations used for the energy balance and exergy destruction are also stated below:

$$(S + D_{ev})(h_{dc} - h_c) = F_1 C(T_1 - T_f) + D_1 L_1 \quad (3.57)$$

$$I_1 = (S + D_{ev})[(h_{dc} - h_c) - T_0(s_{dc} - s_c)] - F_1 C \left[(T_1 - T_f) - T_0 \ln \frac{T_1}{T_f}\right] - D_1 L \left(1 - \frac{T_0}{T_{v1}}\right) \quad (3.58)$$

- **Second effect**

Equations to determine the energy balance and exergy destruction are given as follows:

$$D_1 L + (F_1 - D_1)C(T_1 - T_2) = F_2 C(T_2 - T_f) + D_2 L \quad (3.59)$$

$$I_2 = D_1 L \left(1 - \frac{T_0}{T_1}\right) + (F_1 - D_1)C \left[(T_1 - T_2) - T_0 \ln \frac{T_1}{T_2}\right] - D_2 L \left(1 - \frac{T_0}{T_2}\right) - F_2 C \left[(T_2 - T_f) - T_0 \, ln \frac{T_2}{T_f}\right] \quad (3.60)$$

- **N$^{th}$ effect**

Similarly, equations for the calculation of energy balance and exergy destruction are stated below:

$$D_{i-1}L_{i-1}[(F_1 - D_1) + (F_2 - D_2) + \cdots (F_{i-1} - D_{i-1})]C\Delta T = F_iC(T_i - T_f) + D_i \quad (3.61)$$

$$I_i = \Delta\Psi_i = D_{i-1}L_{i-1}\left(1 - \frac{T_0}{T_{v(i-1)}}\right) + \left(\sum_{k=1}^{i-1}(F_i - D_i)\right)C\left[\Delta T - T_0\, ln\frac{T_{i-1}}{T_i}\right] - D_iL\left(1 - \frac{T_0}{T_{vi}}\right) - F_iC\left[(T_i - T_f) - T_1 \ln\frac{T_i}{T_f}\right] \quad (3.62)$$

- **End Condenser**

Foe end condenser the following equations are generally used for the energy balance and exergy destruction:

$$D_cL_n = (M_{cw} - F_t)C(T_f - T_{cw}) \quad (3.63)$$

$$I_c = \Delta\Psi_c = D_cL_n\left(1 - \frac{T_0}{T_n}\right) - (M_{cw} - F_t)C\left[(T_f - T_{cw}) - T_0\, ln\frac{T_f}{T_{cw}}\right] \quad (3.64)$$

The total desalinated product output is expressed by the following expiration:

$$D_t = \sum D_i = D_1 + D_2 + \cdots + D_n \quad (3.65)$$

### 3.4.3. Thermo-Economic Analysis

Thermo-economics is an engineering discipline that combines thermodynamic assessments on an exergy basis in a manner that is economically appropriate, at the level of system components, it provides information that is useful for designing and operating a cost-effective system, but it is not possible to obtain through the traditional exergy and economic analyses. Figure 3.11 presents the cost balance of a desalination plant.

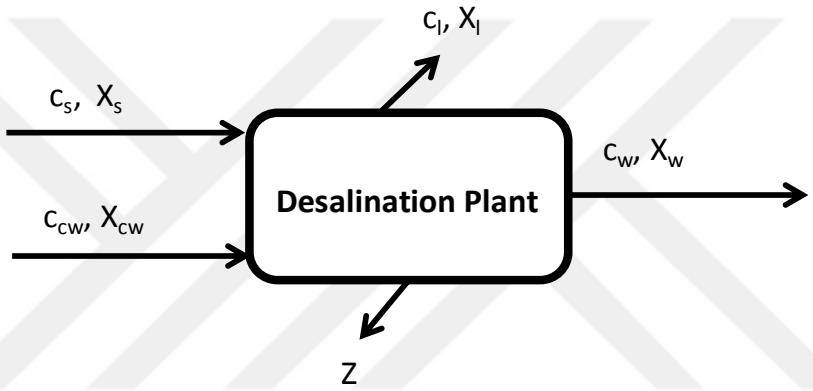


Figure 3.11. Cost balance of a desalination plant

For each flow in a system, a parameter called flow cost rate $\dot{C}$ (\$/h) is defined, and a cost rate balance is expressed for each component as follows:

$$\dot{C}_s + \dot{C}_{cw} + \dot{Z} = \dot{C}_l + \dot{C}_w \tag{3.66}$$

The cost rate balances are usually expressed as positive, as shown below:

$$c_s X_s + c_{cw} X_{cw} + \dot{Z} = c_l X_l + c_w X_w \tag{3.67}$$

The unit product cost is shown by equation (3.78):

$$\text{Unit cost } \left(\$/_{m^3}\right) = \frac{\dot{C}_l + \dot{C}_w}{\dot{m}_w} \quad (3.68)$$

Fuel exergy and product exergy must be defined in this assessment. When the product exergy is defined based on the component in question, the fuel refers to the consumed source in the production. The product and the fuel are shown in terms of exergy. The cost ratios associated with the fuel and product of a component are obtained by changing the rates of exergy.

The investment cost rate for the elements and capital recovery factor are calculated using equations (3.42) and (3.43).

### 3.5. Greenhouse Heating

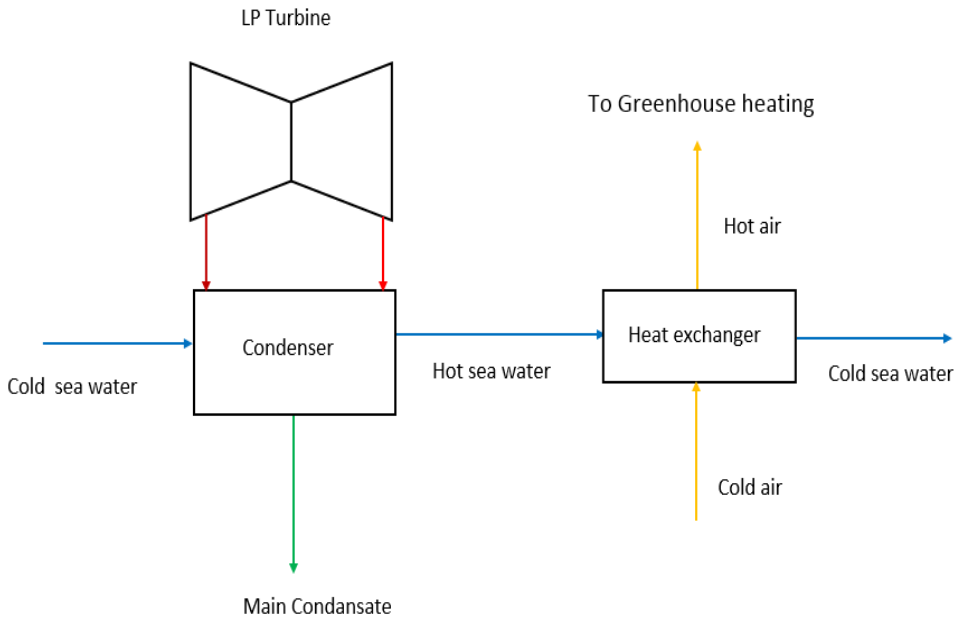


Figure 3.12. Greenhouse heating mechanism

Greenhouse activities around the power plant have been increasing day by day. Together with the increase of greenhouses, the required heat also increases. It

determined to be economical to meet this heat requirement from the waste heat of the power plant and this application upgrades the efficiency of the power plant positively. As can be seen in Figure 3.12, low temperature waste heat sources are sufficient in many cases for greenhouses agriculture industry. Rejected heat to the seawater from the condenser can be recovered using heat exchangers. There are growing applications that heat is transferred to greenhouses is to keep its temperature in the desired temperature range to preserve crops.

Normally in winter time, the cold sea water temperature is around 18 ºC. Hot seawater temperature becomes 25 ºC approximately. The atmospheric air temperature is variable and it is around 10 ºC in winter. The greenhouse needs a constant temperature, but this depends on the type of herbs and vegetables grown and other plants. In this study, the required heat for the tomato greenhouse is considered and the temperature is expected to be kept between 20 ºC and 25 ºC.

### 3.6. Multigeneration System

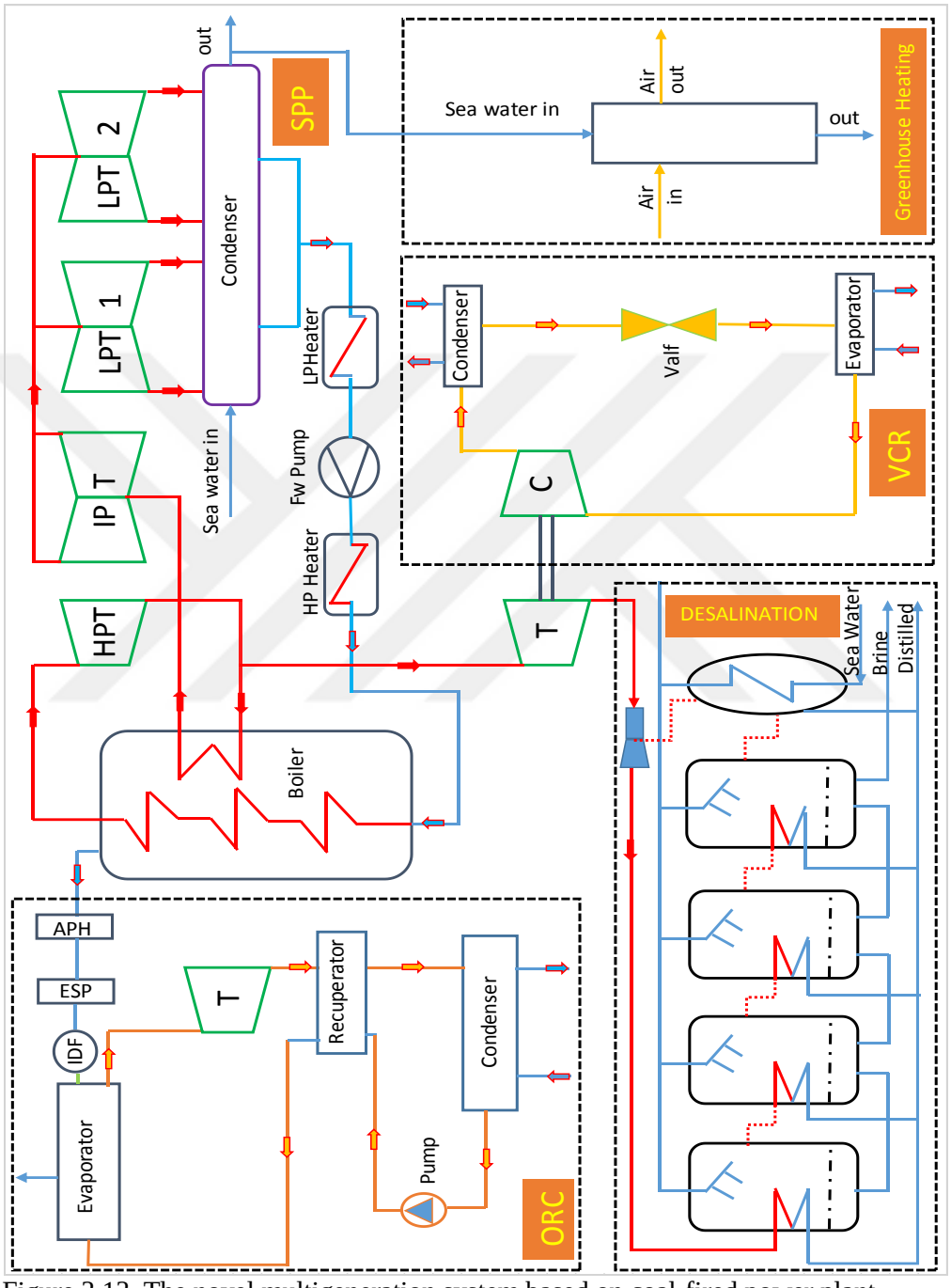


Figure 3.13. The novel multigeneration system based on coal-fired power plant

The novel multigeneration system based on coal-fired power plant is shown in Figure 3.13. The multigeneration system is designed to produce different outputs using waste heat of coal-fired power plant.

This system consists of four different subsystems. These are ORC, VCR, Desalination plant and Greenhouse heating system. The system uses coal as a prime mover to achieve electricity production, distilled water, cooling purposes and greenhouse heating.

The organic Rankine cycle is placed downstream of the boiler to recover the unused heat of flue gas. The ORC produces extra electricity with R245fa working fluid. Flue gas temperatures vary between 150 ºC and 160 ºC. The ORC evaporator recovers heat from flue gas until 110 ºC to avoid acid formation on flue gas channel and stack.

The VCR is designed and modeled to cool indoors of the power plant. The refrigeration cycle is driven by a steam turbine. Normally, the steam is fed to the desalination unit by means of a pressure relief valve which is withdrawn the steam from the cold reheat line of the steam power plant.

In the newly designed system, a steam turbine is installed instead of the pressure reducing valve and the compressor of the refrigeration cycle is driven by this turbine.

Distilled water is used as a working fluid in steam power plants and continuous reinforcement is required. The desalination plant is integrated into the steam power plant to meet water make-up and reduce water costs. Desalination process is a thermal process and brine is extracted from seawater using steam coming from the cold reheat line through the steam turbine.

As it is known that in thermal power plants, the most heat energy loss occurs in the condenser. But the temperature of wet steam in the condenser is very low, namely, it is around 30 ˚C and thermodynamically insignificant. Greenhouse cultivation has been increasing around the thermal power plant since constant and

low heat is required in the greenhouses to keep temperature of greenhouse at desired level.

### 3.6.1. Analysis

The exergy efficiency, defined as the product exergy output divided by the exergy input, for the steam power plant, the greenhouse heating system, the vapor compression refrigeration system, the desalination system, the organic Rankine cycle and overall multigeneration systems, can be expressed as follows (Dincer and Zamfirescu, 2014):

$$n_{single} = \frac{W_{spp}}{X_f} \tag{3.69}$$

$$n_{cogen} = \frac{W_{spp}+X_{ghouse}}{X_f} \tag{3.70}$$

$$n_{tri} = \frac{W_{spp}+X_{ghouse}+X_{cooling}}{X_f} \tag{3.71}$$

$$n_{quat} = \frac{W_{spp}+X_{ghouse}+X_{cooling}+X_{distilled}}{X_f} \tag{3.72}$$

$$n_{multi} = \frac{W_{spp}+X_{ghouse}+X_{cooling}+X_{distilled}+W_{ORC}}{X_f} \tag{3.73}$$

# 4. RESULTS AND DISCUSSION

## 4.1. Steam Power Plant Case

The variation in energy and exergy efficiencies for three types of the boilers such as subcritical, supercritical and ultra-superciritcal are shown in Figure 4.1. As seen from this figure, the exergy efficiency of the three types of system is always lower than the energy efficiency. The higher level of exergy destruction in the boiler is due to the finite temperature differences between the flue gas and the working fluid. The losses in the boiler occur because of an increase in entropy generation of the flue gases. Both the chemical reaction and heat transfer are irreversible processes. The process of combustion generally happens simultaneously with heat transfer. Additionally, substantial amounts of heat loss are conveyed by the flue gases to the environment at a high temperature. High-quality energy is ejected outside via flue gases, so exergy efficiency is lower. As the boiler pressure is increased, efficiencies for three types of boilers are positively affected.

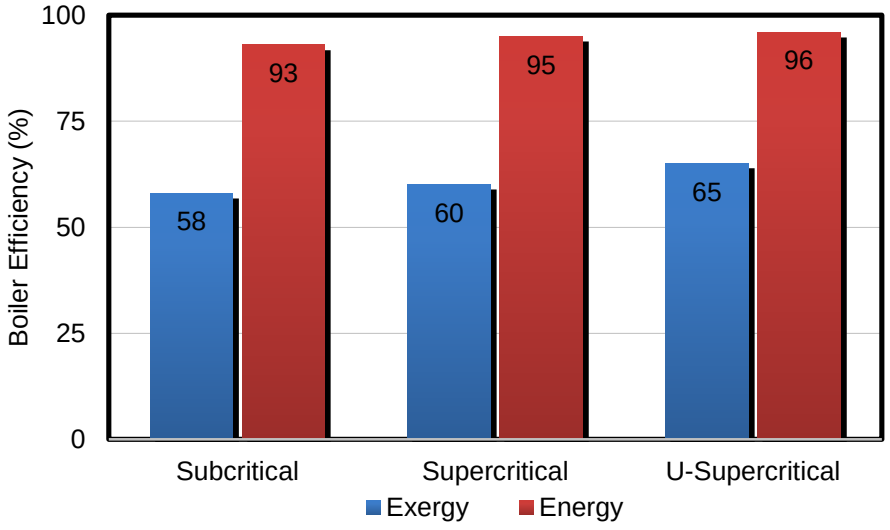


Figure 4.1. Energy and exergy efficiencies of boilers in power plants

Figure 4.2 shows the energy losses of the condensers in power plants. As seen from this figure, the energy loss of a subcritical condenser is always higher than the other power plants such as supercritical and ultra-supercritical power plants. For example, 48.1%, 46.2% and 43.4% of the total energy are ejected to the environment via the condenser for subcritical, supercritical and ultra-supercritical power plants, respectively. The reason for condenser losses is the latent heat of the exhaust steam which is transferred to the cooling water, because the enthalpy of exhaust steam, which comes from the LP turbines, is higher compared to the condensed water.

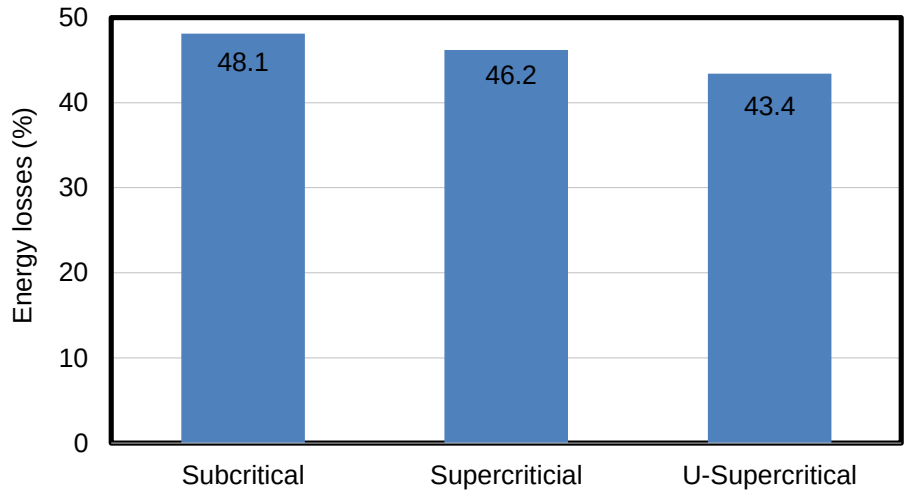


Figure 4.2. Energy losses from condensers in power plants

Figure 4.3 presents the exergy efficiency of the turbines for the three different types of power plant considered. The exergy destructions in the turbines are associated with the pressure drop and expansion process. Fluid friction happens when the fluid expands through the steam turbine blades. These friction losses result in the dissipation of part of its energy into heat itself at the expense of useful work. The fluid then does less work and leaves through the exhausts with a higher

temperature. Greater irreversible processes result in a higher turbine exit temperature and less work. The exergy efficiency in the LP turbines is lower than in the IP and HP turbines because the LP turbines work at vacuum pressure so that the condensation process begins and steam leaves the LP turbines as a water-steam mixture. Therefore, the rate of entropy and irreversibility increases substantially with the condensation process. The value of exergy efficiencies in the $LP_1$ and $LP_2$ turbines are close to each other because the operating conditions are almost the same. All turbine efficiencies in ultra-supercritical power plants are higher than subcritical and supercritical ones due to technological progress in the development of turbines.

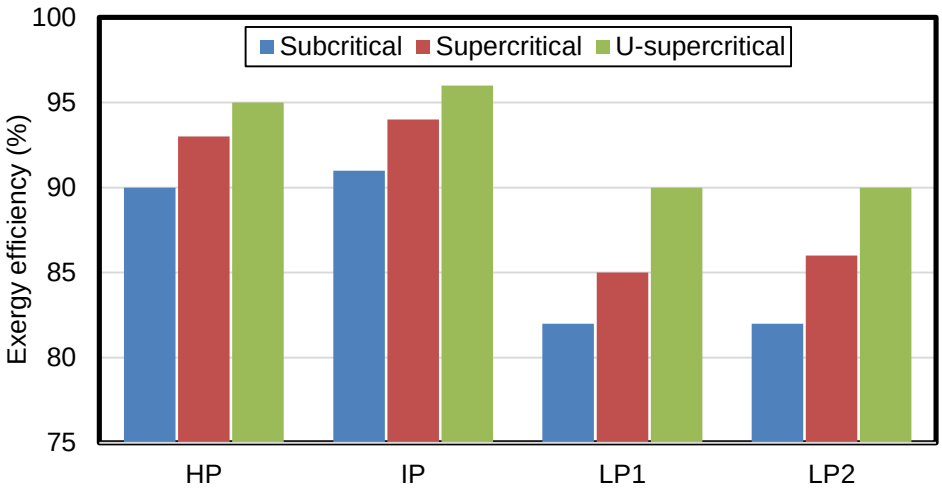


Figure 4.3. Exergy efficiencies for turbines in the three types of power plants

The exergy efficiencies of the boiler feed pumps in power plants are shown in Figure 4.4. The exergy destructions take place in pumps and are associated with friction or irreversibilities in the supercritical power plant, which is usually very small compared to cases of subcritical and ultra-supercritical power plants. Exergy efficiency in pumps is directly proportional to the compression and the type of drive. Supercritical and ultra-supercritical cycle pump efficiencies are far higher

than the subcritical cycle because supercritical and ultra-supercritical pumps are a steam turbine driven so electric energy losses are negligible.

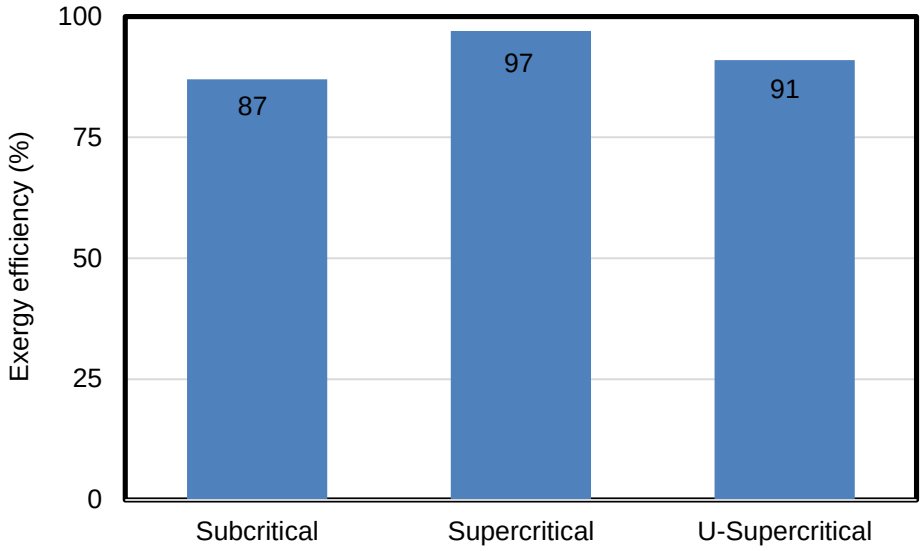


Figure 4.4. Exergy efficiencies for boiler feed pumps in power plants

Figure 4.5 presents the coal consumption per unit of electricity generation in steam power plants. Coal consumptions per MWh of electricity generation is a relevant tool for the unit efficiency. As seen from this figure, the coal consumption of subcritical power plants is higher than other power plants. The values are 372 kg, 352 kg and 318 kg of coal consumed per MWh of electricity generation at subcritical, supercritical and ultra-supercritical power plants, respectively.

Figure 4.6 illustrates the overall energy and exergy efficiencies of power plants. The overall energy values for the subcritical, supercritical and ultra-supercritical power plants were 41.5%, 43.8% and 46.0%, respectively. The corresponding exergy efficiencies for the thermal power plants were calculated to be 39.1%, 40.8% and 41.9%, respectively. The overall power plant efficiency is affected by its components' efficiencies, and those component efficiencies and

overall efficiency increase with increased boiler pressures. Although the amount of energy losses and exergy destructions of power plants are increased, a reduction in the percentage of energy losses and exergy destructions result in an upgrading of the overall efficiencies when the boiler pressure is increased.

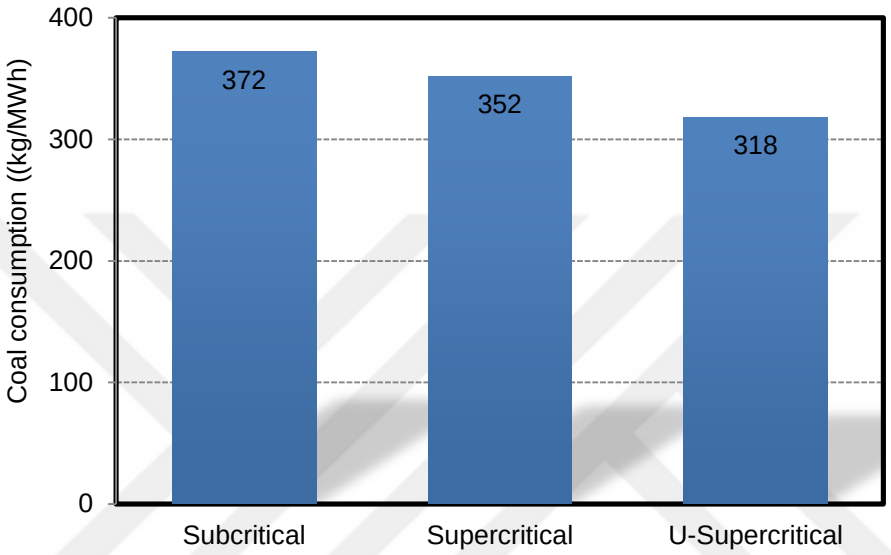


Figure 4.5. Coal consumptions per electricity generation in power plants

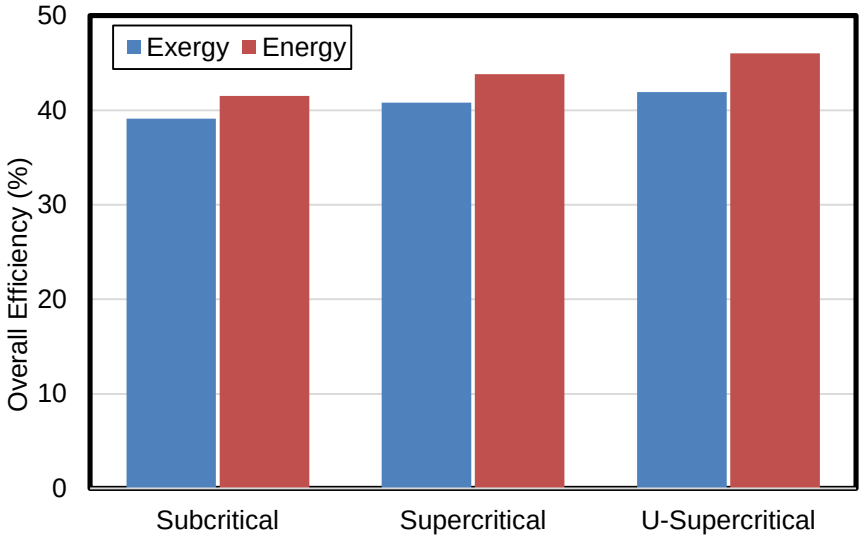


Figure 4.6. Overall energy and exergy efficiencies of power plants

### 4.1.1. Economic Analysis

An assessment regarding the financial aspects of the plant was conducted on the basis of initial capital investment and operating costs. The equipment cost includes boiler, steam turbine, condenser, generator and auxiliary equipment – such as the condensate extraction pump, boiler feed pump and so on. Thus, the total fixed equipment cost can be determined according to the redundancies of respective components as follows (Kumar et al., 2014):

$$C_i = f(C_{boiler} + C_{turbine} + C_{condenser} + C_{BFP} + C_{axuillary}) \quad (4.1)$$

The total operating costs include maintenance, insurance, total operating labor and purchase of coal feedstock as follows:

$$C_{op} = (C_{maint} + C_{ins} + C_{labor} + C_{coal}) \quad (4.2)$$

Where, C is the cost while subscripts *op*, *maint*, *ins*, *labor* and *coal* refer to operating, maintenance, insurance, labor and fuel cost, respectively.

In this study, the salvage value of each power plant was taken to be 5% of the total fixed cost. The economic life is considered to be 25 years for each power plant. Also, the annual working period was estimated to be 8000 hours for each power plant. The discount ratio was determined to be 10%. The discount rate is affected by the market interest rate related to the project and shows the cost of the capital. The discount rate is the minimum rate of yield that the investor expects to achieve from the investment that is considered to be invested. The minimum expected internal productivity rate from an investment, in other words, the profitability of the investment, is determined by the effect of many factors. Those factors are the profit rate in the market, the inflation rate, the interest rate, the efficiency ratio of risk-free investments, the grade of a risk of investment and so on

are factors that are effective in determining the expected internal rate of return or the discount rate. Before investing, the investor is curious to know the present value of the net income that the project will make over its economic life. For this reason, the calculation of the specific cost of a unit production has a very important role in calculating the profitability ratio of the investment.

Thus, by using Net present value (NPV), the expenses for each power plant was calculated for a 25-year economic life as follow:

$$NPV = \sum_{t=1}^{n} C_i + \frac{C_{op}}{(1+k)^t} - \frac{SV}{(1+k)^n} \quad (4.3)$$

Where $k$ is the discount ratio and $SV$ is the salvage value for each power plant.

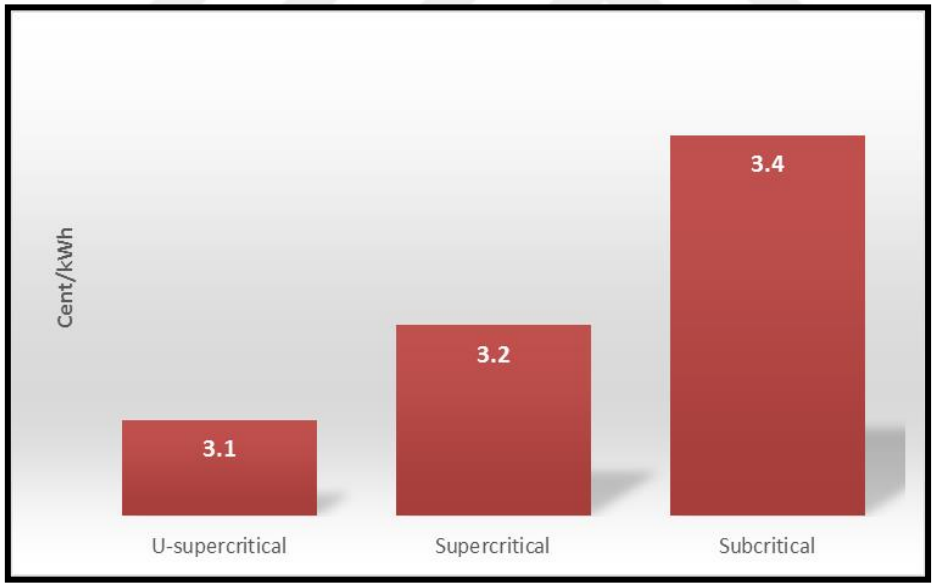


Figure 4.7. Specific cost per unit electricity

Figure 4.7 shows the unit cost electricity generation per kWh according to the power plant type. According to the results, the ultra-supercritical cycle unit cost

per unit of electricity production is lower in comparison to the other power plants. Although the investment cost is higher, the fuel cost is lower due to higher thermal and exergy efficiency.

### 4.2. ORC Case

#### 4.2.1. Effect of Flue Gas Temperature

In this section, the effect of the flue gas temperature on the ORC system performance was determined, analyzed and the results obtained were discussed. Organic working fluids such as R245fa, R236fa, R600 and R236ea were considered as a working fluid in the present ORC system and driven by exhaust waste heat. The thermodynamic properties of these working fluids were determined by the Epsilon Simulation Program for the thermal power plant. The variation in the exergy efficiency of the ORC system as a function of flue gas temperature is presented in Figure 4.8. As it can be seen from the figure, the exergy efficiency of the ORC system decreases with increasing flue gas temperature due to the high amount of exergy destruction which is caused by the increase of temperature differences between the organic working fluid and the flue gas. In addition, calculations indicated that the exergy efficiency values of the R245fa working fluid were higher than other fluids.

Variation of the exergy efficiency of the evaporator unit as a function of flue gas temperature is shown in Figure 4.9. As it can be seen from the figure, the exergy efficiency of the evaporator unit slightly decreases when the flue gas temperature rises. The most important reason for this decrease is the difference in temperature between the flue gas inlet and the evaporator inlet. As the flue gas temperature increases, this temperature difference will increase even more. As a result, exergy destruction is adversely affected, so the exergy efficiency of the evaporator is even lower. So temperature difference between flue gas inlet and the evaporator inlet is the lowest for R245fa, while it is quite high for R236fa.

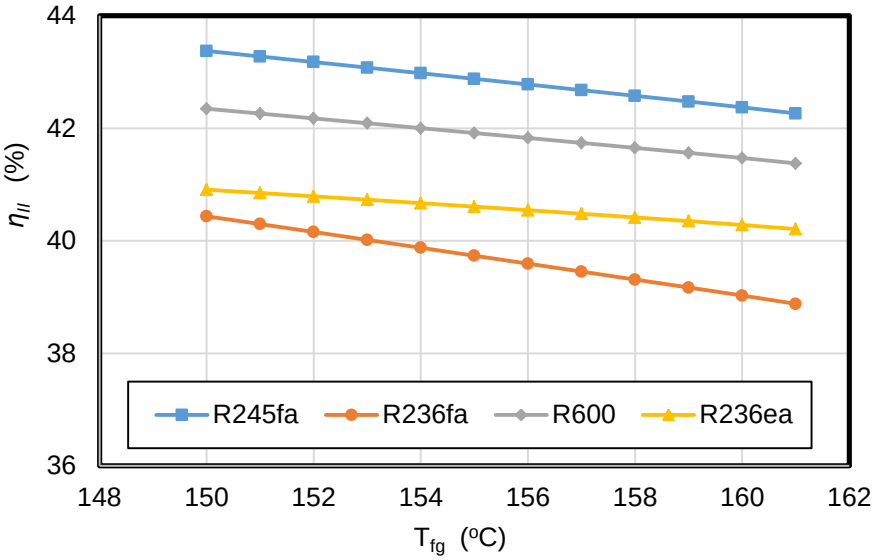


Figure 4.8. Variation in the exergy efficiency of the ORC system as a function of the flue gas temperature

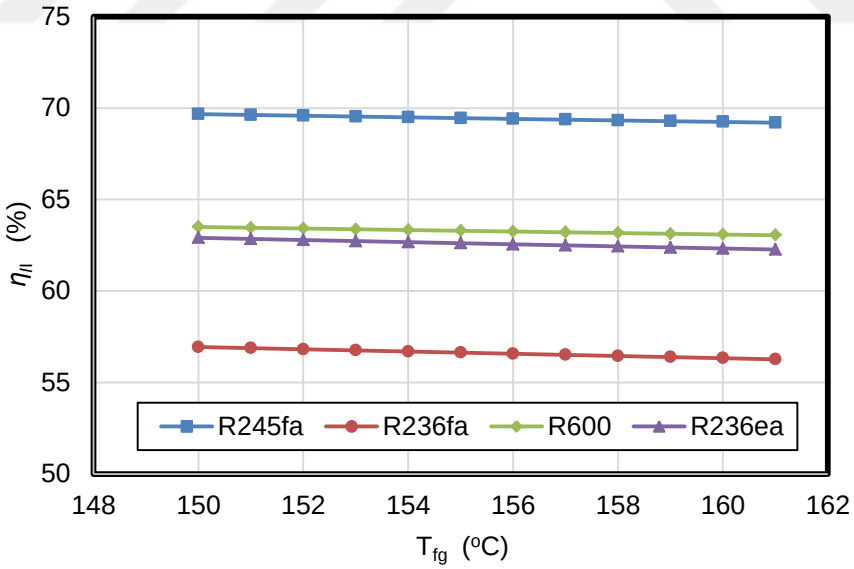


Figure 4.9. Variation in the exergy efficiency of the evaporator unit as a function of the flue gas temperature

Variation of the exergy efficiency of the turbine as a function of flue gas temperature is shown in Figure 4.10. Properties of the turbine, such as design, frictional losses and the pressure ratio cause exergy destruction. The results indicated that the turbine exergy efficiencies for the fluids R245fa, R600, R236ea and R236fa have an ignorable decrease with increasing flue gas temperature. Also, exergy efficiency of R236fa was found lowest among all examined fluids.

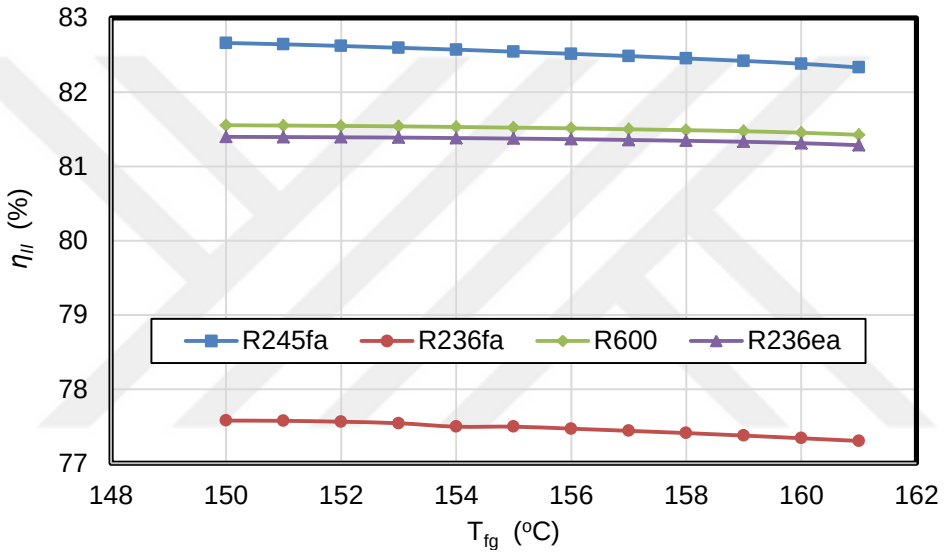


Figure 4.10. Variation in the exergy efficiency of the turbine as a function of the flue gas temperature

Figure 4.11 shows the variation in exergy efficiency of the pump as a function of flue gas temperature. The exergy efficiency of the pump is directly related to the pumping work. As a result of this pumping work, hot organic working fluids caused too much entropy generation inside the pump. For this reason, the exergy efficiency of the pump clearly decreases with an increase in flue gas temperature. R245fa working fluids show better performance compared to other fluids.

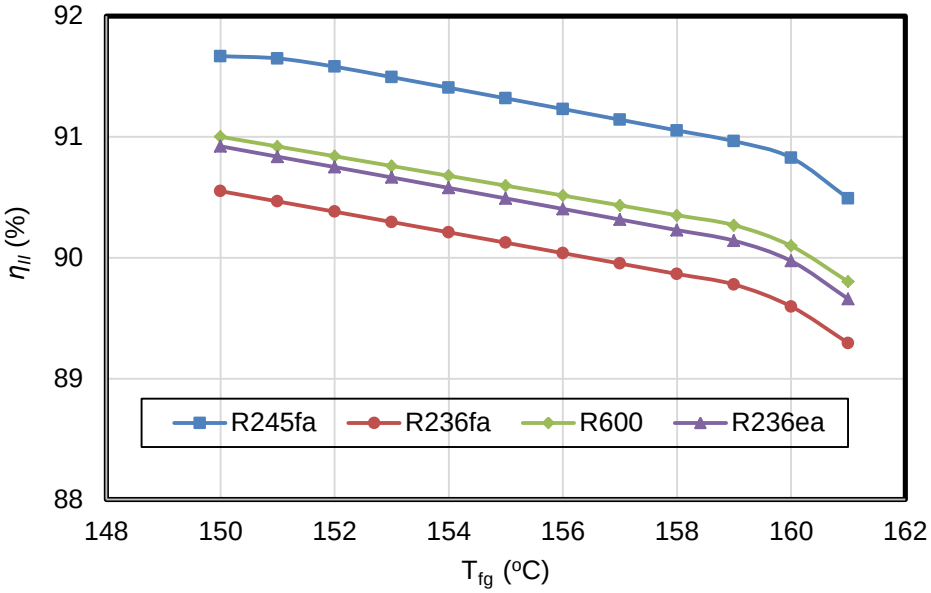


Figure 4.11. Variation in the exergy efficiency of the pump as a function of the flue gas temperature

Variation of the net output power of the ORC system as a function of flue gas temperature is presented in Figure 4.12. It can be observed from the figure that the net output power of the ORC system shows a clear linear increase with an increase in flue gas temperature. So, effective use of exhaust heat and a higher grade of heat source will positively affect and increase the net output power, and the energy efficiency of the ORC system. Furthermore, the best result among the working fluids was obtained with R245fa.

Variation of the energy efficiency of the ORC system as a function of flue gas temperature is presented in Figure 4.13. It is known that energy efficiency only deals with the quantity of energy. However, the exergy efficiency deals with the quality of the energy with an increase of flue gas temperature, although the exergy efficiency of the ORC system decreases slightly, the energy efficiency of the ORC system has a slightly increases.

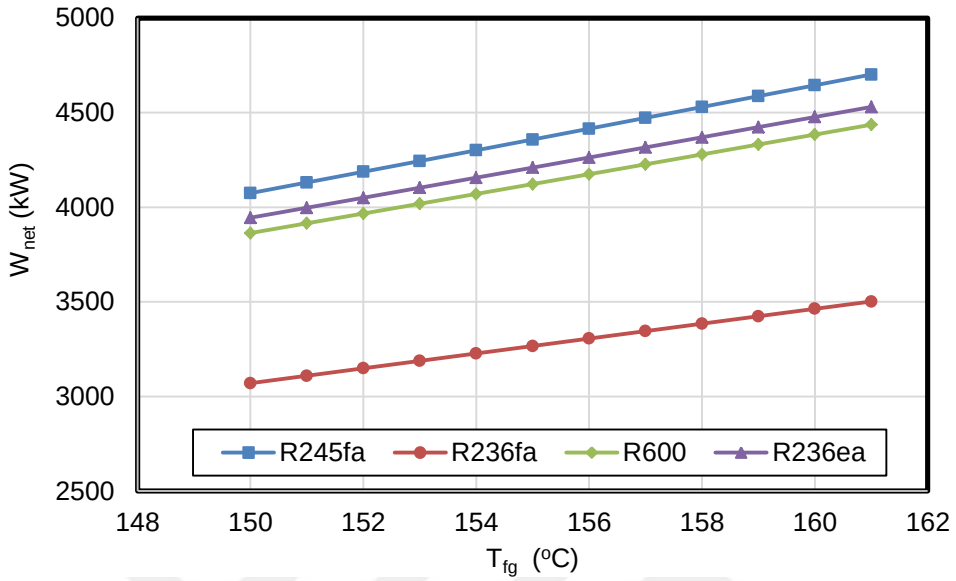


Figure 4.12. Variation in the net output power as a function of the flue gas temperature

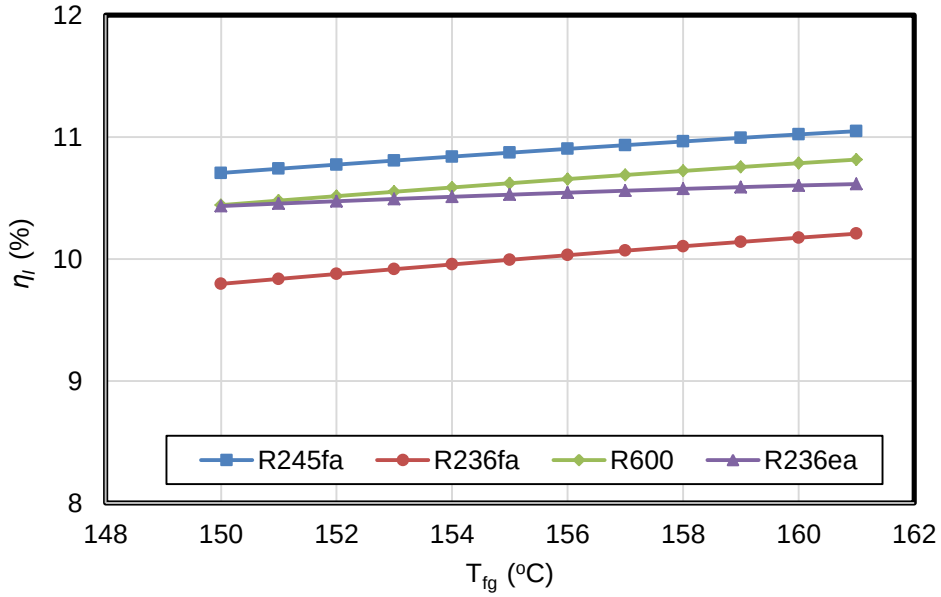


Figure 4.13. Variation in the energy efficiency of the ORC system as a function of the flue gas temperature

### 4.2.2. Effect of Flue Gas Mass Flow Rate

In this section, the influence of the flue gas mass flow rate on the ORC system performance is determined, analyzed and discussed. The variation in the exergy efficiency of the ORC system as a function of the flue gas mass flow rate is presented in Figure 4.14. As the mass flow rate increases, the efficiency of exergy increases for all working fluids considered in the present work. Because of an increase in the mass flow rate, the heat transfer in the evaporator of the ORC system is further raised, and therefore the net output power is upgraded. In addition, the reduction in exergy destruction by the equipment improves the overall system efficiency.

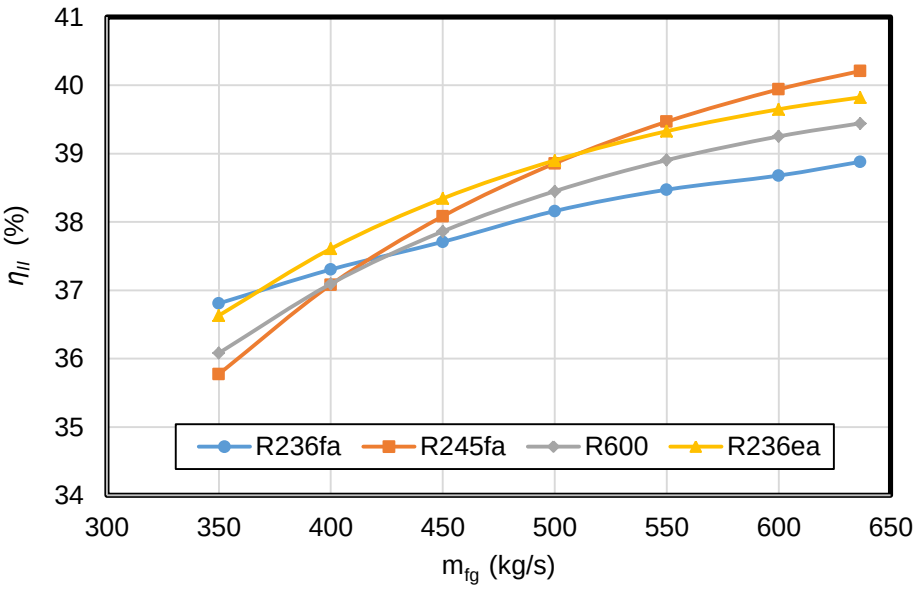


Figure 4.14. Variation in the exergy efficiency of the ORC system as a function of the flue gas mass flow rate

Since the evaporator is the first unit in which the flue gas heat is transferred to the heat recovery system, it is considered as a most important part of the ORC system. Because of this, the waste heat must be efficiently transferred to the power

system. As shown in Figure 4.15, the exergy efficiency of the evaporator unit clearly increases with an increase in the flue gas mass flow rate. In other words, the higher rate of flue gas mass flow rate improves the exergy efficiency of the evaporator unit further. In addition, the result of calculations showed that the exergy efficiency values for the R245fa working fluid were higher than the other working fluids.

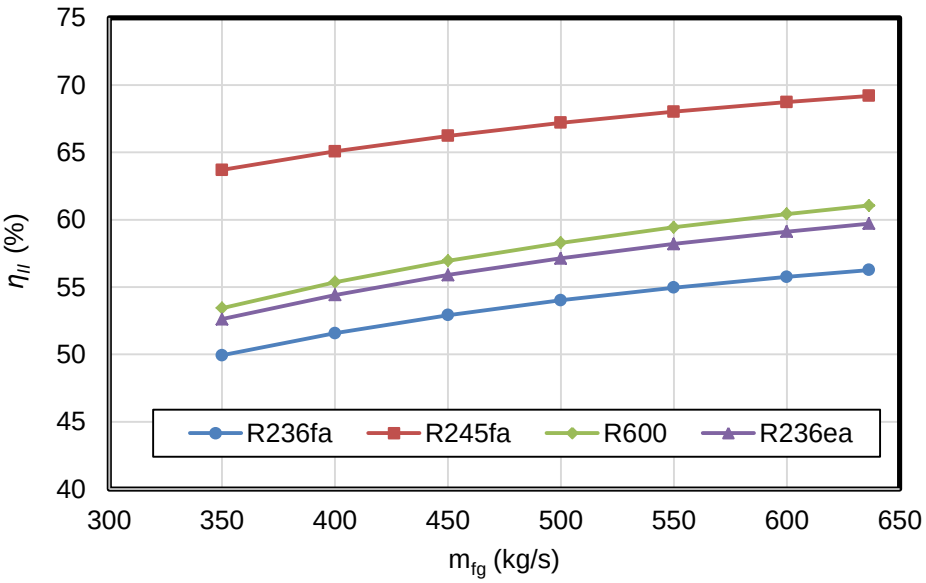


Figure 4.15. Variation in the exergy efficiency of the evaporator unit as a function of the flue gas mass flow rate

The variation of the exergy efficiency of the turbine with the flue gas mass flow rate is illustrated in Figure 4.16. The results indicated in this figure that the turbine exergy efficiencies for working fluids such as R236ea, R600 and R245fa decrease in small quantities with an increase of the flue gas mass flow rate but the exergy efficiency of R236fa decreases more than other working fluids with an increase of the flue gas mass flow rate. R245fa has a maximum efficiency among the other working fluids as a function of the flue gas mass flow rate. On the other

hand, R236fa has the lowest efficiency among the other working fluids for the same case.

The variation in the exergy efficiency of the pump on the flue gas mass flow rate is presented in Figure 4.17. As seen from this figure that the best working fluid in terms of the pump exergy efficiency is R245fa explicitly. For the highest exergy efficiency of the pump calculated as 91.8% for the flue gas mass flow rate of 450 kg/s. This flue gas mass flow rate is an optimum value for the maximum exergy efficiency of the pump which rated as 91.8%.

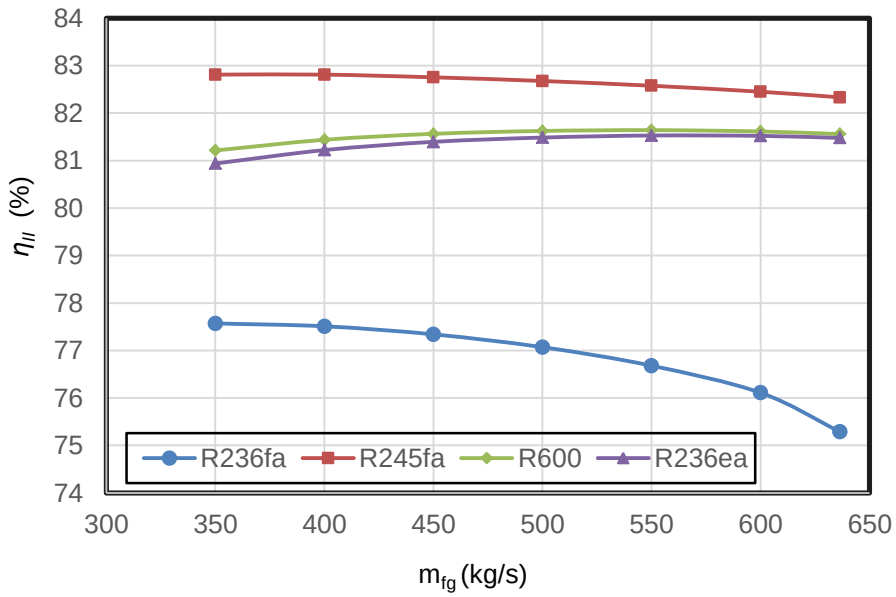


Figure 4.16. Variation in the exergy efficiency of the turbine as a function of the flue gas mass flow rate

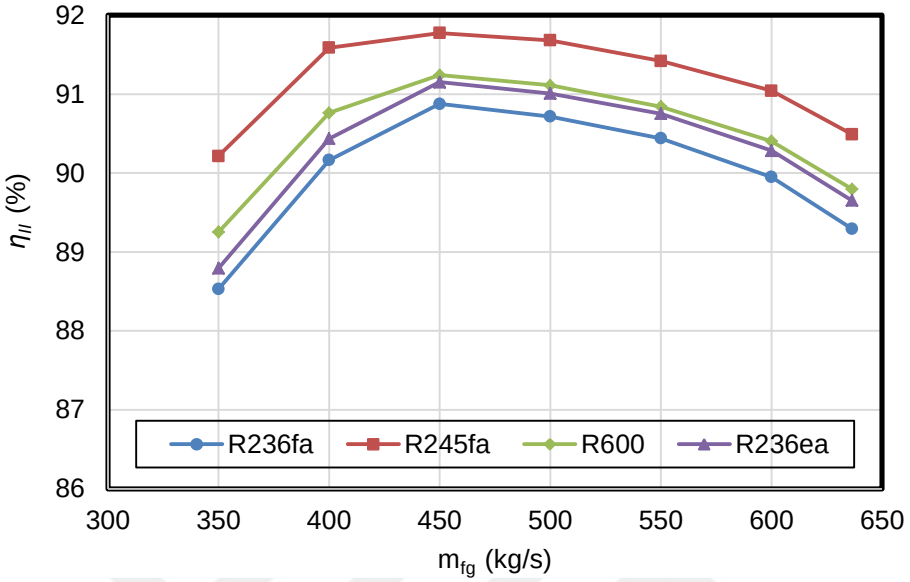


Figure 4.17. Variation in the exergy efficiency of the pump as a function of the flue gas mass flow rate

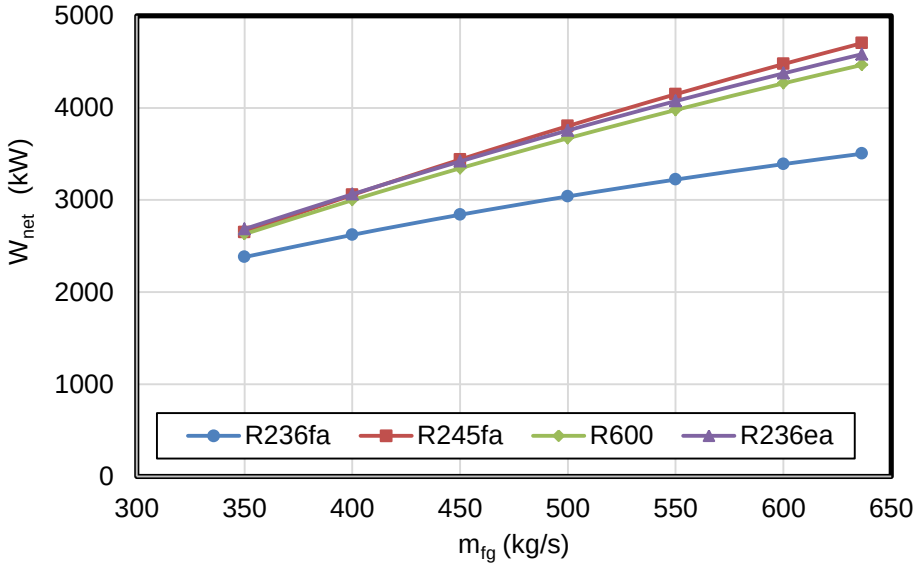


Figure 4.18. Variation in the net output power as a function of the flue gas mass flow rate

Figure 4.19 presents changes in the energy efficiency of the ORC system as a function of the flue gas mass flow rate. It can be seen that the energy efficiency of the ORC system increases as the flue gas mass flow rate increases. Both the turbine inlet pressure and temperature increase because of the flow rate of the flue gas goes up so that the latent heat of the organic fluids decrease, but, the energy efficiency is grown up. The ORC system with R245fa has higher energy efficiency than those of other working fluids under same conditions. The other working fluids present similar results.

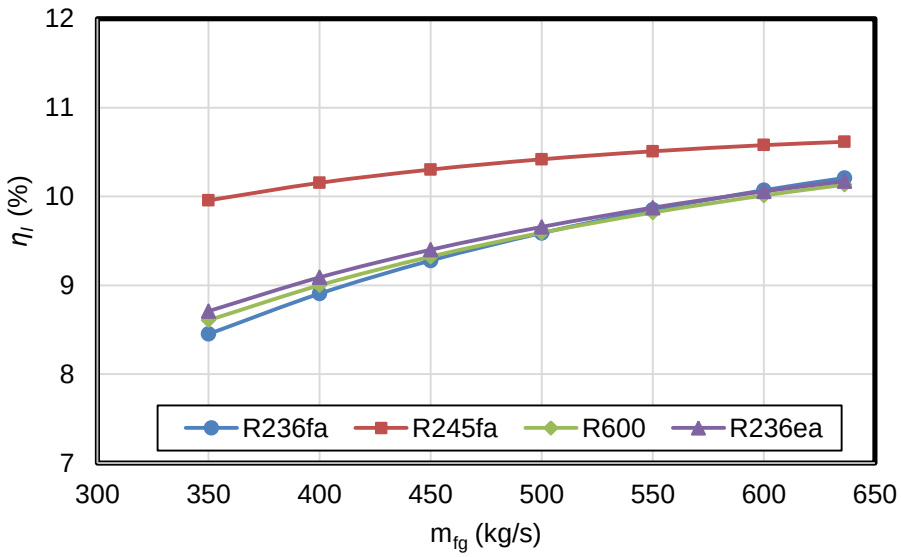


Figure 4.19. Variation in the energy efficiency of the ORC system as a function of the flue gas mass flow rate

### 4.2.3. Effect of Steam Power Plant Unit Load

This section provides the results of analyzes and discusses the effect of the steam power plant unit load on the ORC system performance. The calculated results reveal that an increase in the steam power plant unit load has a similar effect on the ORC system to that of an increase in the flue gas mass flow rate. The variation in the exergy efficiency of the ORC system as a function of the steam

power plant unit load is presented in Figure 4.20. As seen from this figure that the exergy efficiency of the ORC system increases with an increase of the steam power plant unit load, even though the amount of energy loss and exergy destruction of the steam power plant increase. As a consequence, it is highly recommended that the steam plant should be operated at a full load. The best rate of exergy efficiency increase happens with R245fa for the unit load varying from 70% to 100%.

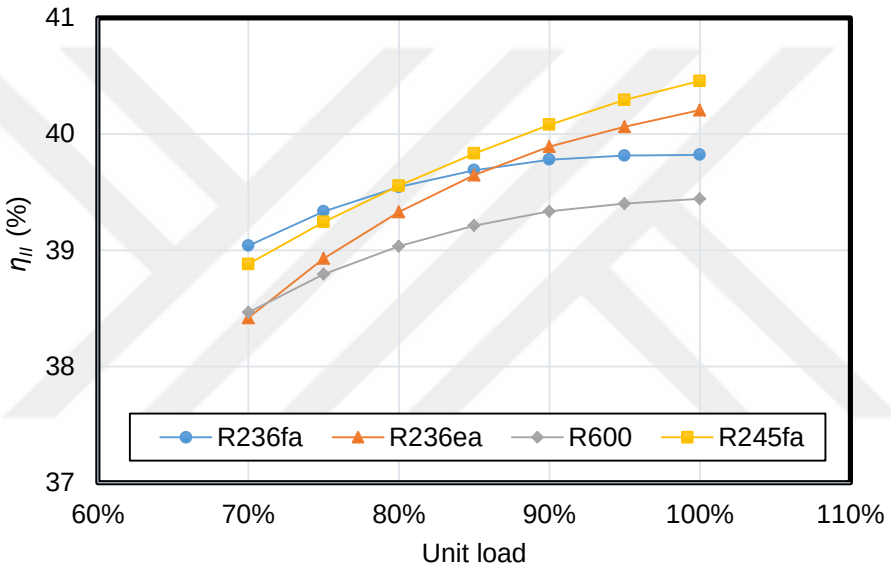


Figure 4.20. Variation in the exergy efficiency of the ORC system as a function of the steam power plant unit load

Figure 4.21 illustrates the exergy efficiency variations through the evaporator unit based on the steam power plant unit load. The exergy efficiency of the evaporator shows a considerable and linear increase with an increase in the steam power plant unit load. In other words, the higher rate of unit load rate improves the exergy efficiency of the evaporator unit. The higher level of exergy loss in the evaporator is caused by the finite temperature differences between the flue gas and the working fluid. The losses in the evaporator happen due to an

increase in entropy generation by the flue gases. However, as the load increases the exergy efficiency of the evaporator increases as it is seen in Figure 4.21. Highest exergy efficiency was calculated as 70% in the case of using of working fluid of R245fa.

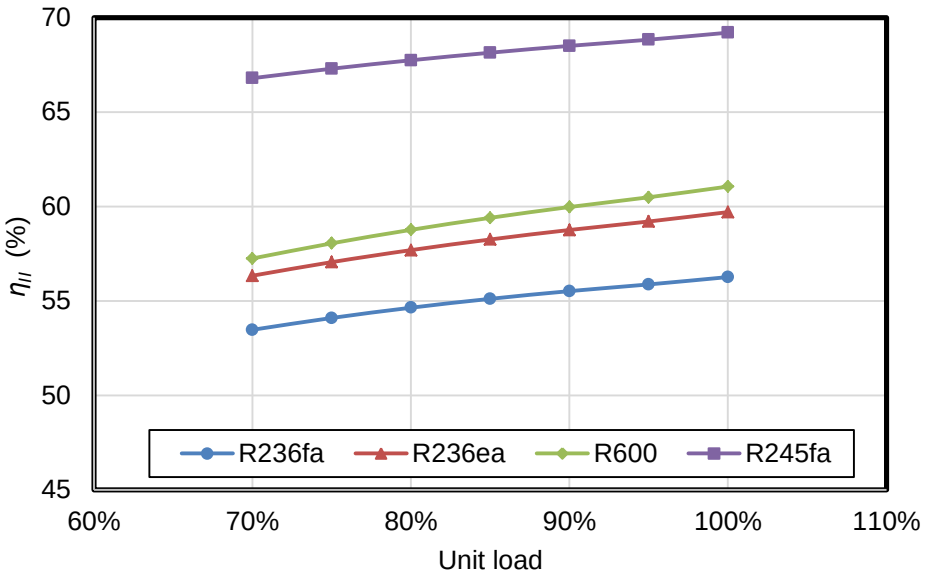


Figure 4.21. Variation in the exergy efficiency of the evaporator unit as a function of the steam power plant unit load

The exergy efficiency of the steam turbine with a steam power plant unit load is shown in Figure 4.22. It is shown that the turbine exergy efficiencies for the fluids R236ea, R245fa and R600 remained nearly constant when the steam power plant unit load is varied. But the exergy efficiency in the case of R236fa decreases by 2%.

Figure 4.23 shows the variation in the exergy efficiency of the pump as a function of the power plant unit load. As seen from this figure, the best working fluid in terms of the pump exergy efficiency is R245fa. For the highest exergy

efficiency of the pump is calculated to be 91.8% which corresponds to the optimum power plant unit load of 80%.

Figure 4.24 presents the variation in the net output power as a function of the steam power plant unit load. It can be seen that the net output power generated by the ORC system increases as the steam power plant unit load increases. The ORC system with R245fa had a higher net output power than those of the other working fluids under the same conditions.

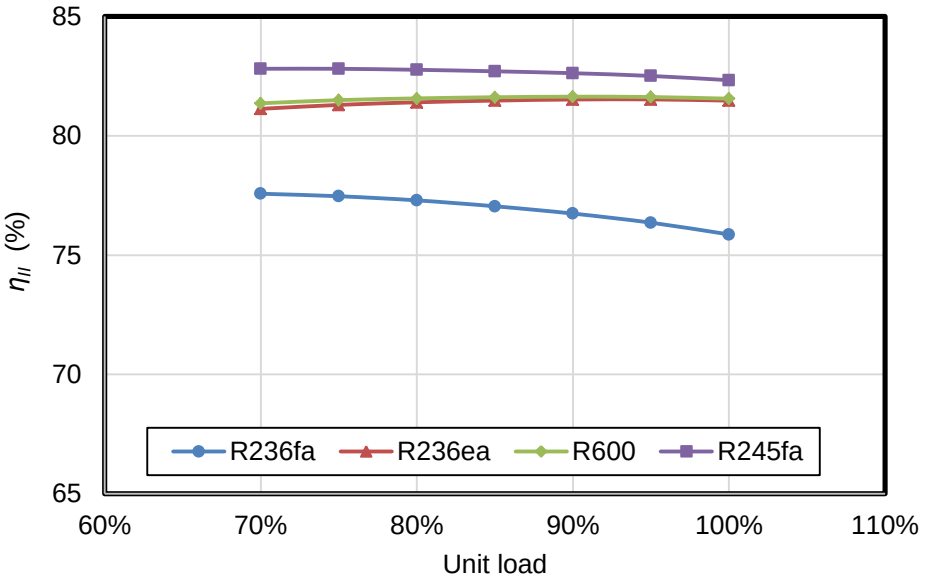


Figure 4.22. Variation in the exergy efficiency of the turbine as a function of the steam power plant unit load

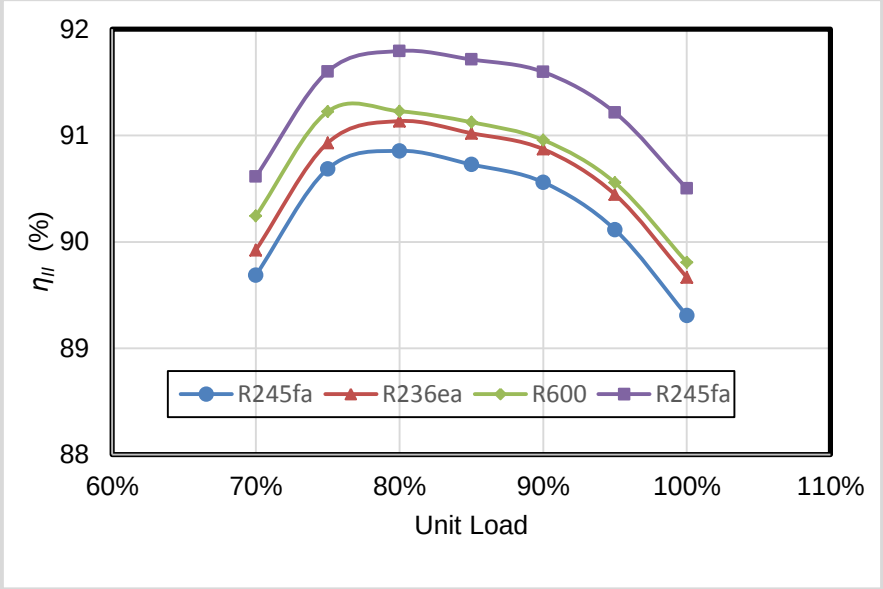


Figure 4.23. Variation in the exergy efficiency of the pump as a function of the power plant unit load

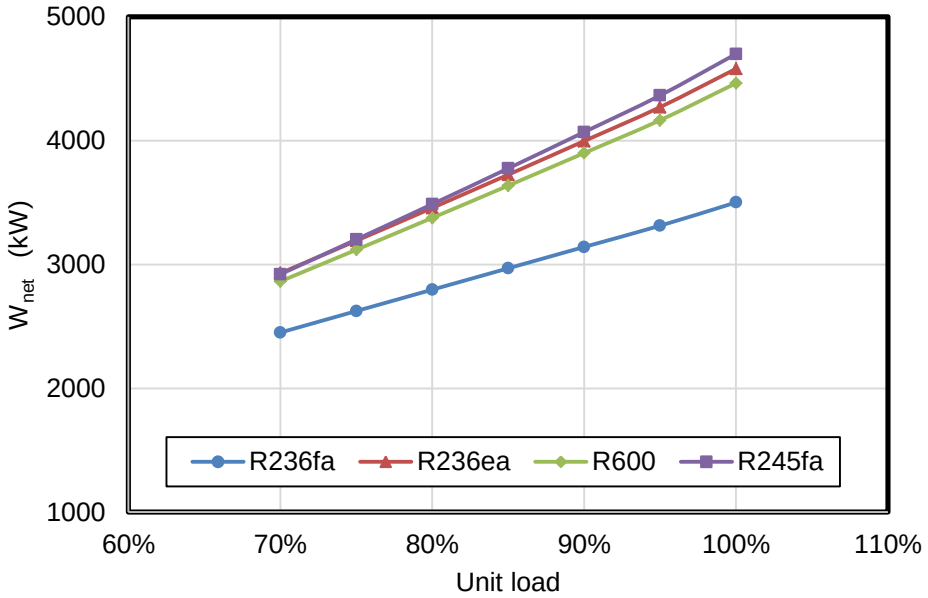


Figure 4.24. Variation of the net output power as a function of the steam power plant unit load

The variation in the energy efficiency of the ORC system as a function of the steam power plant unit load is presented in Figure 4.25. It is indicated that the energy efficiency of the ORC system increases as the steam power plant unit load increases. When the steam power plant unit load is increased, heat transfer from the flue gas to the ORC system increases. This unit load increase mainly upgrades the mass flow rate of the ORC system and the turbine inlet pressure. On the other hand, the latent heat of the organic fluid decreases, so that the energy efficiency of the ORC system increases. The ORC system with R245fa has higher energy efficiency than those of the other working fluids under the same conditions.

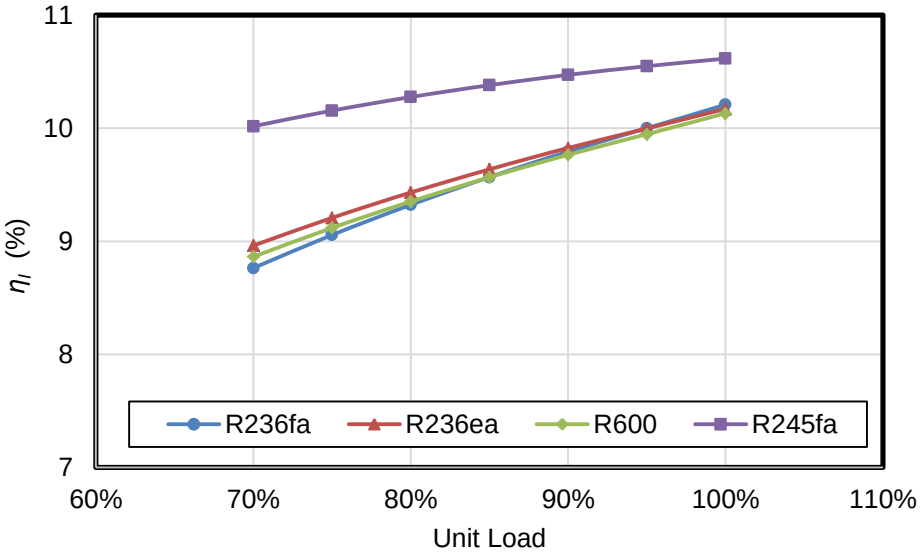


Figure 4.25. Variation in the energy efficiency of the ORC system as a function of the steam power plant unit load

### 4.2.4. Effect of Evaporator Pinch Point Temperature

In this section, the effect of the evaporator pinch point temperature on the ORC system performance is analyzed and discussed. The pinch point is the location in the evaporator where the temperature difference between refrigerants

and chilling water is a minimum at that location. The pinch point (PP) temperature is an important design parameter in heat exchangers. Pinch point of the evaporator is shown in Figure 4.26. An increase in this value can lower the efficiency of the system slightly by decreasing the energy recovered by the evaporator. Figure 4.27 illustrates the influence of varying the pinch point temperature on the cycle's overall exergy efficiencies for different working fluids. The ORC system with R245fa has higher exergy efficiency than those of the other working fluids under the same conditions.

Variations in the exergy efficiency of the evaporator unit as a function of evaporator pinch point temperature are shown in Figure 4.28. When the pinch point temperature of the evaporator increases it adversely affects the heat transfer rate between the flue gas and the working fluid. When the temperature differences between working fluids increase, exergy destruction increases so that exergy efficiency is negatively affected by all working fluids.

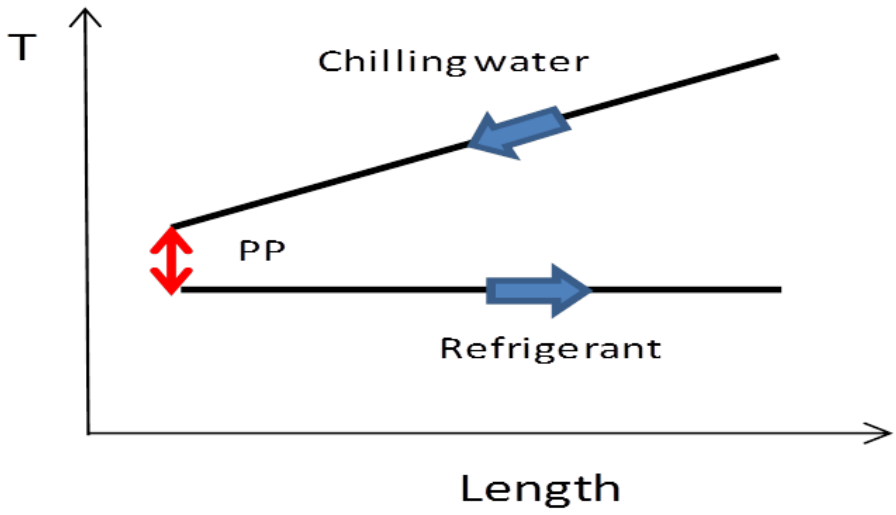


Figure 4. 26. Pinch point of the evaporator

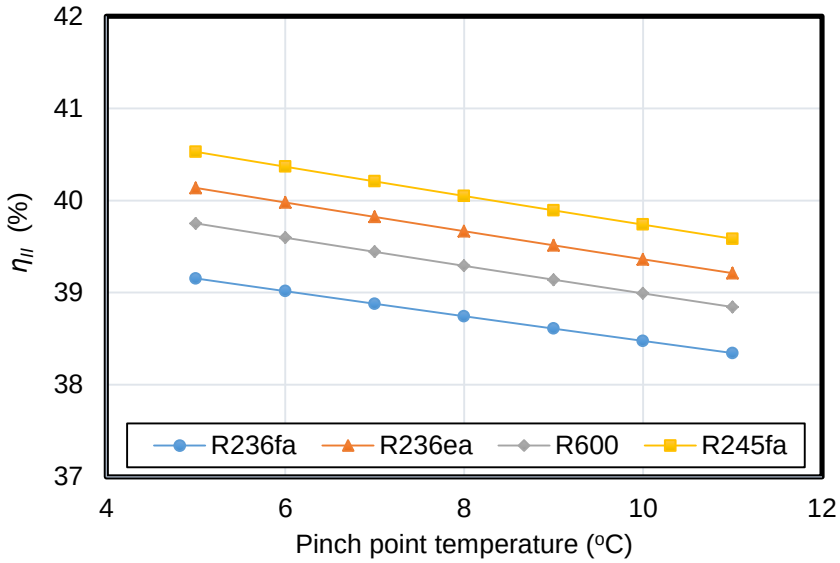


Figure 4.27. Variation in the exergy efficiency of the ORC system as a function of the evaporator pinch point temperature

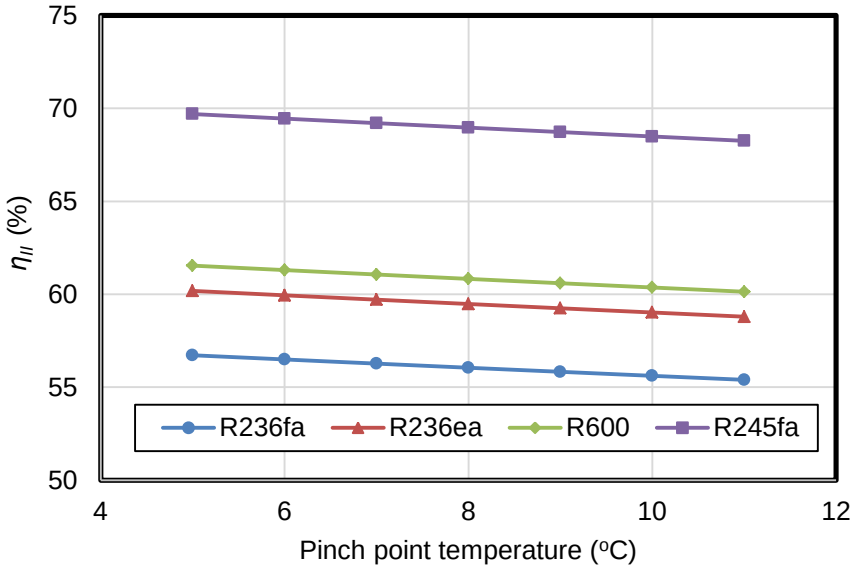


Figure 4.28. Variation in the exergy efficiency of the evaporator unit as a function of the evaporator pinch point temperature

Figure 4.29 shows how the pinch point temperature affects the net output power. Increasing the pinch point temperature negatively affects the net power output. Increasing the pinch point temperature leads to a decrease in the ORC mass flow rate according to the energy balance of the evaporator that finally leads to a decrease in the turbine work.

It is known that a steam power plant produces not only electricity but also produces waste or unused energy. This waste or unused energy can be converted to a usable energy by adding integrated systems to generate different products in multigeneration energy systems. For this reason, every product provides useful exergy outputs. As seen in Figure 4.30 whatever input energy is supplied, single generation exergy efficiencies are lower compared to multi-system exergy efficiencies because multiple outputs have been obtained from a single input energy.

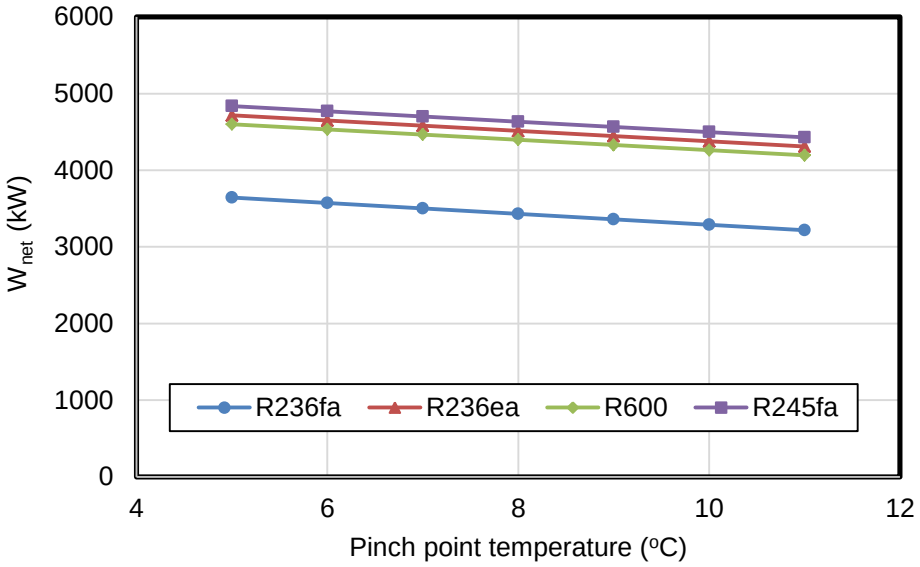


Figure 4.29. Variation in the net output power as a function of the evaporator pinch point temperature

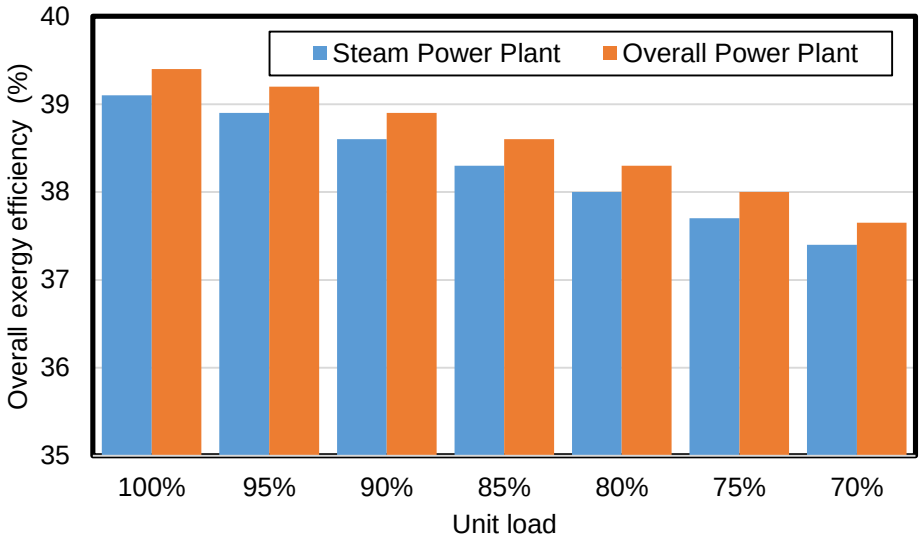


Figure 4.30. Overall exergy efficiency as a function of the steam power plant unit load

### 4.2.5. Exergoeconomic Analysis Case

In this section, an exergoeconomic analysis was performed to determine the cost rate of each exergy stream. R245fa working fluid was selected for the ORC system at design point for exergoeconomic analysis. The design point parameters are the flue gas temperature, the flue gas mass flow rate, the evaporator pinch point temperature and power plant unit load which were 161ºC, 636 kg/s, 7ºC and 100%, respectively.

The solution of the system of cost balance and auxiliary equations gives the value of the costs for the unknown streams of the ORC system. Table 4.1 shows the important exergy and exergoeconomic parameters of the system. The elements with the maximum sum of $\dot{C_D} + \dot{Z}$ are the most significant components from an exergoeconomic point of view. The evaporator has the maximal value for the sum of $\dot{C_D} + \dot{Z}$ and the minimum value for the exergoeconomic factor, *f*. This means that the cost rate of exergy destruction is important for this element. The total exergy destruction in the evaporator is 5113.23 kW. This value consists of 43.25%

of the total exergy input and 56.27% of the total exergy destruction within the system. High exergy destruction in the evaporator is mainly because of the finite temperature differences between the flue gas and the organic fluid. An increase in the costs can cause a decrease in the exergy destruction costs of the evaporator. . However, the greatest value for the exergoeconomic factor, $f$ in the recuperator is 73.18%, which is 63.10% for the pump and 61.15% for the turbine. Exergoeconomic improvement of one unit of energy production can be achieved by having a reduction in the initial investment of each component. Also, the highest $f$ value for the recuperator indicates that it can affect the costs to lower the investment by decreasing the surface area. Exergy loss from the system can be defined as the exergy stream leaving the heat exchanger and expelled to the environment. The exergy loss was determined to be 35.58 kW, and the cost flow rate associated with the exergy loss was 532 $/kJ.

In this study, the period of repayment was also calculated taking the annual operation hours of the power plant into account using economic analysis. The operating period of the steam turbine is taken to be 8000 hours annually. Based on this working period, the payback period is found to be 5.02 years. To be able to shorten the payback period it is necessary to consider different options, for example, maximizing the waste heat recovery from flue gas. It is possible to reduce the flue gas temperature below 120 °C if a new coating material resistant against acid deformation is applied, through the flue gas channels and chimneys in order to improve the waste heat recovery further (Karaoglu, 2018)

Table 4.1. Exergy and exergoeconomic system parameters for ORC

| **System component** | $X_D$ **(kW)** | $n_{ıı}$ **(%)** | $y$ **(%)** | $c_f$ **($/KJ)** | $c_p$ **($/KJ)** | $\dot{Z}$ **($/h)** | $\dot{C_D}$ **($/h)** | $\dot{C_D} + \dot{Z}$ **($/h)** | $r$ **(%)** | $f$ **(%)** |
|---|---|---|---|---|---|---|---|---|---|---|
| Condenser | 1089.30 | 51.23 | 9.21 | 5.48 | 8.31 | 322.00 | 5969.36 | 6291.36 | 51.64 | 5.12 |
| Recuperator | 35.58 | 42.76 | 0.30 | 5.48 | 5.75 | 532.01 | 195.00 | 727.01 | 4.93 | 73.18 |
| Pump | 104.13 | 89.29 | 0.88 | 6.30 | 9.26 | 1121.68 | 656.01 | 1777.69 | 46.98 | 63.10 |
| Evaporator | 5113.23 | 56.27 | 43.25 | 3.00 | 5.31 | 670.34 | 15339.69 | 16010.03 | 77.00 | 4.19 |
| Turbine | 779.38 | 77.58 | 6.59 | 5.48 | 6.30 | 6721.41 | 4270.99 | 10992.39 | 14.96 | 61.15 |

### 4.2.6. Environmental Analysis Case

In this section, an environmental analysis was carried out to determine the emission values of the steam power plant and the overall system, and the results obtained are shown in Table 4.2. It is known that $CO_2$ emissions adversely affect global warming. In the case of a multigeneration system designed in the present work, the input energy of the system is reduced. This means that fewer emissions are generated when less input energy is used. As a result, the environmental impact of a steam power plant can be minimized with the integration of the ORC system.

The amount of emissions produced by a steam power plant integrated with the ORC system appears to have a lower environmental impact than the emission level generated by the steam power plant alone, as shown in Table 4.2. Namely, a steam power plant integrated with the ORC system reduces $CO_2$, CO and $NO_x$.

Table 4.2. Unit emissions of harmful gases (kg/MWh)

| | $CO_2$ | $NO_x$ | CO |
|---|---|---|---|
| Steam power plant | 230 | 510 | 25 |
| Overall power plant | 228 | 502 | 24 |

### 4.3. Vapor Compression Refrigeration Case

The performance of the proposed system is calculated considering varying turbine inlet temperature, steam mass flow rate and turbine inlet pressure, and four different working fluids (R134a, R410a, R407c and R717 in the VCR system). Figure 4.31 displays the effect of steam turbine flow rate on turbine output power and exergy efficiency.

The exergy destructions in turbines are associated with pressure drop and expansion process. Fluid friction happens when the fluid expands through the steam turbine blades. These friction losses result in the dissipation of part of its energy into heat itself at the expense of beneficial work. The fluid then does less work and leaves through the exhausts with a higher temperature. As expected, both

turbine output power and exergy efficiency increase while steam mass flow rate increases. In Figure 4.31, the variation of turbine steam mass flow rates is varied between 1 kg/s and 6 kg/s by keeping the turbine inlet pressure and temperatures constant such as 55 bar and 355 °C respectively. Due to the ventilation effect inside the turbine, the turbine exergy efficiency increases by 1% as the steam turbine mass flow increases.

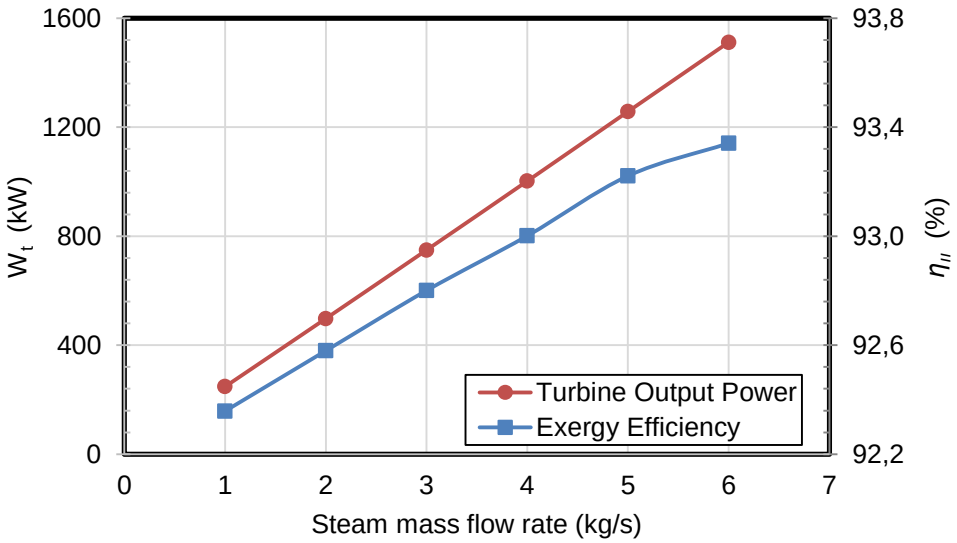


Figure 4.31. Variation of turbine power and exergy efficiency as a function of steam mass flow rates

The influence of varying the inlet temperature of the turbine on the exergy efficiency of the turbine and turbine output power are displayed in Figure 4.32. Variation of turbine inlet temperatures between 330 °C and 355 °C is investigated by keeping the turbine inlet pressure and mass flow rate at 55 bar and 6 kg/s respectively. As it is seen, the effect of changing the inlet temperature of the turbine on the net electricity generation and exergy efficiency are significant. The net electrical energy generation increases by 8 % as the turbine inlet temperature increases. Also, the exergy efficiency of the turbine is more or less is constant for

variation of temperatures from 330°C to 345°C then increasing the turbine inlet temperature further as seen in Figure 4.32, negligibly slight changes occur in the exergy efficiency rates.

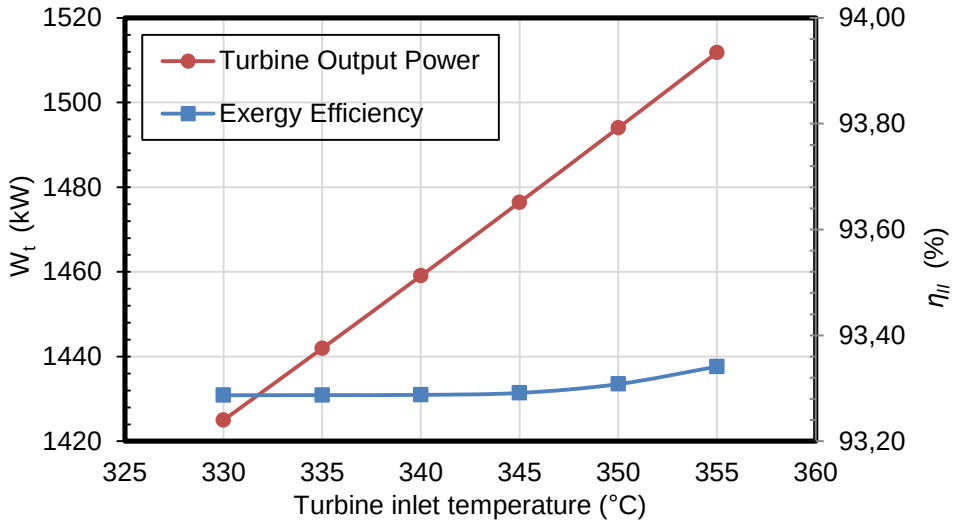


Figure 4.32. Variation of turbine power and exergy efficiency as a function of turbine inlet temperature

In Figure 4.33, turbine inlet pressure is monitored between 45 bar and 55 bar while maintaining fixed turbine inlet temperature and mass flow rate at 355 °C and 6 kg/s respectively. It can be seen that varying the inlet pressure on the turbine of the net electricity generation and progress in the efficiency of the exergy are quite important. Net electricity generation increased by 15% when the turbine inlet pressure increased. Conversely, the exergy efficiency of the turbine increases from 93.35% at 45 bar to 93.6 % at 55 bar. The increase in the steam pressure results in an increase in the density of the steam so the steam velocity decreases and causes less friction inside the turbine.

Effect of steam mass flow rate on the cooling load is examined as seen in Figure 4.43. Changing of the steam mass flow is important for cooling load. As the steam mass flow raises the steam turbine generates a higher electricity and also

drives the compressor with a higher power. Therefore, the cooling load increases by increasing the mass flow rate of refrigerant. According to fluid types, cooling load of R134a was always higher than other working fluids. On the contrary, R717 displays the least performance.

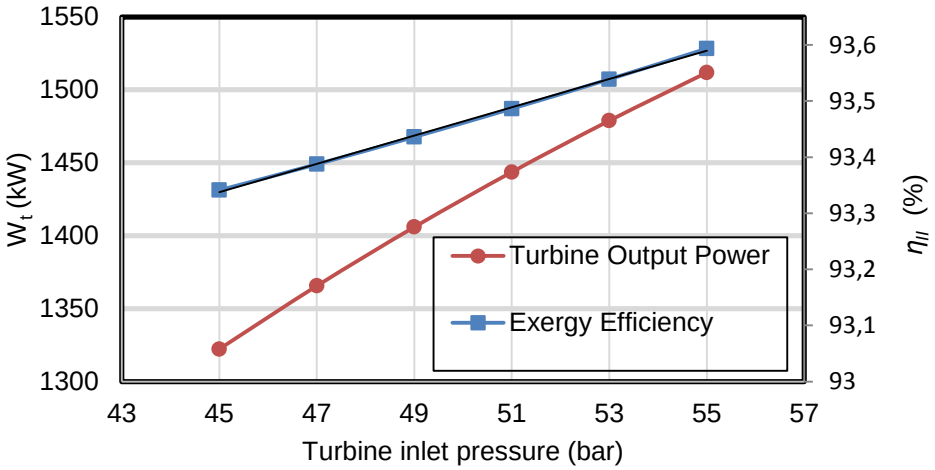


Figure 4.33. Variation of turbine power and exergy efficiency as a function of turbine inlet pressures

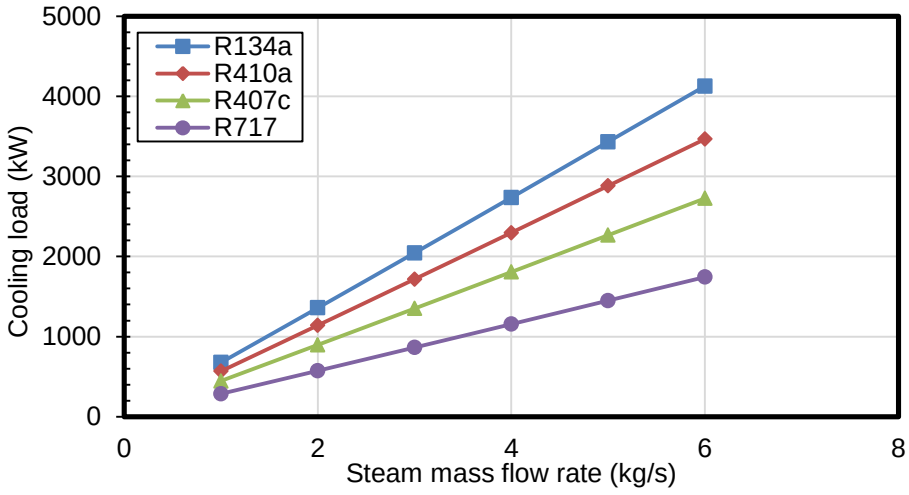


Figure 4.34. Variations of cooling loads as a function of steam mass flow rates

The cooling load as a function of the turbine inlet temperature is illustrated in Figure 4.35. By increasing the steam temperature, the steam provides better enthalpy at the inlet of the turbine to generate better electricity and drive compressor with a higher power. The variation of the cooling load of the vapor compression cycle depends on the type of working fluids. For example, the cooling load of R134a is always higher than the other working fluids. On the contrary, R717 displays the worst performance.

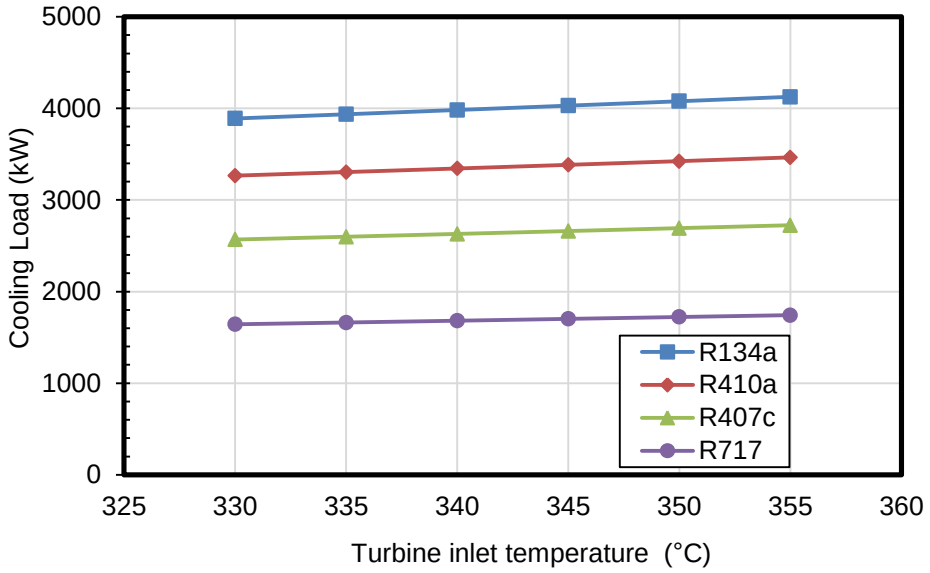


Figure 4. 35. Variation of cooling loads as a function of turbine inlet temperatures

Variation of cooling loads as a function of turbine inlet pressures is presented in Figure 4.36. The turbine output power increases with increasing turbine inlet pressure, as it is displayed in Figure 4.35. Therefore, the driven power of vapor compression cycle rises when the mass flow rate of refrigerants increases. As a consequence, the cooling load gets better. In conclusion, the cooling load of R134a is always higher than the other working fluids. On the other hand, R717 clearly shows the least performance as seen for turbine inlet pressure changes.

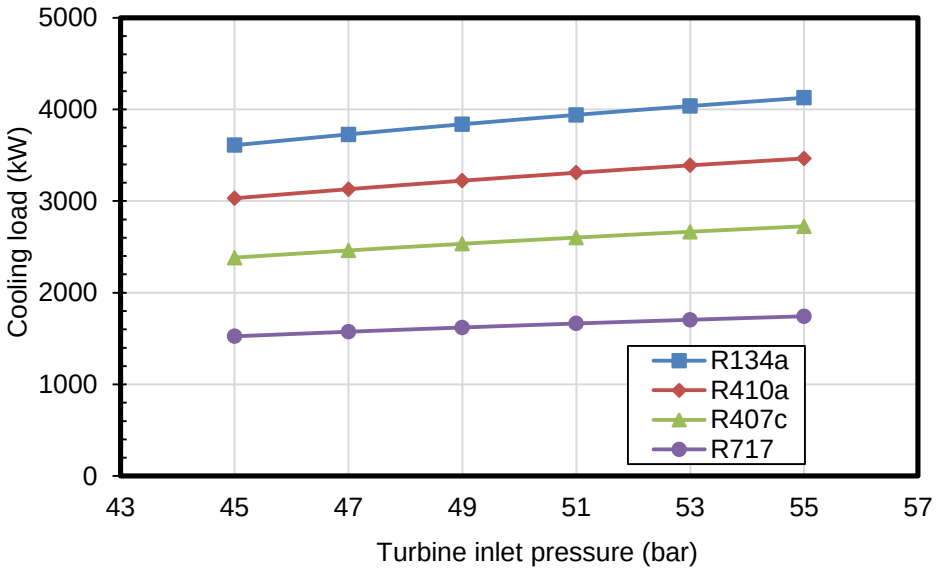


Figure 4.36. Variation of cooling loads as a function of turbine inlet pressures

Exergy efficiency and the COP of vapor compression cycle are investigated at a design load of the steam turbine. It is observed from Figure 4.37 that the working fluid of R134a has the best performance in terms of the COP as well as the exergy efficiency compared to other working fluids considered in the present work. It is worth noting that although the working fluid of R717 has high exergy efficiency, from COP viewpoint, the R717 working fluid has the lowest COP among other working fluids considered in the present work.

Exergy efficiency and exergy destruction rate of the compressor for each working fluid are shown in Figure 4.38. Exergy destruction is directly proportional to pressure ratios of compressor outlet and inlet. The pressure ratios are 2.63, 4, 5.26 and 15.35 for R134a, R410a, R407c and R717 respectively. As the pressure ratio increases exergy efficiency is positively affected. Therefore, the working fluid of R717 has a maximum exergy efficiency however the working fluid of R134a has minimum exergy efficiency and has maximum exergy destruction rate.

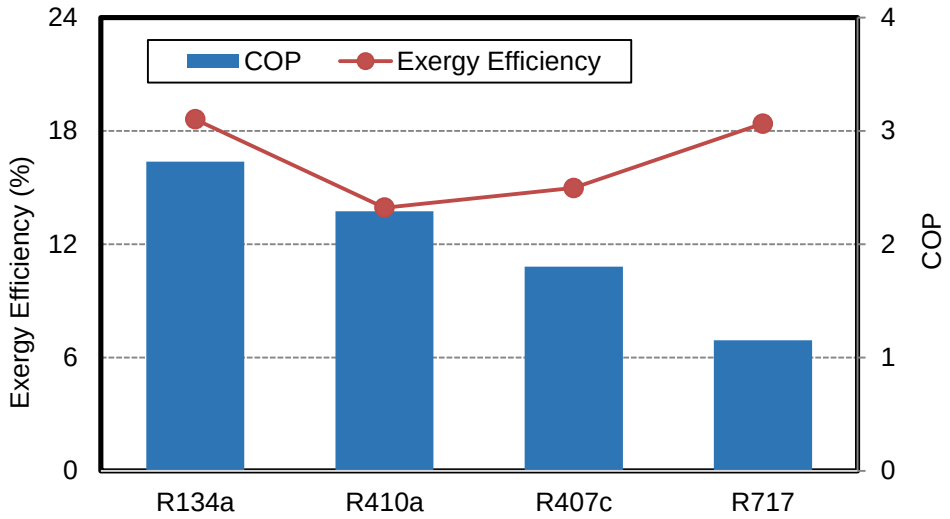


Figure 4.37. Variations of exergy efficiency and the COP of vapor compression cycle with different working fluids.

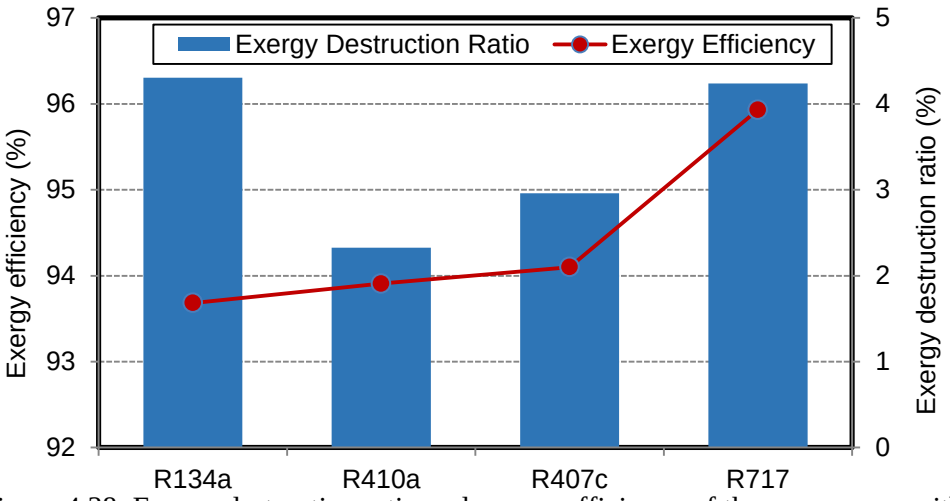


Figure 4.38. Exergy destruction ratio and exergy efficiency of the compressor with working fluids

Variation in exergy efficiency and exergy destruction rate of the condenser is demonstrated in Figure 4.39. Exergy destruction in the condenser is directly proportional to temperature differences between cold inlet and hot inlet fluid

temperatures. Temperature differences are 56.44 °C, 68.69 °C, 79.56 °C and 219.92°C for working fluids of R134a, R410a, R407c and R717 respectively. Therefore, the working fluid of R134a has the highest exergy efficiency however, R717 has minimum exergy efficiency, but has the maximum exergy destruction rate.

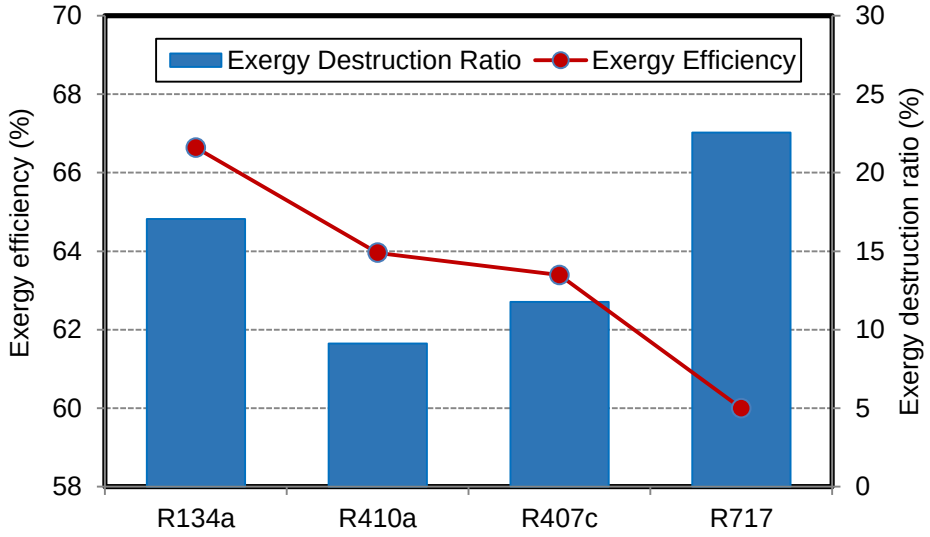


Figure 4.39. Exergy destruction ratio and exergy efficiency of the condenser with working fluids

Throttling is the irreversible process even though enthalpy is constant on both sides of the expansion valve. A significant exergy is destroyed due to internal energy converted into kinetic energy. Variation of exergy destruction and exergy efficiency of the expansion valve according to different working fluids is displayed in Figure 4.40. The working fluid of R410a has both the highest exergy destruction and the exergy efficiency rate. However, the exergy efficiency of R717 is considered the worst working fluid because the pressure differences of the expansion valve are higher compared to others. Also, minimum exergy destruction rate occurs in the case of R134a working fluid.

Variations in the exergy destruction rate and exergy efficiency of the evaporator are presented in Figure 4.41. Exergy destruction occurs due to temperature differences between the cold inlet temperature and the hot inlet temperature in the evaporator. Temperature differences are 19 °C, 14.58 °C, 11.12 °C and 14.19°C for working fluids of R134a, R410a, R407c and R717 respectively. In summary, R407c has maximum exergy efficiency, but, R134a has minimum exergy efficiency along with maximum exergy destruction rate.

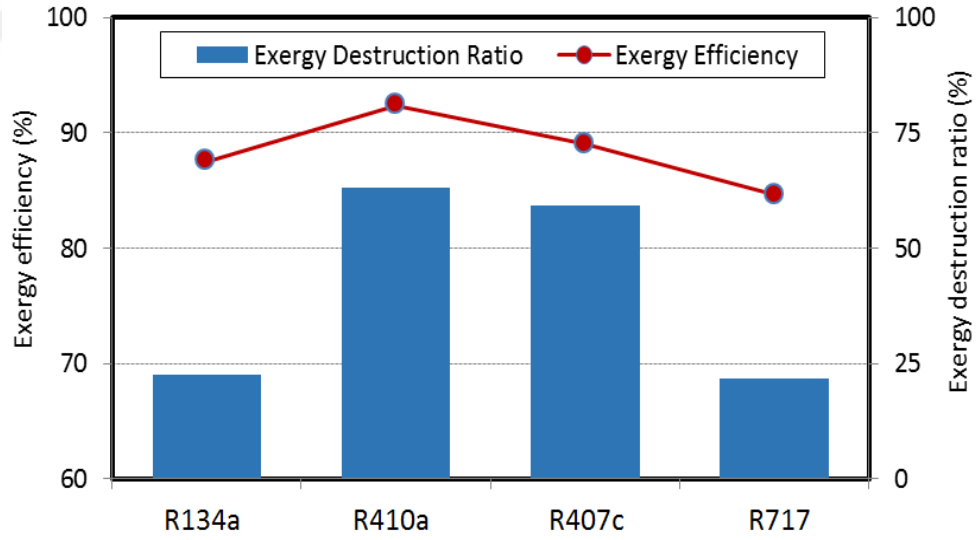


Figure 4.40. Exergy destruction ratio and exergy efficiency of the expansion valve with working fluids

Entire system and steam power plant exergy efficiency are illustrated in Figure 4. 42. All working fluids taken into account in this study contribute to the efficiency of the entire system. But, the efficiency of the R134a working fluid is much higher than that of other working fluids. Calculated steam power plant exergy efficiency is 39.1%. As a consequence of integrating vapor compression cycle, entire exergy efficiencies are 39.36%, 39.32%, 39.27% and 39.21% for R134a, R410a, 407c and R717 respectively.

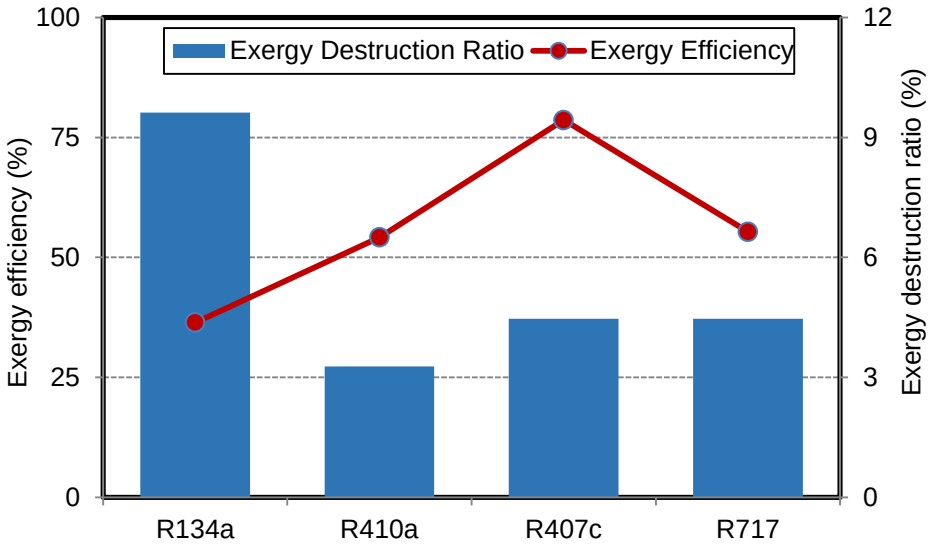


Figure 4.41. Exergy destruction ratio and exergy efficiency of the evaporator with working fluids

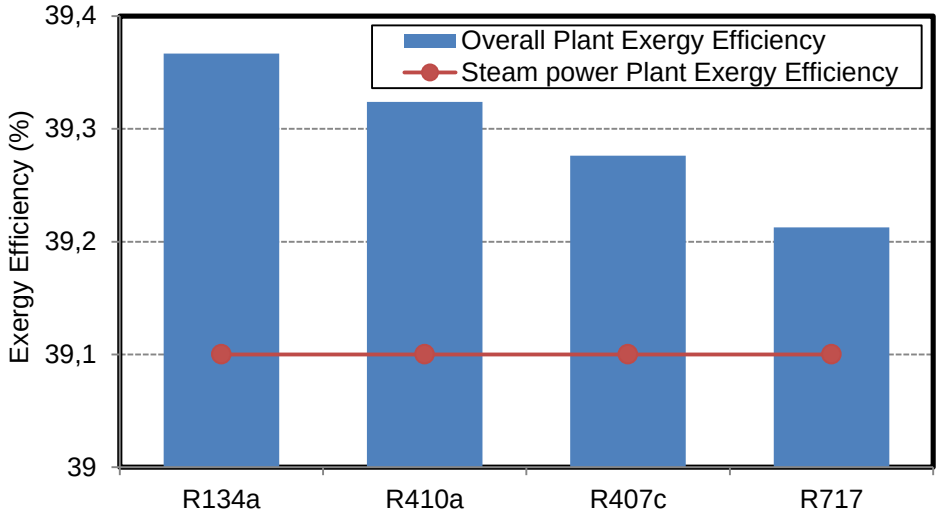


Figure 4.42. Variation of exergy efficiency of the entire system and steam power plant with working fluids

The exergoeconomic analysis is conducted for each element of total equipment of a vapor compression cycle to determine the cost rate of each exergy

stream for R134a fluids at a design point. Design point parameters of the vapor compression cycle are 355 ºC of steam inlet temperature 6 kg/s of steam mass flow rate and 55 bar of steam turbine inlet pressure.

The system of cost equivalence and auxiliary equations is resolved to get the cost of unknown flows of the system. Parameters used in the exergy and economic analyses to be considered for the system is given in Table 4.3. The elements with the greatest value of $\dot{C}_D + \dot{Z}$ is the most important element for economic analysis. The expansion valve has the maximal value of total $\dot{C}_D + \dot{Z}$ and the minimal value of the exergoeconomic factor which means that the cost ratio of the exergy destruction is noticeable for this element. Total exergy destruction in the expansion valve is 1635. 10 kW, which accounts for 68.70% of total exergy input and 69.03% of total exergy destruction in the system. The high exergy destruction in the expansion valve is a non-reversible process, mainly due to throttling, but if both enthalpy side expansion valves are fixed, too much exergy is destructed due to the kinetic energy conversion of the internal energy. Although increasing the investment cost can lead to a decrease in the cost of the exergy destruction of the expansion valve. The compressor has the maximal value of the exergoeconomic factor. In addition, this value is 49.76% for the compressor and 43.49% for the steam turbine.

Exergoeconomic improvement of one unit of energy production can be achieved by having a reduction in the initial investment of each component. Also, the highest *f* value of the compressor recommends that it may possibly to be a cost-effective to pull down the initial investment cost by lowering the amount of production. Exergy losses from the system are in balance with the exergy of the stream leaving the compressor and stack to the surrounding. The amount of exergy losses is computed to be 101.95 kW and the cost of the exergy losses in unity is determıned to be 1641.4 $/h.

Table 4.3. Exergy and exergoeconomic parameters for VCR

| | $\boldsymbol{X_D}$ **(kW)** | $\boldsymbol{n}$ **(%)** | $\boldsymbol{y}$ **(%)** | $\boldsymbol{c_f}$ **($/KJ)** | $\boldsymbol{c_p}$ **($/KJ)** | $\boldsymbol{\dot{Z}}$ **($/h)** | $\boldsymbol{\dot{C}_D}$ **($/h)** | $\boldsymbol{\dot{C}_D + \dot{Z}}$ **($/h)** | $\boldsymbol{r}$ **(%)** | $\boldsymbol{f}$ **(%)** |
|---|---|---|---|---|---|---|---|---|---|---|
| Turbine | 107.85 | 93.34 | 4.55 | 15 | 16.10 | 1245 | 1617.75 | 2862.75 | 7.33 | 43.49 |
| Compressor | 101.95 | 93.68 | 4.30 | 16.10 | 17.20 | 1626 | 1641.40 | 3267.40 | 6.83 | 49.76 |
| Condenser | 403.79 | 66.64 | 17.05 | 13.80 | 18.20 | 946 | 5572.30 | 6518.30 | 31.88 | 14.51 |
| Expansion Valve | 1635.10 | 68.70 | 69.03 | 13.80 | 20.10 | 15 | 22564.38 | 22579.38 | 45.65 | 0.07 |
| Evaporator | 227.94 | 36.43 | 9.62 | 9.00 | 10.90 | 575 | 2051.46 | 2626.46 | 21.11 | 21.89 |

### 4.4. Desalination System Case

A thermo-economic analysis was applied to an existing MED-TVC system operating in Turkey. The variation in the gain output ratio as a function of the production load is presented in Figure 4.43. As seen from this figure, the gain output ratio (GOR) increased with increasing production load and seawater temperature. When the production load and seawater temperature were 100% and 33°C, respectively, the gain output ratio obtained was 7.33. When the seawater temperature rises, the required steam decreased to increase its temperature to the upper brine temperature, and as a result, the GOR value increases.

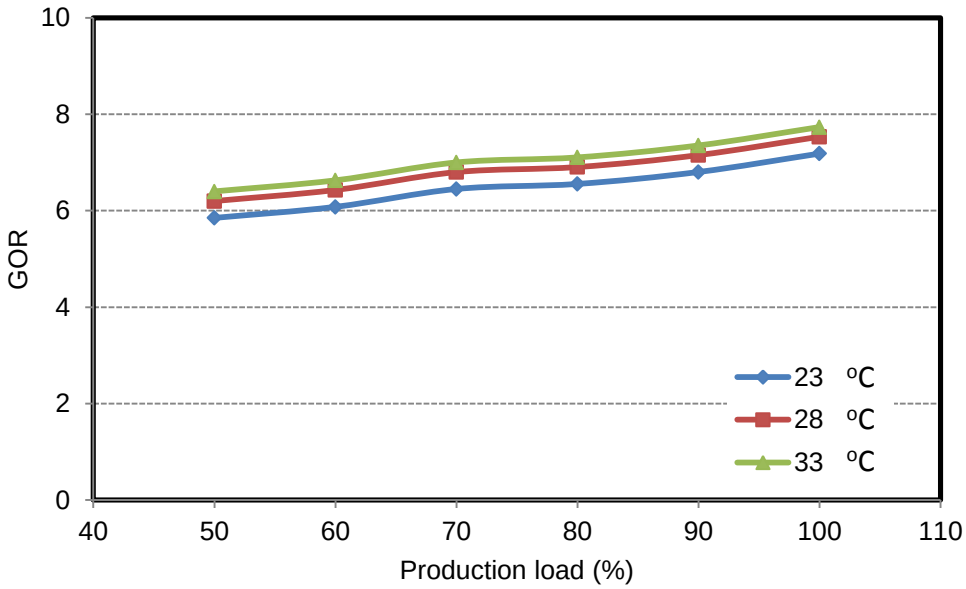


Figure 4.43. Variation of the gain output ratio as a function of the production load at different seawater temperatures

Variation of the exergy efficiency of the overall desalination plant as a function of the production load is presented in Figure 4.44. Results revealed that the exergy efficiency of the overall desalination plant increases with increasing production load and seawater temperature. The desalination process is an energy-

intensive process; accordingly, high-quality energy is converted into low-quality energy, as motive steam energy is converted into the distilled water so that the exergy efficiency of the system is around 1 to 2 %, which increases with rising operating load and increasing seawater temperatures.

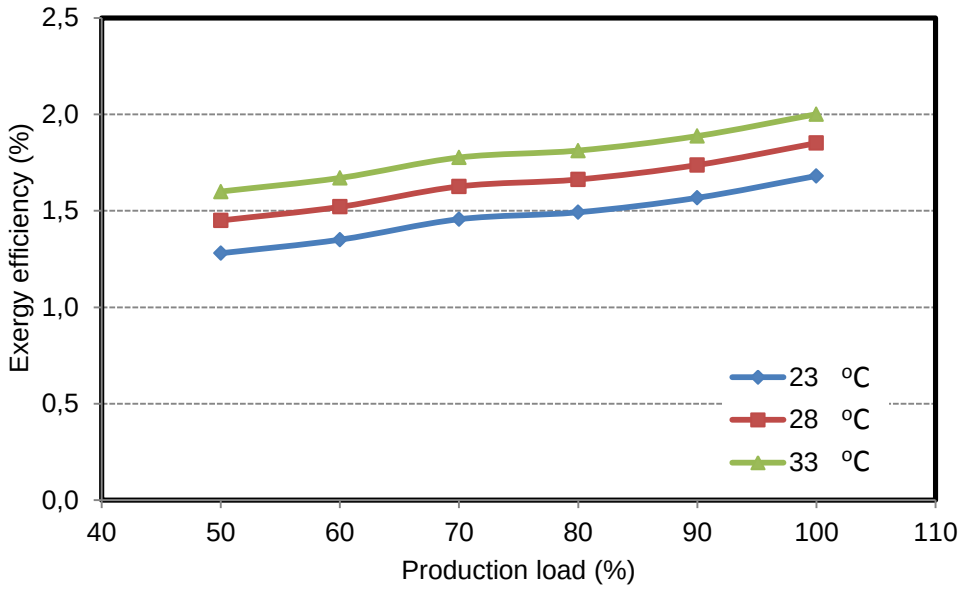


Figure 4.44. Variation of the exergy efficiency of the overall plant as a function of the production load for different seawater temperatures

Variation of the specific heat consumption as a function of the production load for different seawater temperatures is shown in Figure 4.45. Calculations showed that the specific heat consumption decreased with increased seawater temperatures. In addition, the reduction in the production load across the system, which can be achieved by decreasing the rate of flow of motive steam, increases the specific heat consumption and, as a result, decreases the specific exergy consumption. The specific enthalpy of the motive vapor increases in parallel to the rising pressure. The increased rate of specific enthalpy is lower compared to the

decreasing amount of steam required so that the specific heat consumption is reduced.

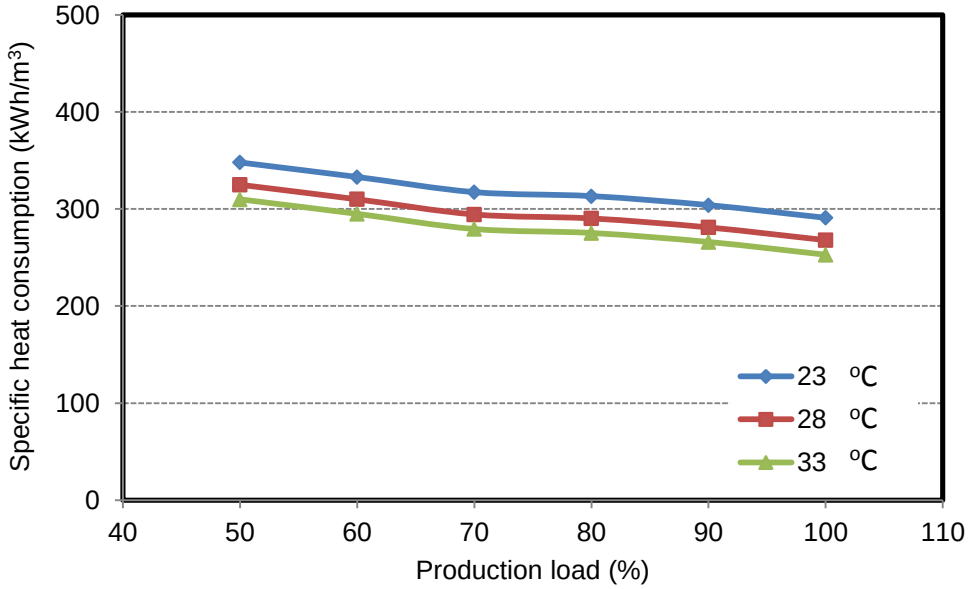


Figure 4.45 .Variation of the specific heat consumption as a function of the production load for different seawater temperatures

Specific exergy destruction is associated with an assessment of the performance. Variation of the specific exergy destruction as a function of the production load for different seawater temperatures is shown in Figure 4.46. The specific exergy destruction decreased with increased production load and seawater temperature. The desalination process is an inefficient process. Too much exergy is destroyed when the steam flows through the steam ejector, in addition, the steam energy disappears during heat transfer by heat exchangers.

Figure 4.47 presents the variation of the gain output ratio as a function of upper brine temperature (temperature of brine entering the first stage) for different seawater temperatures. As seen from this figure, the gain output ratio is inversely proportional to the upper brine temperature. As the upper brine temperature increased, the vacuum pressure of the effect was adversely affected. Therefore, a

high amount of energy is needed to evaporate seawater. In the system, the potential for scale formation, corrosion and pretreatment costs are reduced by a lower brine temperature.

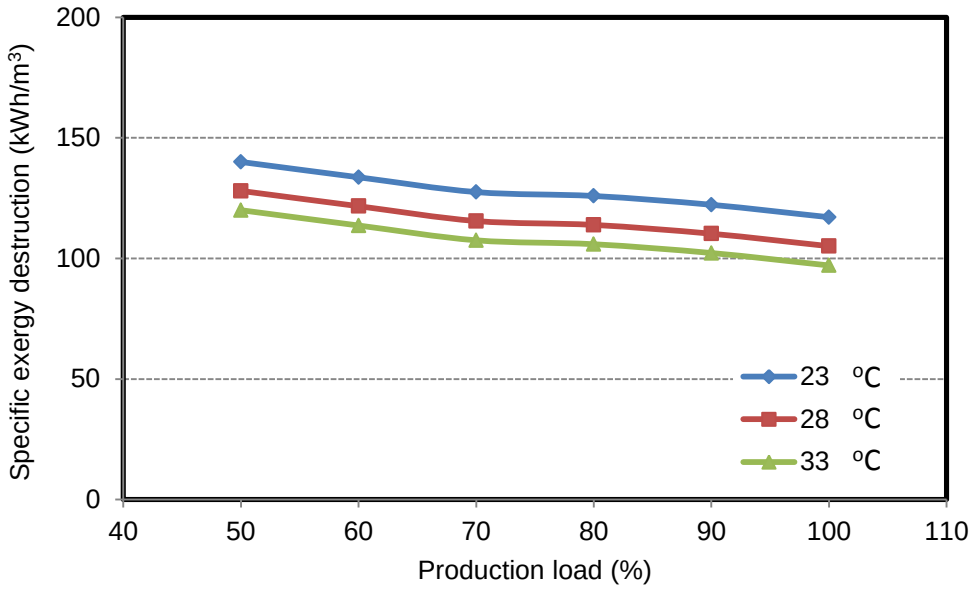


Figure 4.46. Variation of the specific exergy destruction as a function of the production load for different seawater temperatures

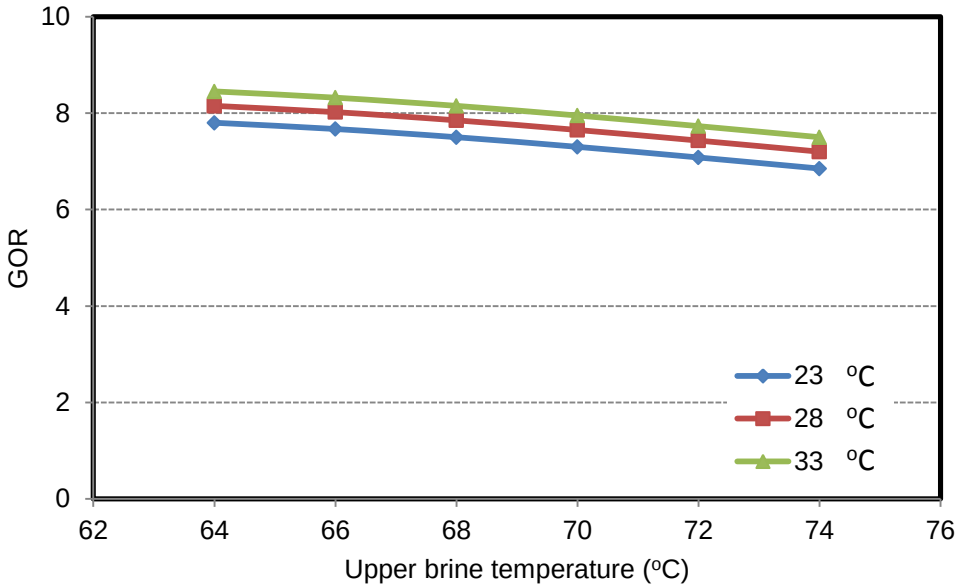


Figure 4.47. Variation of gain output ratio as a function of upper brine temperature for different seawater temperatures

Figure 4.48 shows the variation of the specific heat consumption as a function of upper brine temperature. The obtained results have revealed that as the upper brine temperature increased, the specific heat consumption significantly increased for all three seawater temperatures. So, the specific heat consumption is directly proportional to the upper brine temperature. In the desalination process, the heat transfer area is decreased when the upper brine temperature rises. Therefore, the heat transfer rate gets lower and therefore a higher amount of energy is needed.

Variation of specific exergy destruction as a function of upper brine temperature is shown in Figure 4.49. The increase in the specific total exergy destruction is noteworthy as the upper brine temperature increases in the three configurations because of an increase in the ejector compression ratio, which leads to higher irreversibilities.

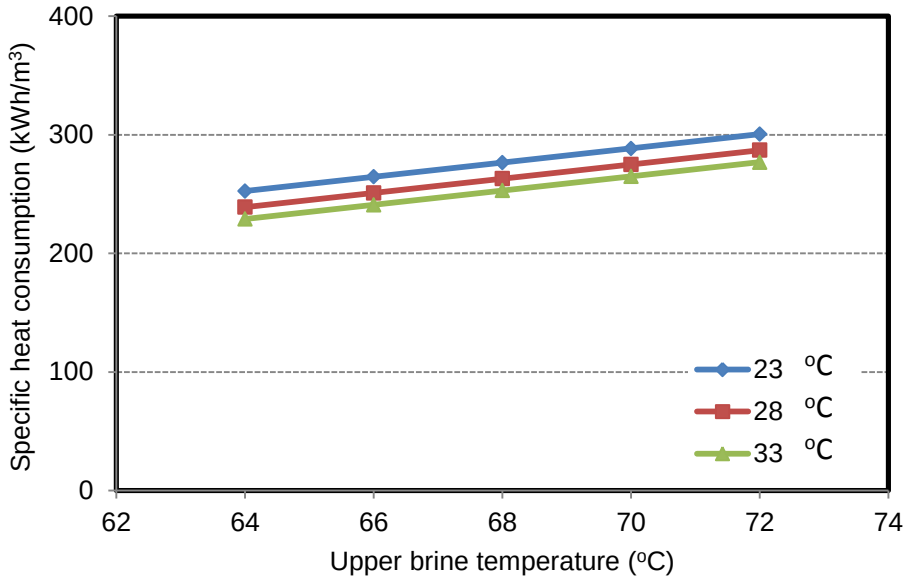


Figure 4.48. Variation of specific heat consumption as a function of upper brine temperature for different seawater temperatures

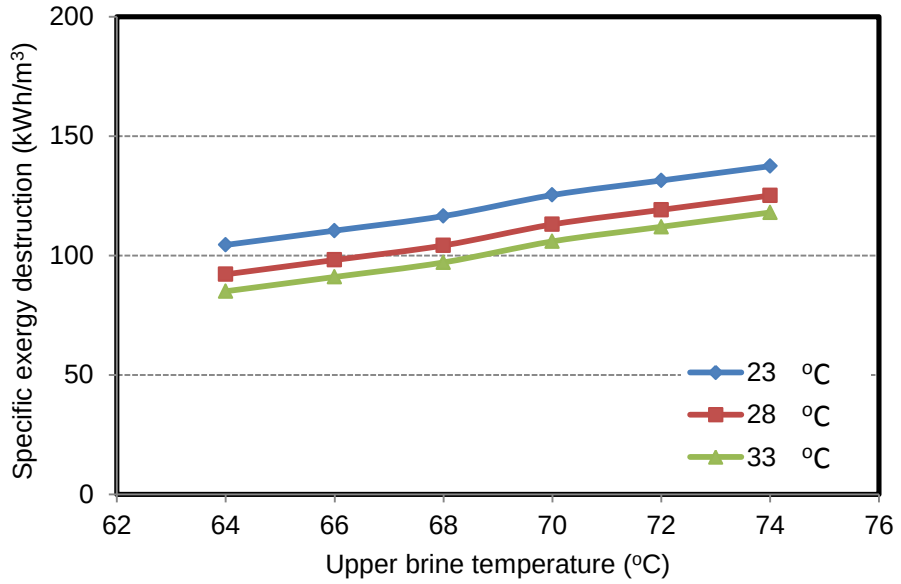


Figure 4.49. Variation of specific exergy destruction as a function of upper brine temperature for different seawater temperatures

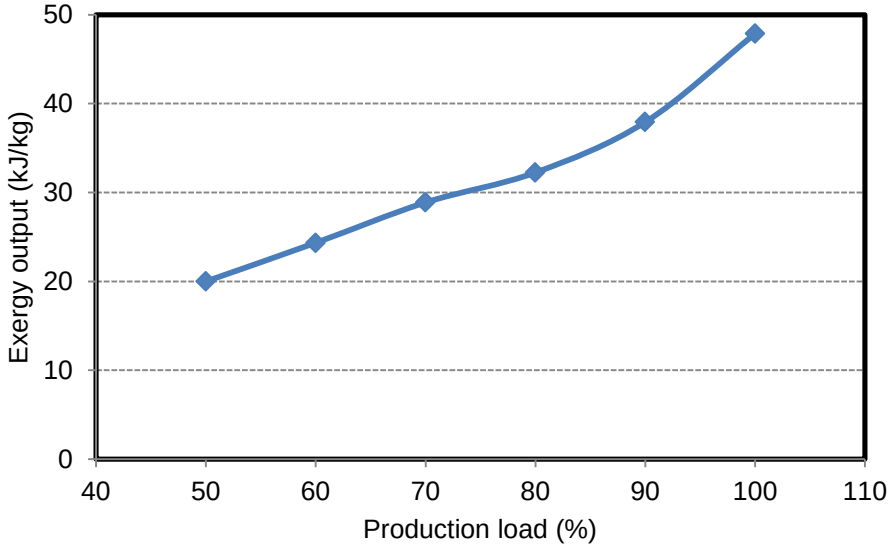


Figure 4.50. Variation of exergy output of distilled water as a function of the production load

Figure 4.50 presents the variation of the exergy output of distilled water as a function of the production load at a seawater temperature of 23ºC. As seen from this figure, the exergy output increases with increasing operating load due to the combination of rising exergy efficiency and distilled water production.

The subsystem that causes exergy destruction in the desalination system is the steam jet ejector, due to the high temperature and high pressure of its heat input. In the thermal vapor compression (TVC) system, the steam jet ejector is responsible for a loss of 45% of the total input exergy, with the second highest loss of exergy (20%) due to the effects. Subsystem exergy destruction ratios at full load and a seawater temperature of 23°C are shown in Figure 4.51.

The regulation of the distillated water can be maintained by controlling the flow rate of the motive steam to the steam ejector (Shen et al., 2011). The increase in the motive steam flow rate automatically provides an increase in the distillated water output as seen Figure 4.52. Calculations indicated that as the production load and seawater temperature increased, the amount of distilled water production

significantly increases. An increase in production load from 50% to 100% provides an increase of 119.1%, 105.6% and 96.6% of distilled water production at seawater temperatures of 23ºC, 28ºC and 33ºC, respectively.

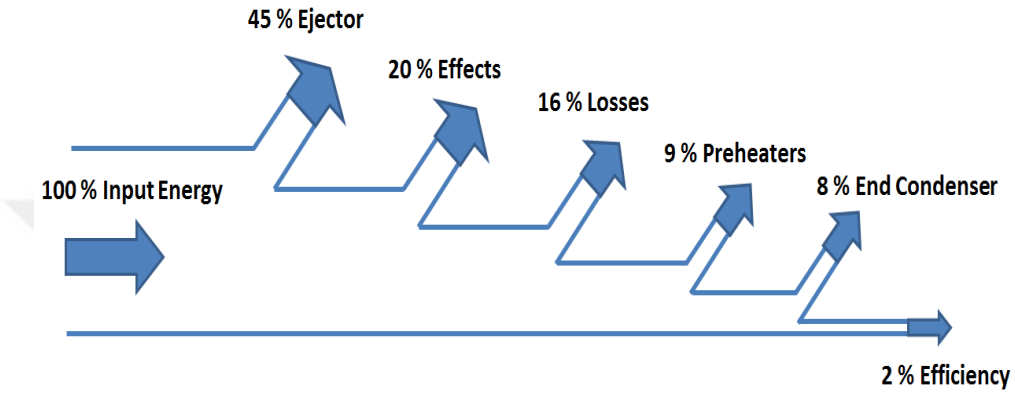


Figure 4.51. Exergy destruction ratios of the subsystem at full load

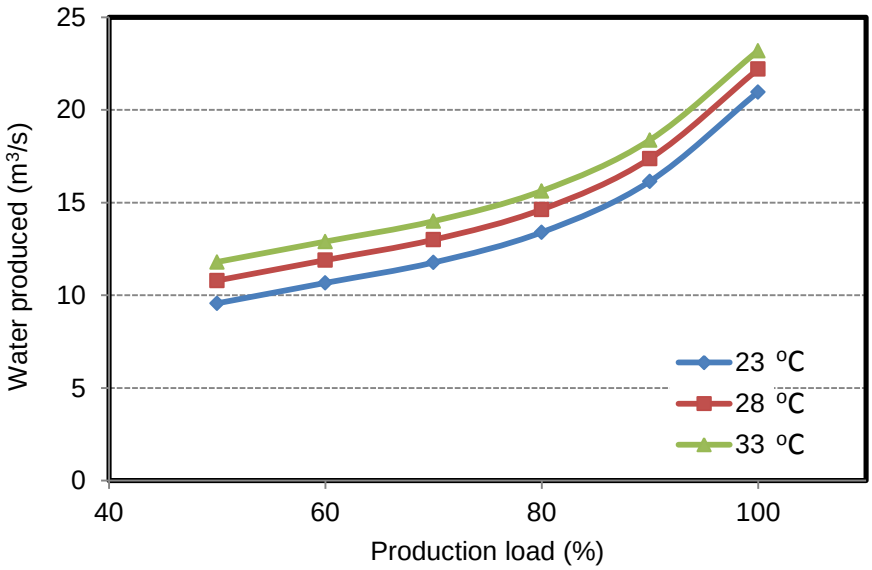


Figure 4.52. Variation of water produced as a function of production load

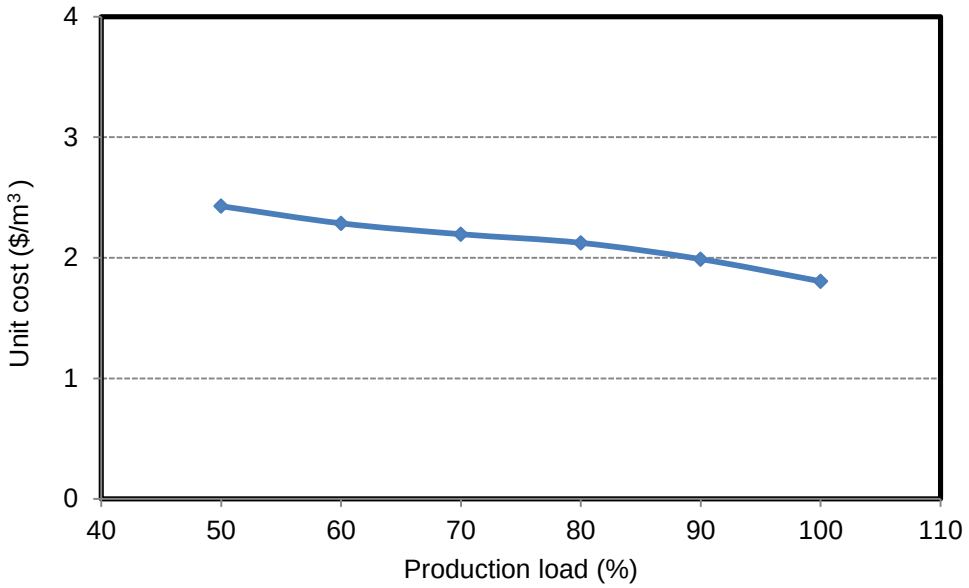


Figure 4.53. Variation of unit production cost as a function of the production load for seawater temperature of 23ºC

Figure 4.53 shows the unit production cost obtained by thermo-economic analysis. As seen from the figure, unit cost is decreased when the production load is increased. The production cost of the desalinated water is 1.8 $/m$^3$ at full load and a seawater temperature of 23ºC. The high costs related to the rejected brine shows that recovering these expenses may prove to be cost-effective for the plant.

### 4.5. Greenhouse Heating System Case

The heat transfer rate is calculated by taking different sea water temperatures into account at an air temperature of 10 ºC which is shown in Figure 4.54. As it can be seen from the figure, the amount of heat transferred from the hot seawater to the air increases when the seawater temperature rises.

The heat transfer rate is calculated by varying the air temperatures at 16 ºC seawater temperature which is presented in Figure 4.55. As it can be seen from the

figure, the amount of heat transferred from the hot seawater to the air decreases as the air temperature increases.

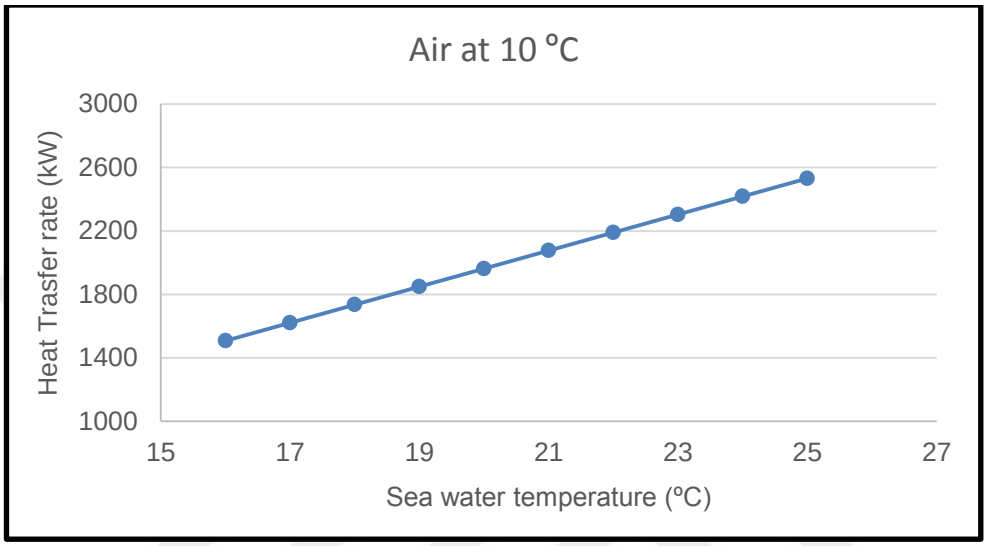


Figure 4.54. Heat transfer rate from the steam power plant at air 10 ºC

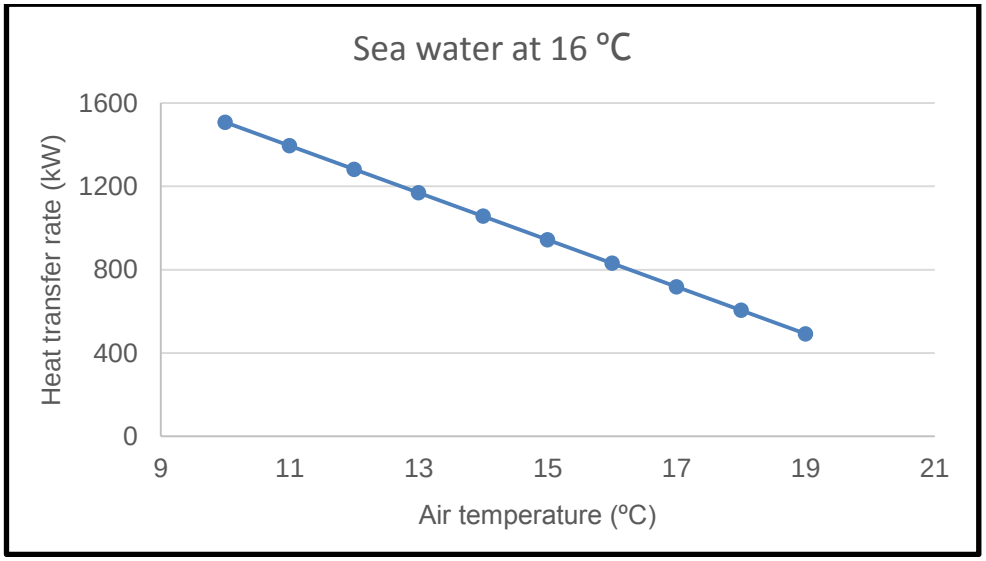


Figure 4.55. Heat transfer rate from the steam power plant at seawater 16 ºC

### 4.6. Multigeneration System Case

As it is known that a single generation system produces not only electricity but also produce waste or unused energy. This waste or unused energy is converted to the useful work by integrating additional systems to generate different products by multigeneration energy system. Although the multigeneration system has multiple outputs, the energy efficiency and exergy efficiency are higher compared to the systems with multiple input energy when the multigeneration system has a single energy input.

As it is indicated Figure 4.56 shows that calculated exergy efficiency of single generation is 39.1 % , but, in the case of the cogeneration system, the system efficiency becomes 39.25%, furthermore, in the second step using trigeneration systems the efficiency increases to a value of 39.49 In addition to the trigeneration systems, when the desalination plant and the organic Rankine cycle are integrated into the evaporation plant, the efficiency of the multi-production system increases to 39.84%. As in the case of exergy efficiency, energy efficiency is 41.5% for only power generation. On the other hand, the energy efficiency with cogeneration becomes 41.66 %. In the case of trigeneration, this efficiency increases up to 41.92 %. Finally, after integration of the desalination plant and the organic Rankine cycle to reuse waste heat to convert into electricity, the multigeneration system energy efficiency reaches to 42.29 %. As noted earlier, the overall efficiency of the existing thermal power plant is %41.5. However, as a result of the analyzes carried out in the present study, the efficiency of the thermal power plant increases to 42.29% with the reuse of waste heat and the production of additional useful work in the system. As can be seen, the efficiency of the thermal power plant rises up by 0.72%. Considering the fact that this increase returns back to the company as an additional income. Now, one can conclude that the present work reveals that the outcome of the study is very rewarding.

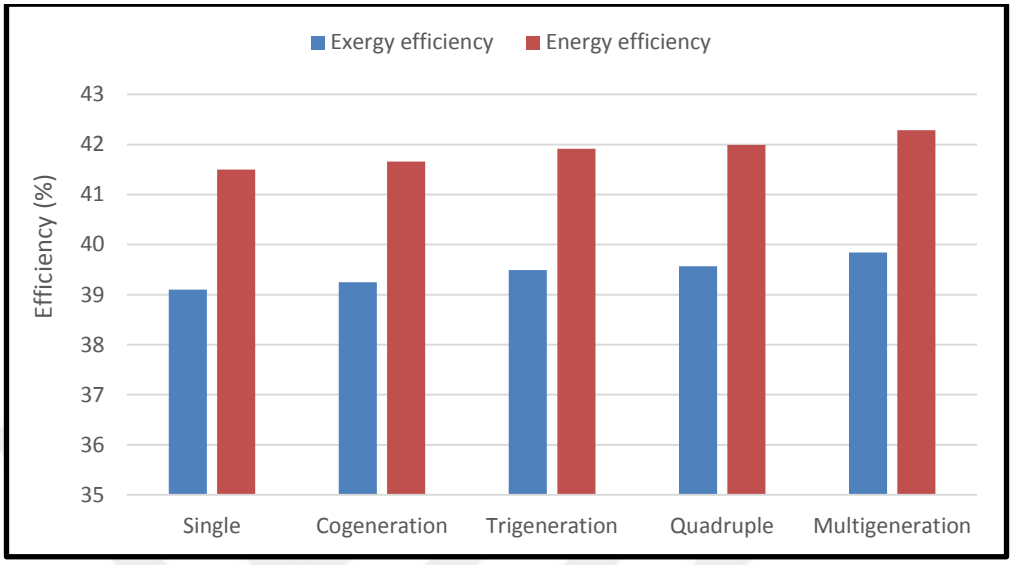


Figure 4.56. Energy and exergy efficiencies of integrated energy systems

$CO_2$ emissions of single and multigeneration systems are summarized in Figure 4.57. $CO_2$ emissions adversely affect global warming. In order to eliminate the permanently harmful effect of $CO_2$, multigeneration replaced with a single generation. While the system is converted into multigeneration system, input energy of system drops down thus less amount of input energy used then it provides less emission. As a result environmental impact of a single generation can be minimized with multiple outputs.

As it is known, these days, scientific and engineering studies are being carried out extensively to improve the technology of capturing and storing of $CO_2$ gas which causes global warming. However, when the majority of the energy contained in the coal is converted into useful works, the amount of coal consumption can be reduced in the thermal power plant. This reduces the amount of $CO_2$ produced. Thus, the investment cost of both the thermal power plant and the $CO_2$ capture and storage system is reduced as the capacities of those systems are reduced.

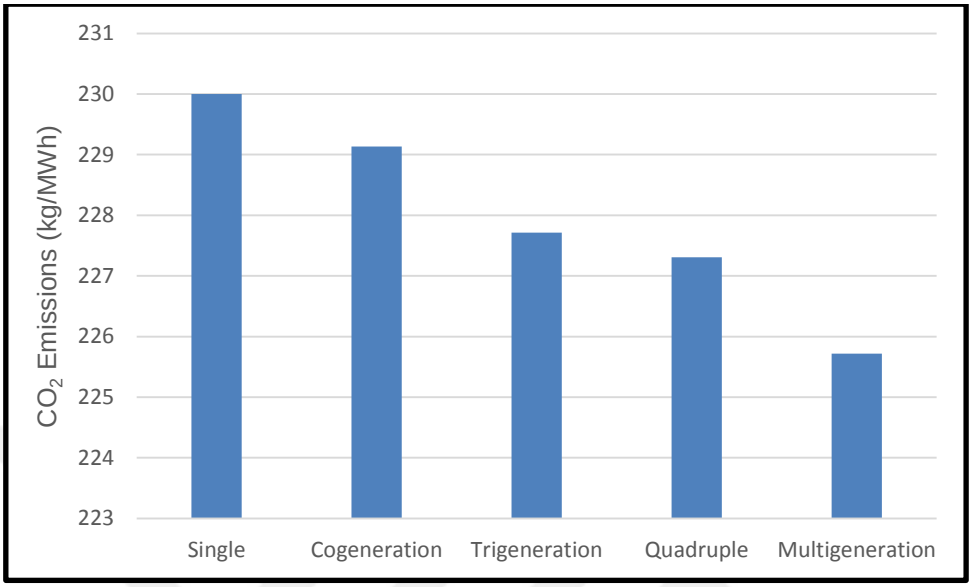


Figure 4.57. $CO_2$ emissions of integrated energy systems

## 5. CONCLUSION AND RECOMMENDATIONS

The comprehensive thermodynamic modeling, energy and exergy analyses and environmental evaluations of this newly proposed multigeneration system for electricity generation, refrigeration, greenhouse heating and distilled water production have provided useful insights. These applications are of great importance and receive a great deal of attention because of efficient performance and environmentally less harmful.

- The effects of three types of power plants on an operating power plant were examined by carrying out energy and exergy analyses. The highest loss of input energy to the environment in this power cycle was determined to be in the condenser. In addition, this was followed by the energy efficiency in the boiler system which was calculated to be approximately 93%, 95% and 96% for subcritical, supercritical and ultra-supercritical cycles, respectively. Moreover, the exergy efficiency of the boilers was found to be 58%, 60% and 65% for subcritical, supercritical and ultra-supercritical cycles, respectively. The calculated energy efficiencies for subcritical, supercritical and ultra-supercritical systems were 41.5%, 43.8% and 46%, respectively. However, energy loss in the condenser was determined to be thermodynamically insignificant because of the low quality of the condenser. With respect to exergy efficiencies, the biggest exergy efficiency was seen in the ultra-supercritical power plant and was 39.1%, 40.8% and 41.9% for subcritical, supercritical and ultra-supercritical type power plants, respectively. Lastly, the main conclusion is that the highest overall efficiency of the steam power

plant is achieved by the ultra-supercritical power plant due to the greatest boiler pressure.

- In the desalination plant, energy and exergy analyses were conducted by considering different operating loads, different seawater temperatures as well as upper brine temperatures. The purpose of the study was to determine the exergy destroyed in every component of the plant, which indicates overall plant performance. To enhance the thermodynamic performance of desalination plants, exergy destruction within the plant's components should be decreased. When the operating load increases, the observed performance parameters are improved.When the production load and seawater temperatures are 100% and 33$^{o}$C, respectively, the gain output ratio obtained becomes 7.33. Desalination process is an energy-intensive process. Accordingly, high-grade energy is converted into low-grade energy, as motive steam energy is converted into distilled water. So, the exergy efficiency of the system is around 1% or 2 %, which increases with rising operating load and increasing seawater temperatures. Increased seawater temperatures can also improve performance parameters. In addition, the ejectors and effects were the main sources of exergy destructions. The steam jet ejector controls approximately 45% of the total exergy destruction of effect. Finally, the unit cost of distilled water is computed to be 1.8 \$/m$^3$ at full load.
- As a novel system, the Vapor Compression Cooling (STD-VCR) system, in which the steam turbine is installed, is proposed. The compressor is driven by a turbine which replaces the expansion valve. Based on the vapor compression cycle a new refrigeration cycle driven by a steam turbine is introduced in this work. The system is also compared to equivalent systems by performing energy, exergy

and economic analysis. The inlet vapor of back pressure steam turbine comes from cold reheat line of the steam power plant and the exhaust stream of the back pressure turbine is fed to desalination plant of the steam power plant. The applicable COP of the proposed cycle is investigated for four different working fluids, for example, R134a, R410a, R407c and R717. A performance of each working fluid is examined. The results obtained by thermodynamic and thermoeconomic analyses reveal that the working fluid R134a is the most efficient fluid among the other fluids considered in the present work. By performing a comprehensive parametric study, the thermodynamic parameters that are effective in defining the performance criteria of the system were defined. Some of the main results of the present study can be summarized as follows.

- ✓ Among all examined working fluids, R134a is suggested as the best candidate from thermodynamic and thermoeconomic, viewpoints, revealing cooling capacity, COP and exergy efficiency values of 4127 kW, 2.73, 18.61%, respectively.
- ✓ The turbine inlet parameters such as pressure, temperature, and steam mass flow positively affect an improvement of the cooling load for each fluid.
- ✓ Among all elements, the expansion valve is accounted for the biggest exergy destruction rate due to the non-isentropic expansion process.
- ✓ Exergy efficiencies of evaporator and condenser are directly proportional to the temperature differences of hot and cold inlet fluid.
- ✓ COP values are obtained as 2.73, 2.29, 1.8 and 1.15 for working fluids of R134a, R410a, 407c and R717 respectively. Also, exergy

efficiency is found to be 18.61 %, 13.93%, 14.97 % for those fluids mentioned above.

- ✓ The steam power plant exergy efficiency is determined to be 39.1% with a single output. As a consequence of integrating vapor compression cycle with the ORC, the overall exergy efficiencies of the whole systems are 39.36%, 39.32%, 39.27% and 39.21% for working fluids of R134a, R410a, R407c and R717 respectively.
- ✓ The expansion valve has the maximal value of the sum $\dot{C}_D + \dot{Z}$ and $r$, also, has the minimal $f$ value which is the exergoeconomic factor.

- In the ORC cycle, the influence of parameters such as the flue gas temperature, the flue gas mass flow rate, the steam power plant unit load and the evaporator pinch point temperature on the thermodynamic performance of the ORC system integrated with the steam power plant was examined as a waste heat recovery system. Detailed energy, exergy and exergoeconomic-environmental analyses of the ORC system were performed. Exergy and energy efficiencies were also calculated and the values of exergoeconomic variables were determined for each component as well as the entire ORC system. In summary, some concluding remarks are presented below:
  - ✓ The increase in flue gas temperature causes an overall decrease in the ORC exergy efficiency and evaporator efficiency, which in contrast, positively affects the net power generation and energy efficiency.
  - ✓ The flue gas mass flow rate directly affects all efficiency parameters, net power output, overall energy efficiency, exergy

efficiency and evaporator efficiency, which all have a tendency to rise when the mass flow rate is increased.

- ✓ Increasing evaporator pinch point temperature negatively affects the overall exergy efficiency, the net power output and the evaporator efficiency.
- ✓ Steam power plant unit load improvement is directly proportional to the performance parameters such as net power output, overall energy and exergy efficiencies. Evaporator efficiency increases when the unit load is increased.
- ✓ The R245fa fluid reveals the extraordinary performance in terms of exergy efficiency in the Organic Rankine Cycle for all varied parameters.
- ✓ The steam power plant exergy efficiency is 39.1% on its own, but when the ORC system is integrated this overall becomes 39.4%. This 0.3% efficiency difference corresponds to energy gain of 4.7 MW.
- ✓ The best operating point for the ORC pump was determined to have a 80% steam power plant unit loads and a flue gas flow rates of 450 kg/s.
- ✓ The evaporator had the maximal value for the sum $\dot{C_D} + \dot{Z}$ and the minimal value for the exergoeconomic factor *f*. Based on this working period, the payback period is found to be 5.02 years.
- ✓ $CO_2$, $NO_x$ and CO emissions are lowered by integrating the ORC system with the steam power plant.

- Calculated exergy efficiency of a single generation as 39.1 %. In the case of the cogeneration system, the efficiency of the system becomes 39.25%, furthermore, using trigeneration systems the efficiency

increase to the value of 39.49 %. Besides trigeneration systems multigeneration system efficiency increase to 39.84 % when desalination plant and organic Rankine cycle are integrated into the steam power plant. As in the case of exergy efficiency, the energy efficiency is 41.5% for only power generation. The energy efficiency with cogeneration becomes 41.66 %. In the case of trigeneration, the efficiency increases up to 41.92 %. Finally, after integration of the desalination plant and the organic Rankine cycle, multigeneration system energy efficiency reaches the value of 42.29 %.

- $CO_2$ emissions are lowered from 230 kg/MWh to 225 kg/MWh by integrating four subsystems with the steam power plant.

The results of this PhD thesis can be used for designing new multigeneration systems based on the subcritical coal-fired power plant. These outcomes can assist designers in developing more energy efficient systems in an integration fashion. In this study, the multigeneration system was analyzed and assessed. The results obtained from this thesis strongly suggest integrating the ORC system and all other systems examined presently with the coal-fired power plant.

## REFERENCES


Afanasyeva, O. V., and Mingaleeva, G. R., 2015. Comprehensive exergy analysis of the efficiency of a low-capacity power plant with coal gasification and obtaining sulfur. Energy Efficiency, 8: 255-265.

Ahmadi, P., Dıncer, I., and Rosen, M. A., 2012a. Exergo-Environmental Analysis of an Integrated Organic Rankine Cycle for Trigeneration, Energy Conversion and Management, 64: 447-453.

Ahmadi, P., Dıncer, I., Rosen, M. A., 2014. Thermoeconomic multi-objective optimization of a novel biomass based ıntegrated energy systems, Energy, x, 1-13.

Ahmadi, P., Rosen, M. A., Dincer, I., 2012b. Multi-objective exergy-based optimization of a polygeneration energy system using an evolutionary algorithm. Energy. 46: 21-31.

Al-Ali, M., and Dincer, I., 2014. Energetic and exergetic studies of a multigenerational solar-geothermal system, Applied Thermal Engineering, 71: 16-23.

Alasfour, F. N., and Alajmi, H. F., 2010. Integration of TVC desalination system with cogeneration plant: Parametric study. Fourteenth International Water Technology Conference, Cairo, Egypt, 117-132.

Aljundi, I. H., 2009. Energy and exergy analysis of a steam power plant in Jordan, Applied Thermal Engineering, 29:324-328.

Al-Mutaz. I. S., and Wazeer. I., 2014. Comparative performance evaluation of conventional multi-effect evaporation desalination processes. Applied Thermal Engineering; 73: 1192-1201.

Al-Sulaıman, F. A., Dincer, I., and Hamdullahpur, F., 2012. Energy and exergy analyses of a biomass trigeneration system using an organic Rankine cycle, Energy, 45: 975-985.

Anvari, S., Saray R. K., Bahlouli, K., 2015. Conventional and advanced exergetic and exergoeconomic analyses applied to a tri-generation cycle for heat, cold and power production, Energy, 91:925-939.

Aphornratana, S., and Sriveerakul. T., 2010. Analysis of a combined Rankine-vapour-compression refrigeration cycle. Energy Conversion and Management. 51: 2557-2564.

Askari, I. B., Ameri. M., Calise. F., 2018. Energy, exergy and exergo-economic analysis of different water desalination technologies powered by Linear Fresnel solar field. Desalination, 425:37-67.

Bejan A, Tsatsaronis G, Moran M. Thermal design and optimization, John Wiley & sons ,1996, 470s.

Bıcer, Y., and Dıncer, I., 2016. Analysis and performance evaluation of a renewable energy based multigeneration system, Energy, 94: 623-632.

Bin Amer, A. O., 2009. Development and optimization of ME-TVC desalination system. Desalination. 249: 1315-1331.

Brogioli, D., La Mantia, F., Yip, N. Y., 2018. Thermodynamic analysis and energy efficiency of thermal desalination processes. Desalination, 428: 29-39.

Carcasci, C., and Winchler, L., 2016. Thermodynamic analysis of an Organic Rankine Cycle for waste heat recovery from an aeroderivative intercooled gas turbine. Energy Procedia, 101: 862-869.

Chen, H., Goswami, D. Y., Stefanakos, E. K., 2010. A review of thermodynamic cycles and working fluids for the conversion of low-grade heat. Renewable and Sustainable Energy Reviews, 14: 3059-3067

Dai, Y., Wang, J., Gao, L., 2009. Parametric optimization and comparative study of organic Rankine cycle (ORC) for low grade waste heat recovery. Energy Conversion and Manageme, 50: 576-582.

Demirkaya, G., Padilla, RV., Goswami, DY., 2013. A review of combined power and cooling cycles. WIREs Energy Environ, 2: 534-547.

Deng, N., Zhou, M., Zhang, Y., Zhang, Z., Zhang, Y., Wang, H., Li, X., 2017. Experimental research of a new steam heat pump system for recovering industrial waste heat. Journal of Energy Engineering, 143(5):040-035.

Dincer I, and Kanoglu M. Refrigerations system and analysis, Wiley, 2010, 464 p.

Dincer I, Rosen MA, Pouria A. Optimization of Energy Systems, Wiley, 2017, 453p.

Dinçer, I., and Rosen, M. A., 2007. Exergy: Energy, Environment and Sustainable Development. Elsevier Science Publishers, Amsterdam.

Dinçer, I., and Rosen, M. A., 2011. Thermal energy storage; systems and applications. John Wiley and Sons.

Dincer, I., and Zamfirescu, C., 2012. Renewable-energy-based multigeneration systems. International Journal of Energy Research.

Dıncer, I., and Zamfirescu, C., Advanced power generation systems, Elsevier, 2014.

Esen, M., and Yuksel, T., 2013. Experimental evaluation of using various renewable energy sources for heating a greenhouse. Energy and Buildings, 65:340-351.

Eyidogan, M., Kilic, F. C., Kaya, D., Coban, V., 2016. Cagman S. Investigation of Organic Rankine Cycle (ORC) technologies in Turkey from the technical and economic point of view. Renewable and Sustainable Energy Reviews. 58: 885-895.

Fellah, G., Shuia, E., Rohoma, A., 2014. Exergy assessment for a typical multi-effect thermal vapor compression desalination unit (MED-TVC). Journal of Engineering Research, 20: 57-66.

Fitzsimons, L., Corcoran, B., Young, P., Foley, G., 2015. Exergy analysis of water purification and desalination: A study of exergy model approaches. Desalination, 359: 212-224.

Galloni, E., Fontana, G., Staccone, S., 2015. Design and experimental analysis of a mini ORC (organic Rankine cycle) power plant based on R245fa working fluid. Energy, 90: 768-775.

Hamed, O. A., Zamamiri, AM., Aly, S., Lior, N., 1996. Thermal performance and exergy analysis of a thermal vapor compression desalination system. Energy Conversion and Management, 37: 379-387.

Hasti, S., Aroonwilas, A., Veawab, A., 2013. Exergy analysis of ultra-super-critical power plant. Energy Procedia, 37: 2544-51.

Hepbasli, A., Erbay, Z., Icier, F., Colak, N., Hancioglu, E., 2009. A review of gas engine driven heat pumps (GEHPs) for residential and industrial applications. Renew Sustain Energy Rev, 13: 85–99.

ISKEN, 2018. Isken sugözü steam power plant, http://www.isken.com.tr/fotograflar-detay.aspx?id=1 (Accessed 10 march 2018)

Karaoglu, Ç., 2018. Flue gas heat recovery in steam power plant, MSc thesis, Cukurova University, Adana.

Kaşka, O., 2014. Energy and exergy analysis of an organic Rankine for power generation from waste heat recovery in steel industry. Energy Conversion and Management, 77: 108-117

Khalid, F., Dincer, I., and M. A., 2015. Rosen, Energy and exergy analyses of a solar-biomass integrated cycle for multigeneration, Solar Energy, 112: 290-299.

Khalid, K. A., Antar, M. A., Khalifa, A., Hamed, O. A., 2018. Allocation of thermal vapor compressor in multi effect desalination systems with different feed configurations. Desalination, 426:164-173.

Khanmohammadi, S., Atashkari, K., and Kouhikamali, R., 2015. Exergoeconomic multi-objective optimization of an externally fired gas turbine integrated with a biomass gasifier, Applied Thermal Engineering, 91: 848-859.

Kim, K. H., Perez-Blanco, H., Performance analysis of a combined organic Rankine cycle and vapor compression cycle for power and refrigeration cogeneration. Applied Thermal Engineering, 91: 964-974.

Kotas, T. J., 1995. The exergy method of thermal plant analysis, Krieger Publishing Company, Malabar, 296s

Kumar, R., Sharma, A. Kr., Tewari, P. C., 2014. Thermal Performance and Economic Analysis of 210 MWe Coal-Fired Power Plant. Journal of Thermodynamics, Article ID 520183, 10 pages.

Li, L., Ge, Y. T., Luo, X., Tassou, SA., 2018a. Experimental analysis and comparison between $CO_2$ transcritical power cycles and R245fa organic Rankine cycles for low-grade heat power Generations. Applied Thermal Engineering, 136: 708-717.

Li, Z., Siddiqi, A., Anadon, L. D., Narayanamurti, V., 2018b. Towards sustainability in water-energy nexus: Ocean energy for seawater desalination. Renewable and Sustainable Energy Reviews, 82: 3833-3847.

Long, R., Bao, YJ., Huang, XM., Liu, W., 2014. Exergy analysis and working fluid selection of organic Rankine cycle for low grade waste heat recovery. Energy, 73: 475-483. ,

Lu, Y., Wang, Y., Dong, C., Wang, L., Roskilly, A. P., 2015. Design and assessment on a novel integrated system for power and refrigeration using waste heat from diesel engine. Applied Thermal Engineering, 91: 591-599.

Mabrouk, A. A., Nafey, A. S., Fath, H. E. S., 2007. Thermoeconomic analysis of some existing desalination processes. Desalination, 205: 354-373.

Malik, M., Dıncer, I., and Rosen, M. A., 2015. Development and analysis of a new renewable energy-based multi-generation system, Energy, 79: 90-99.

Moran, M. J., and Shapiro, H. N., 2000. Fundamental of Engineering Thermodynamics, John-Wiley & Sons.

Ozlu, S., and Dıncer, I., 2015. Development and analysis of solar and wind energy based multigeneration systems, Solar Energy, 122: 1279-1295.

Ozturk, M., and Dıncer, I. 2013. Thermodynamic assessment of an integrated solar power tower and coal gasification system for multi-generation purposes, Energy Conversion and Management, 76: 1061-1072.

Safarian, S., and Aramoun, F., 2015. Energy and exergy assessments of modified Organic Rankine Cycles (ORCs). Energy Reports, 1: 1-7.

Sahin, H.E., and Aydın, M., 2012. Energy and exergy analysis of a supercritical power plant with 660 MW output Turkey, Global Conference on Global Warming (GCGW-2012), July 8-12, 1590-1594, Istanbul, Turkey

Saleh, B., 2016. Parametric and working fluid analysis of a combined organic Rankine-vapor compression refrigeration system activated by low-grade thermal energy. Journal of Advanced Research, 7: 651-660.

Seyedkavoosi, S., Javan, S., Kota, K., 2017. Exergy-based optimization of an organic Rankine cycle (ORC) for waste heat recovery from an internal combustion engine (ICE). Applied Thermal Engineering, 126:447–457.

Shen, S., Zhou, S., Yang, Y., Yang, L., Liu, X., 2011. Study of steam parameters on the performance of a TVC-MED desalination plant. Desalination and Water Treatment, 33:300-308.

Suleman, F., Dıncer, I., and Agelin-Chaab, M.,2014. Development of an integrated renewable energy system for multigeneration, Energy, 78: 196-204.

Sun, W., Yue, X., Wang, Y., 2017. Exergy efficiency analysis of ORC (Organic Rankine Cycle) and ORC based combined cycles driven by low-temperature waste heat. Energy Conversion and Management, 135: 63-73.

Tchanche, B. F., Lambrinos, G., Frangoudakis, A., Papadakis G., 2011. Low-grade heat conversion into power using organic Rankine cycles – A review of various applications. Renewable and Sustainable Energy Reviews. 15: 3963-3979.

Tchanche, B. F., Pétrissans, M., Papadakis, G., 2014. Heat resources and organic Rankine cycle machines. Renewable and Sustainable Energy Reviews, 39: 1185-1199.

Unal, F., 2009. Exergy analysis of a thermal power plant, Msc Thesis, Yıldız Teknik University, The Institute of Science, Istanbul, Turkey.

Vélez, F., Segovia, J. J., Martín, M. C., Antolín, G., Chejne, F., Quijano, A., 2012. A technical, economical and market review of organic Rankine cycles for the conversion of lowgrade heat for power generation. Renewable and Sustainable Energy Reviews, 16: 4175-4189.

Wang, H., Peterson, R., Harada, K., Miller, E., Ingram-Goble, R., Fisher, L., Yih, J., Ward, C., 2011a. Performance of a combined organic Rankine cycle and vapor compression cycle for heat activated cooling. Energy, 36: 447-458.

Wang, H., Peterson, R., Herron, T., 2011b. Design study of configurations on system COP for a combined ORC (organic Rankine cycle) and VCC (vapor compression cycle). Energy, 36: 4809-4820.

Wei, D., Lu, X., Lu, Z., Gu, J., 2007. Performance analysis and optimization of organic Rankine cycle (ORC) for waste heat recovery. Energy Conversion and Management, 48: 1113-1119.

WER, 2016. World Energy Resources, https://www.worldenergy.org (accessed, 20 may 2016)

Yuksel, Y. E., Ozturk, M., Dincer, I., 2016. Thermodynamic performance assessment of a novel environmentally benign solar energy based integrated system, Energy Conversion and Management. 119: 109-120.

Zarzo, D., and Prats, D., 2018. Desalination and energy consumption. What can we expect in the near future? Desalination, 427:1-9.

**CURRICULUM VITAE**

Mehmet TONTU was born in 15.08.1986 in Ceyhan. He lives in Adana province. He graduated from Ceyhan High School in 2003. He enrolled in the Mechanical Engineering Department of University of Çukurova in 2005. He graduated from the Mechanical Engineering Department in 2010 and he started to his MSc education in 2011. He completed MSc education at 2013. And he began his PhD education at the Department of Mechanical Engineering of Çukurova University in the same year.

Mehmet TONTU has been working in ISKEN Sugözü steam power plant since 2011 as an operation lead engineer. He is expert about power plant operation and its components. He is married.